The diverse roles of Collapsin Response Mediator Protein 4 in mitosis and nerve regeneration

Stephan Ong Tone

Department of Neurology and Neurosurgery

McGill University, Montreal

February 2011

A thesis submitted to McGill University in partial fulfillment of the requirements of the degree of Doctor of Philosophy

ABSTRACT

Microtubule-actin interactions underlie a diverse number of biological processes including cell motility, neuronal outgrowth, cellular wound healing, cell division and cortical flow. CRMPs (Collapsin Response Mediator Proteins) are a family of cytosolic phosphoproteins that play roles in regulating both actin and microtubule dynamics. The roles of the CRMP family of proteins in regulating these cellular processes have only been partially described. Our lab has been particularly interested in the function of the CRMP4 isoform because of its unique ability to complex with RhoA, a master regulator of the actin cytoskeleton. **In this thesis we explore the function of CRMP4 in two biological processes that are dependent on actin and microtubule dynamics: mitosis (Chapter 2) and axon regeneration (Chapter 3 and 4).** In Chapter 2, we identify CRMP4 as an important regulator of mitotic chromosomal alignment. We show that CRMP4 localizes to spindle microtubules during mitosis and that loss of CRMP4 disrupts chromosomal alignment, mitotic progression and spindle morphology. Furthermore, we demonstrate that these processes are dependent on CRMP4 phosphorylation, which may be important for recruitment of additional proteins to the mitotic machinery. In Chapter 3, we investigate the ability of an adeno-associated virus (AAV) encoding a CRMP4 antagonist C4RIP (CRMP4-RhoA inhibitory peptide) to enhance adult retinal ganglion cell (RGC) axon regeneration in an *in vivo* preclinical optic nerve injury model. We describe the inability of AAV-C4RIP to promote RGC regeneration and discuss the likelihood that AAV-mediated expression levels of C4RIP may be insufficient to promote regeneration. In Chapter 4, we describe the development and validation of cell permeable recombinant C4RIP (TAT-C4RIP) and discuss our data testing the effects of TAT-C4RIP on regeneration *in vitro* and *in vivo*. Together, these studies identify CRMP4 as an important regulator of mitosis, and describe our ongoing studies testing the effects of a CRMP4 antagonist on nerve regeneration.

RÉSUMÉ

Les interactions entre l'actine et les microtubules sont sous-jacentes à divers processus biologiques incluant la motilité cellulaire, le guidage neuronal, la cicatrisation cellulaire, la division cellulaire et la circulation corticale. Les protéines CRMPs

(Collapsin Response Mediator Protein) sont une famille de phosphoprotéines cytosoliques jouant un rôle dans la régulation de la dynamique de l'actine et des microtubules. Cependant, cette régulation du cytosquelette par les CRMPs n'a été que partiellement décrite. Notre laboratoire s'intéresse à la fonction de l'isoforme CRMP4 en raison de sa capacité unique d'interagir avec RhoA, un régulateur important du cytosquelette d'actine. **Dans cette thèse, nous explorons la fonction de CRMP4 dans deux processus biologiques qui dépendent de la dynamique de l'actine et des microtubules: la mitose (chapitre 2) et la régénération des axones (chapitre 3 et 4).** Dans le chapitre 2 sera présentée notre identification de CRMP4 en tant que régulateur important de l'alignement chromosomique durant la mitose. Nous démontrons que, pendant la mitose, CRMP4 se situe sur les fuseaux mitotiques formés de microtubules et que la perte de CRMP4 perturbe l'alignement chromosomique, la progression de la mitose et la morphologie des fuseaux. En outre, nous démontrons que ces processus sont dépendants de la phosphorylation de CRMP4. Ceci pourrait être crucial pour le recrutement de protéines supplémentaires nécessaire pour la mitose. Dans le chapitre 3, nous étudions la capacité d'un virus adéno-associé (AAV) codant pour l'antagoniste de CRMP4, nommé C4RIP (CRMP4-RhoA inhibitory peptide), de favoriser la régénération de l'axone de cellules ganglionnaires de la rétine (RGC) chez l'adulte. Pour cela, nous utilisons un modèle *in vivo* de traumatismes du nerf optique chez le rat adulte. Nous décrivons l'incapacité des virus AAV-C4RIP de favoriser la régénération des RGCs et discutons de la probabilité que les niveaux de AAV-C4RIP exprimés puissent être insuffisants afin de favoriser la régénération. Le chapitre 4, quant à lui, est consacré à la description du développement et de la validation de la protéine recombinante TAT-C4RIP qui a le potentiel de traverser la membrane cellulaire. Nous y discutons les données concernant les effets de TAT-C4RIP sur la régénération *in vitro* et *in vivo*. Dans l'ensemble, ces études caractérisent CRMP4 comme important régulateur de la mitose et décrivent une nouvelle méthode de purification pour des protéines perméables à la membrane cellulaire.

TABLE OF CONTENT

LIST OF FIGURES

Chapter 1

Chapter 2

Chapter 3

Chapter 4

LIST OF ABBREVIATIONS

AAV	Adeno Associated Virus
ANT-1	Adenine Nucleotide Translocator-1
APC	Anaphase-Promoting Complex
BBB	Basso, Beattie, and Bresnahan
BDNF	Brain Derived Neurotrophic Factor
BSA	Bovine Serum Albumin
C4RIP	CRMP4b RhoA Inhibitory Peptide
Ca^{2+}	Calcium
CaMKII	Ca^{2+}/Calmodulin–Dependent Protein Kinase II
cAMP	cyclic Adenosine Monophosphate
cdk	Cyclin-Dependent Kinase
chABC	Chondroitinase ABC
CHO	Chinese Hamster Ovary
CNS	Central Nervous System
CNTF	Ciliary Neurotrophic Factor
CREB	cAMP Response Element Binding
CRMP	Collapsin Response Mediator Protein
CSPG	Chondroitin Sulfate Proteoglycan
CST	Corticospinal Tract
CTβ	Cholera toxin beta
DHPase	Dihydropyrimidinase
DMEM	Dulbecco's Modified Eagle Medium
DN	Dominant Negative
DN-NgR1	Dominant Negative Nogo-66 Receptor
DRG	Dorsal Root Ganglion
DRP	Dihydropyrimidinase-Related Protein
DYRK	Dual tyrosine Regulated Kinase
E15	Embryonic day 15
ER	Endoplasmic Reticulum
Erk1/2	Extracellular Signal-Regulated Kinase 1/2
ES	Embryonic Stem
EGFR	Epidermal Growth Factor Receptor
F-actin	Filamentous actin
FBS	Fetal Bovine Serum
FGF	Fibroblast Growth Factor
GAG	Glycoaminoglycan
GAP	GTPase Activating Protein
GAP-43	Growth Associated Protein-43
GBM	Glioblastoma Multiform
GDI	Guanine Nucleotide Dissociation Inhibitors
GDP	Guanosine Diphosphate
GEF	Guanine Exchange Factor
GFP	Green Fluorescent Protein
GPI	Glycosyl Phosphatidyl Inositol

GSK	Glycogen Synthase Kinase
GST	Glutathione S transferase
GTP	Guanosine Triphosphate
GTPase	Guanosine Triphosphatase
HeLa	Henrietta Lacks'
His	Histidine
HBS	Hepes buffered Saline
HRP	Horse radish peroxidase
HSV	Herpes Simplex Virus
ICD	$p75^{NTR}$ Intracellular Domain
INL	Inner Nuclear Layer
IP	Immunoprecipitation
IP_3	Inositol 1,4,5-triphosphate
IPL	Inner Plexiform Layer
IRES	Internal Ribosomal Entry Site
kDa	KiloDalton
LINGO1	LRR and Ig containing Nogo Receptor interacting protein
LPA	Lysophosphatidic Acid
LRR	Leucine Rich Repeat
LTP	Long Term Potentiation
LZK	Leucine Zipper Kinase
MAD2	Mitotic-Arrest Deficient homologue-2
MAG	Myelin Associated Glycoprotein
MAI	Myelin Associated Inhibitor
MAP	Microtubule Associated Protein
MAPK	Mitogen-Activated Protein Kinase
mDia	Mammalian homolog of *Drosophila* Diaphanous
MLCII	Myosin Light Chain II
MMP	Matrix Metalloproteinase
mRFP	Monomeric Red Fluorescent Protein
Mst3b	Mammalian Ste20-like Protein Kinase-3b
MTOC	Microtubule Organizing Center
mTOR	Mammalian Target of Rapamycin
NEB	Nuclear envelope breakdown
NF	Nerve fiber
NGF	Nerve Growth Factor
NgR1	Nogo-66 Receptor
NLS	Nuclear Localization Signal
NT	Neurotrophin
OCT	Optimal Cutting Temperature
OMgp	Oligodendrocyte Myelin glycoprotein
ONH	Optic Nerve Head
ONL	Outer Nuclear Layer
OPL	Outer Plexiform Layer
OS	Outer Segment
$p75^{NTR}$	p75 neurotrophin receptor

PBS	Phosphate Buffered Saline
PCR	Polymerase Chain Reaction
PFA	Paraformaldehyde
PH	Pleckstrin-Homology Domain
PI3K	Phosphoinositide 3-Kinase
PI-PLC	Phosphatidyl Inositol-Phospholipase C
PirB	Paired immunoglobulin-like receptor B
PKA	Protein Kinase A
PKC	Protein Kinase C
PLC	Phospholipase C
PlexA1	PlexinA1
PLL	Poly L Lysine
PLP	Proteolipid Protein
PNS	Peripheral Nervous System
PP	Protein Phosphatase
PTD	Protein Transduction Domain
PTEN	Phosphatase and Tensin Homolog
PTPσ	Protein Tyrosine Phosphatase Sigma
PVDF	Polyvinylidene fluoride membrane
RIPA	Radioimmunoprecipitation assay
RBD	Rho Binding Domain
RFP	Red fluorescent protein
RGC	Retinal Ganglion Cell
RhoGDI	Rho Guanine Dissociation Inhibitor
RNA	Ribosylnucleic Acid
ROCK	Rho-associated Kinase
RST	Rubrospinal tract
RTN	Reticulon
SAC	Spindle Assembly Checkpoint
SAP	Shrimp Alkaline Phosphatase
SCI	Spinal Cord Injury
SDS	Sodium Dodecyl Sulfate
SEM	Standard Error of Mean
Sema3A	Semaphorin 3A
Ser	Serine
SH3A	Src Homology 3A
siRNA	Short interfering Ribonucleic Acid
SV2	Synaptic Vesicle Protein 2
TAT	Trans-acting activator of transcription
TBS	Tris Buffered Saline
TBST	Tris Buffered Saline Tween-20
Thr	Threonine
TROY	Tumor necrosis factor superfamily member 19 or Taj
Tyr	Tyrosine
ULIP	Unc-33 Like protein

ACKNOWLEDGMENTS

I first started in Alyson's lab as an undergraduate student in the summer of 2004, and I continued to work in her lab as a research assistant and as a medical student over the following two and a half years. After spending four years as a graduate student, it has been a total of six and half years that I have had the privilege to be part of her lab. I would like to thank Alyson for her support and guidance through my early scientific training. Alyson has helped me develop my critical thinking, has encouraged me to try new experimental techniques and has improved my scientific writing skills. I have especially appreciated the scientific working environment that she has created, filled with people that are not only intelligent but also approachable and kind-hearted.

I would like to thank my collaborators throughout my graduate studies, Drs. Craig Mandato and Adriana Di Polo, for their valuable insight into my vastly different projects. I have spent just as much time in both of their lab as I have in Alyson's lab over my graduate studies, and they have always welcomed me and supported me as if I was their graduate student. I would also like to thank my committee members, Drs. Edward Ruthazer and Michel Cayouette, for their guidance and encouragement through all of my graduate school training. I appreciate all of their constructive feedback and their approachability to engage in conversation, scientific or non-scientific. I would also like to thank Drs. Jean-Francois Cloutier and Mitra Cowan for their advice and work on generating our knockout mice.

My graduate studies were funded through a Canadian Institute of Health Research MD-PhD Studentship, McGill's MD-PhD Program and through various McGill Medicine research bursaries, for which I am grateful.

I feel extremely fortunate to have found myself in a lab filled with great colleagues and friends. I am especially thankful to Dr. Madeline Pool for her continual guidance and her willingness to help troubleshoot any of my scientific problems. Her passion for science is contagious, and I have learnt so much from her. I would also like to thank Gino Ferraro for our many discussions over the course of our scientific training. I would also like to thank Isabel Rambaldi and Angie Giannakopoulos for their technical help, facilitating ordering of reagents, but mostly for our engaging conversations. I would

like to thank Bama Dayanandan for her guidance during my first year in a lab, and for her technical expertise and help with my project. Thanks to current and former lab members for providing a great working environment, specifically: Chris Kent, Dr. Yazan Alabed, Sidney Hsieh, Horia Pribag, Dr. Tadayuki Shimada and Dr. Mammad Khazei. To Emad, Mo, Gina, Martin, Miguel, Jin, Francois, Vess, Joseph, Robyn, Wiam, Ajit, Dalinda, Patricia, Carole, and many others, thank you all for making it such a great place to learn science but to also have fun. The training path that I have undertaken as an MD-PhD student has been challenging and I am extremely grateful to have had the initial guidance from Dr. Mike Jain and the continual support from Dr. Brett Burstein. Their advice has been invaluable to me.

To all of my friends that have always provided support and also much need distractions from my studies. Paul, Dhan, Jr – you guys are my bestfriends I am lucky to have you guys. Thanks to Tyler, Kathy, Christine and Van for your friendship and support throughout these years.

To Meghan, thank you for everything that you contribute to my life. Through your support and our conversations, I have been able to make it through this difficult training period. I am excited about continuing our journey together.

To all of my extended family, thank you all for caring so much about me, and your continual words of encouragement throughout my studies. To my brother and sisters, Chris, Jen and Mel, thank you all for your support and helping me have fun when I'm away from the lab.

To my dad and mom, I can never put into words what you have contributed to my life. From an early age you have taught me the importance of family, academics and of leading a balanced life. Your unconditional support and love throughout all of my life has been amazing. To my Dad, thank you for being the person that you are and for always looking out for our family. To my Mom, not a day goes by that I don't think about you and what you have done for me and our family – thank you.

CONTRIBUTION OF AUTHORS

Chapter 2: **"GSK3 regulates chromosomal alignment through CRMP4"**

Stephan Ong Tone: Performed experiments, analysis and revisions pertaining to Figures 1-10 and Supplemental Figures 1-3. Design of project, analysis of data, writing and editing of the manuscript.

Bama Dayanandan: Performed some of the immunocytochemistry pertaining to Figures 1,7 and 9a. Performed analysis of Figure 2c.

Alyson E. Fournier: Design of project, analysis of data, writing and editing of the manuscript.

Craig A. Mandato: Design of project, analysis of data, writing and editing of the manuscript.

Chapter 3: **"Adeno-associated virus-mediated delivery of C4RIP as a therapeutic agent to promote CNS regeneration"**

Stephan Ong Tone: Performed experiments and analysis pertaining to Figures 3, 4, 5a, 5c, 6 and 7. Analysis of data and writing of the chapter.

Ariel Wilson: Performed experiments and analysis pertaining to Figure 5a and 5b.

Alyson E. Fournier: Overall supervision of the project and editing of the chapter.

Adriana Di Polo: Supervised and designed the *in vivo* experiments.

Chapter 4: **"The development of TAT-C4RIP, a cell permeable RhoA-L-CRMP4 competitive antagonist"**

Stephan Ong Tone: Performed experiments and data analysis pertaining to Figures 2, 3, 4, 5 and 6. Wrote the chapter. Designed the strategy to generate cell permeable TAT mRFP and TAT C4RIP.

Samuel Montcalm: Designed the strategy to generate cell permeable TAT mRFP and TAT C4RIP and performed the purification of TAT mRFP and TAT C4RIP.

Alyson E. Fournier: Designed the strategy to generate cell permeable TAT mRFP and TAT C4RIP. Supervised the overall project and editing the chapter.

Yves Durocher: Designed the strategy to generate cell permeable TAT mRFP and TAT C4RIP. Supervised the purification of TAT mRFP and TAT C4RIP.

Adriana Di Polo: Supervised and designed the *in vivo* experiments.

CHAPTER 1

1 GENERAL INTRODUCTION

1.1 INTRODUCTION

Cells are dynamic structures that must be mechanically strong and resilient, while still labile enough to organize themselves correctly and adapt to their changing environment. They must be able to rearrange their internal compartment in response to internal and external signals, which results in complex and specialized functions. For example, during cell division the cell positions chromosomes, pulls them apart and separates into two daughter cells. During infections, white blood cells crawl and migrate along the endothelial lining of blood vessels patrolling for foreign bodies. Following an injury, fibroblasts and macrophages proliferate and invade into the injury site, respectively. During the formation of our nervous system, neurons extend processes from their cells bodies that grow long distances yet accurately innervate their designated targets. The ability of a cell to participate in these highly dynamic and regulated processes is dependent on a system of filaments called the cytoskeleton.

The cytoskeleton is composed of an interconnected network of actin and tubulin monomers that can assemble into microfilaments and microtubules, respectively, and associate with intermediate filaments. Regulation of the assembly and disassembly of these structures, as well as the interactions between them, are important determinants of how a single cell or a network of cells can perform a specific biological function. In this thesis, we attempt to elucidate the role of Collapsin Response Mediator Protein 4 (CRMP4), a cytosolic phosphoprotein that has been shown to regulate the cytoskeleton, in the biological processes of mitosis and nerve regeneration.

1.1.1 COLLAPSIN RESPONSE MEDIATOR PROTEINS (CRMPs)

CRMPs are cytosolic phosphoproteins that are highly expressed in the nervous system during development (Goshima, Nakamura et al. 1995; Wang and Strittmatter 1996; Gaetano, Matsuo et al. 1997; Byk, Ozon et al. 1998; Quinn, Gray et al. 1999; Quach, Duchemin et al. 2004). The CRMPs are homologs of UNC-33, a protein originally identified in Caenorhabditis elegans to be important for axon extension and guidance (Hedgecock, Culotti et al. 1985; Siddiqui and Culotti 1991). The CRMP family members have been previously identified as TOAD-64 (turned on after division, 64 kDa), Ulip (UNC-33 like protein), DRP (dihydropyrimidinase related protein) and TUC

(TOAD-64/Ulip/CRMP) (Goshima, Nakamura et al. 1995; Minturn, Fryer et al. 1995; Byk, Dobransky et al. 1996; Gaetano, Matsuo et al. 1997; Inatome, Tsujimura et al. 2000; Quinn, Chen et al. 2003). Although the CRMP sequences are similar to those of dihydropyrimidinase (DHPase), a liver enzyme involved with pyrimidine catabolism, they do not share any related enzymatic activity (Wang and Strittmatter 1997). The CRMP family is composed of five family members (CRMP1-5) in vertebrates, where CRMP1-4 share 70-80% amino acid homology while CRMP5 shares only 50-51% (Goshima, Nakamura et al. 1995; Minturn, Fryer et al. 1995; Byk, Dobransky et al. 1996; Gaetano, Matsuo et al. 1997; Wang and Strittmatter 1997; Inatome, Tsujimura et al. 2000; Quinn, Chen et al. 2003). Each CRMP allele produces two transcripts that differ in their amino terminal domains producing long (L-CRMP) and short (S-CRMP) isoforms that have been alternatively referred to as 'a' and 'b' isoforms (Fig. 1) (Quinn, Chen et al. 2003; Yuasa-Kawada, Suzuki et al. 2003; Alabed, Pool et al. 2007; Pan, Chao et al. 2009; Alabed, Pool et al. 2010). Although the CRMPs share a high degree of homology, their physiological roles in different biological processes are diverse and in certain cases have been shown to be antagonistic (Brot, Rogemond et al. 2010). Additionally, CRMPs can form multimers and hetero-oligomers with other CRMPs (Wang and Strittmatter 1997; Fukada, Watakabe et al. 2000; Inatome, Tsujimura et al. 2000; Yuasa-Kawada, Suzuki et al. 2003; Brot, Rogemond et al. 2010). However, the functional relevance of these CRMP multimers and hetero-oligomers has not been fully elucidated.

1.1.1.1 Expression pattern

1.1.1.1.1 Embryonic Central Nervous System

The CRMPs are highly expressed throughout the developing embryonic nervous system, with levels peaking in the first postnatal week and decreasing into adulthood (Wang and Strittmatter 1996; Fukada, Watakabe et al. 2000). While CRMP1, CRMP2, CRMP4 and CRMP5 are ubiquitously expressed throughout the embryonic day 15 rat brain, CRMP3 expression is restricted to the brain stem and spinal cord (Wang and Strittmatter 1996; Quinn, Gray et al. 1999; Fukada, Watakabe et al. 2000). CRMP4 is highly expressed during corticogenesis in postmitotic neurons as they migrate out of the ventricular zone into the developing cortical plate (Minturn, Geschwind et al. 1995).

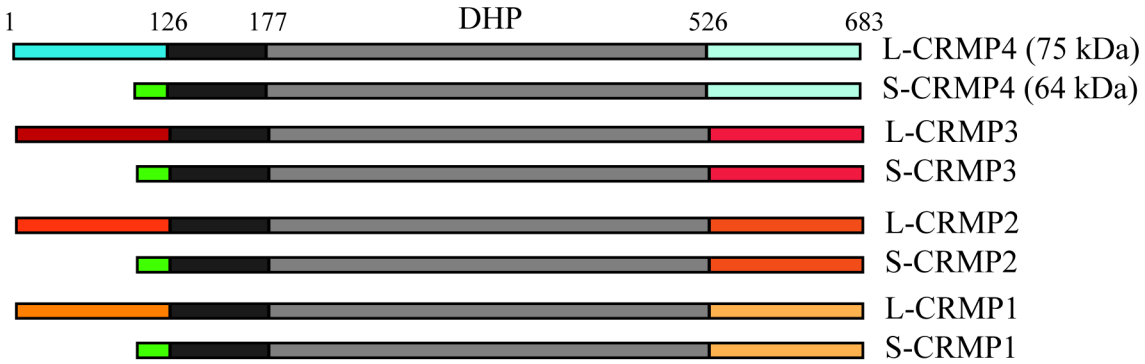

Chapter 1 - Figure 1. Schematic representation of the short and long CRMP family members.

CRMP1-4 family members contain 2 isoforms: long (L) and short (S). While CRMP1-4 contain a dihydropyrimidinase-like (DHP) domain, they do not have its enzymatic activity. CRMP4 consists of a C-terminus common domain and a unique N-terminus domain of 126 amino acids for the long isoform and 13 amino acids for the short isoform.

The expression of CRMP4 in early postmitotic neurons but not in mitotic cells of the ventricular zone has resulted in its use as a neuronal marker for cells that have committed to a neuronal fate (Minturn, Fryer et al. 1995). The CRMP5 expression pattern in the brain is very similar to CRMP4 (Fukada, Watakabe et al. 2000). In contrast to CRMP4, CRMP2 is expressed in both neurons and their progenitors in the developing cortical plate and the ventricular zone (Wang and Strittmatter 1996). All the CRMPs are expressed in the embryonic and post-natal retina, with strongest expression in the postmitotic retinal ganglion cells (Wang and Strittmatter 1996; Fukada, Watakabe et al. 2000). Additionally, CRMP1, CRMP2, CRMP3 and CRMP4 are also expressed in oligodendrocytes, but not astrocytes, during all stages from progenitor to the differentiated cell (Ricard, Stankoff et al. 2000). The expression profiles of the CRMPs in the developing brain indicate that CRMP1, CRMP4 and CRMP5 are similarly regulated, while CRMP2 and CRMP3 are not (Fukada, Watakabe et al. 2000).

1.1.1.1.2 Spinal Cord

The CRMPs are also expressed in the embryonic rat spinal cord with highest levels in the marginal zone during embryonic day 16 and day 20, a period a rapid axonal outgrowth (Geschwind, Kelly et al. 1996; Wang and Strittmatter 1996). At earlier embryonic day 13, CRMP1 and CRMP4 are expressed in the ventral horn while CRMP2 and CRMP3 are expressed throughout the spinal cord. However, by embryonic day 15 CRMP1, CRMP2 and CRMP4 are expressed through out the entire spinal cord, while CRMP3 is limited to the dorsal germinal matrix layer (Wang and Strittmatter 1996; Quinn, Gray et al. 1999). CRMP5 has a similar expression profile to CRMP1, CRMP2 and CRMP4 in the mouse embryonic day 17 spinal cord (Fukada, Watakabe et al. 2000).

1.1.1.1.3 Peripheral Nervous System

CRMP expression is not restricted to the CNS as DRG neurons show strong expression (Minturn, Fryer et al. 1995; Wang and Strittmatter 1996; Fukada, Watakabe et al. 2000; Quinn, Chen et al. 2003). CRMP4 is also regulated in neuronal cell lines in response to nerve growth factor (NGF) or retinoic acid, and in dorsal root ganglion (DRG) neurons by ciliary neurotrophic factor (CNTF) (Byk, Dobransky et al. 1996; Gaetano, Matsuo et al. 1997; Jang, Shin et al. 2010).

1.1.1.1.4 Adult Nervous System

Compared to the developing brain, CRMP expression levels are much lower in the adult brain, except for CRMP2 and CRMP3 levels (Wang and Strittmatter 1996; Charrier, Reibel et al. 2003; Cnops, Van de Plas et al. 2004; Bretin, Reibel et al. 2005). CRMP3 expression is primarily restricted to the hippocampus, pontine nuclei and olivary complex and granule cells of the cerebellum (Wang and Strittmatter 1996; Quach, Mosinger et al. 2000; Quach, Massicotte et al. 2008). CRMP4 expression in adult nervous tissue is highest in areas where ongoing neurogenesis occurs: the subventricular zone, the dentate granular layer of the hippocampus, the olfactory bulbs and the rostral migratory stream (Nacher, Rosell et al. 2000; Liu, Yang et al. 2003; Liu and Martin 2003). However, CRMP4 expression is also observed in other regions of the brain that are not associated with ongoing neurogenesis such as the cerebral cortex, hypothalamus, interpeduncular nucleus, median raphe, superior colliculus, granule cerebellar neurons and the visual cortex (Nacher, Rosell et al. 2000; Cnops, Van de Plas et al. 2004). Intriguingly, many of these regions have been shown to exhibit synaptic rearrangement and axonal outgrowth into adulthood (Nacher, Rosell et al. 2000).

CRMP1, CRMP2, CRMP3 and CRMP4 are all expressed in adult rat oligodendrocytes. While CRMP2 mRNA is detected in the majority of oligodendrocytes, CRMP2 protein is observed only in a subpopulation of oligodendrocytes increasing in a rostro-caudal gradient, where strongest expression is seen in the cerebellum, brainstem and spinal cord (Ricard, Stankoff et al. 2000).

1.1.1.1.5 Outside the Nervous System

CRMP expression levels outside the nervous system are relatively low, although expression is detected in the developing heart and muscles (Goshima, Nakamura et al. 1995; Byk, Dobransky et al. 1996). However, this expression pattern could be attributed to the neural constituents of these organs (Quinn, Gray et al. 1999). More recently, CRMPs expression has been associated with prostate, lung and glial cancer (Shih, Yang et al. 2001; Shih, Lee et al. 2003; Gao, Pang et al. 2010).

1.1.1.2 Diverse Roles of the CRMPs

1.1.1.2.1 Neural Development

The CRMPs were originally characterized as intracellular proteins that mediate collapsin/semaphorin signal transduction based on the finding that an antibody to CRMP2 inhibited growth cone collapse in chick DRG neurons in response to collapsin-1/sema D (Goshima, Nakamura et al. 1995). CRMP2 is also necessary for lysophosphatidic acid (LPA)-induced growth cone collapse (Arimura, Inagaki et al. 2000). Furthermore, CRMP1 can form a complex with the neuronal receptor PlexinA1 (PlexA1) to mediate Sema3A–induced axonal repulsion (Deo, Schmidt et al. 2004). However, the expression of CRMPs in neurons that do not respond to semaphorins, such as retinal ganglion cells, suggests that CRMPs participate in other semaphorin-independent processes (Takahashi, Nakamura et al. 1998). The expression pattern of CRMPs through out the nervous system suggests that CRMPs could play roles in neurogenesis, neuronal migration and axonal growth.

In addition to its role in growth cone collapse, CRMP2 also plays a role in axon/dendrite fate and neuronal polarity. Overexpression of CRMP2 in hippocampal neurons induces supernumerary axons while the expression of truncated CRMP2 mutants suppressed the formation of primary axon (Inagaki, Chihara et al. 2001; Yoshimura, Kawano et al. 2005; Yoshimura, Arimura et al. 2006). CRMP2 overexpression can also promote neurite outgrowth and branching (Hall, Brown et al. 2001; Fukata, Itoh et al. 2002). Similarly, L-CRMP4 overexpression, but not S-CRMP4, results in an increase in neurite length and branching in embryonic cortical neurons (Quinn, Chen et al. 2003). However, S-CRMP4 overexpression in neonatal hippocampal neurons does promote axon elongation (Cole, Causeret et al. 2006), while CRMP4 depletion in DRGs does not affect neurite outgrowth (Alabed, Pool et al. 2007). In mature cerebellar granule neurons overexpression of CRMP3 inhibits neurite outgrowth, whereas CRMP3 depletion promotes neurite outgrowth (Aylsworth, Jiang et al. 2009). Similarly, in N1E-115 cells, overexpression of CRMP5 inhibit neurite outgrowth, while CRMP5 depletion promotes outgrowth (Brot, Rogemond et al. 2010). In hippocampal neurons, CRMP5 regulates neuronal polarity through its ability to inhibit dendrite initiation but not axon initiation

(Brot, Rogemond et al. 2010). These observations indicate that the CRMP family participates in neurite outgrowth where CRMP2 and CRMP4 can promote neurite outgrowth while CRMP3 and CRMP5 inhibit neurite outgrowth.

The expression of CRMPs in oligodendrocytes suggests that they may play a role in oligodendrocyte function. The application of Sema3A conditioned medium to a purified mature oligodendrocyte culture results in oligodendrocytes that remain rounded and fail to extend processes (Ricard, Stankoff et al. 2000). These findings indicate that in addition to its role in regulating neurite outgrowth, CRMP may also participate in oligodendrocyte process outgrowth during myelination and remyelination.

The genetic deletion of CRMP1 and CRMP3 has provided significant insight into CRMP function. CRMP1 gene disruption in mice leads to an alteration of granule cell precursor proliferation, apoptosis and migration during postnatal cerebellar development, and a delay in Reelin-mediated neuronal migration in the cerebral cortex (Charrier, Mosinger et al. 2006; Yamashita, Uchida et al. 2006). CRMP1 gene disruption also results in an impairment in long-term potentiation (LTP) and spatial learning and memory, which has been attributed to improper neurite outgrowth (Su, Chien et al. 2007). CRMP3 gene disruption leads to abnormal dendrite and spine morphogenesis in the hippocampus but not the cerebral cortex (Quach, Massicotte et al. 2008). Further, no axonal abnormalities are observed in these mice suggesting that CRMP3 specifically regulates dendrite arborization and patterning in the hippocampus. These morphological abnormalities also result in a functional impairment in LTP (Quach, Massicotte et al. 2008).

1.1.1.2.2 Cellular Proliferation

CRMP2 has also been implicated in pathways that regulate the proliferation of non-neuronal cells (Tahimic, Tomimatsu et al. 2006). CRMP2 can be dephosphorylated in response to contact inhibition-induced quiescence and is hyperphosphorylated in tumor-derived cell lines and the tumor tissue (Tahimic, Tomimatsu et al. 2006). Although the CRMPs localize to the mitotic spindle and midbody in various cell lines, a functional role for CRMP in mitosis and cytokinesis has not been identified (Gu and Ihara 2000;

Fukata, Itoh et al. 2002; Yoshimura, Kawano et al. 2005; Tahimic, Tomimatsu et al. 2006).

1.1.1.2.3 Pathological Conditions

High CRMP expression levels have been implicated in neurological pathological conditions such as Alzheimer's disease and epilepsy (Czech, Yang et al. 2004; Good, Alapat et al. 2004; Uchida, Ohshima et al. 2005; Cole, Noble et al. 2007). The presence of CRMP5 autoantibodies in patient serum has also been associated with a variety of paraneoplastic neurological disorders, however it is not clear if these autoantibodies are merely a marker of a host immune response or are involved with the manifestation specific neurological symptoms (Antoine, Honnorat et al. 1993; Camdessanché, Lassablière et al. 2006; Honnorat, Cartalat-Carel et al. 2009). High titers of CRMP5 autoantibodies are associated with paraneoplastic optic neuropathy and vitritis in patients with small cell lung carcinoma (Thambisetty, Scherzer et al. 2001; Cross, Salomao et al. 2003; Czech, Yang et al. 2004; Margolin, Flint et al. 2008). CRMP3 and CRMP4 autoantibodies in patient serum have also been associated with limbic encephalitis and thymoma, when classical onconeural antibodies such as CRMP5 are not found (Knudsen, Bredholt et al. 2007).

More recently, CRMPs have been identified as metastatic and invasion suppressors in prostate, lung and glial cancer (Shih, Yang et al. 2001; Shih, Lee et al. 2003; Gao, Pang et al. 2010). These studies demonstrate that CRMP1 expression is inversely associated with the invasive potential of human lung adenocarcinoma cell lines and advanced disease stage in patients, and CRMP4 expression is inversely associated with lymph node metastasis of prostate cancer (Shih, Yang et al. 2001; Shih, Lee et al. 2003; Gao, Pang et al. 2010). Similarly, loss of CRMP1 promotes invasion of human glioblastoma multiform (GBM) cells expressing oncogenic mutations of EGFR (Mukherjee, DeSouza et al. 2009). Additionally, CRMP2 has also been identified as potential marker of colorectal carcinoma through a comparative analysis of cancer cell secretomes (Wu, Chen et al. 2008).

CRMP2 is expressed in T lymphocytes and is involved with both spontaneous and chemokine-induced T lymphocyte migration. The increased expression of CRMP2 in T

lymphocytes from patients suffering for neuroinflammatory disease suggests that a pathological role for CRMP2 in T lymphocytes may exist (Vincent, Collette et al. 2005; Vuaillat, Varrin-Doyer et al. 2007). The implication of CRMPs in pathological conditions that do not involve the nervous system provides evidence for a broader role for CRMPs in diverse physiological processes.

1.1.1.3 Mechanism of action

1.1.1.3.1 Microtubule Polymerization and Depolymerization

While all the CRMPs bind tubulin, they vary in their ability to promote microtubule polymerization (Fukata, Itoh et al. 2002). CRMP2 has the ability to bind tubulin heterodimers and promote microtubule assembly (Fukata, Itoh et al. 2002). It has been proposed that CRMP2 carries tubulin heterodimers to the assembly plus end of nucleation sites or growing microtubules and can then co-polymerize with tubulin heterodimers into microtubules (Fukata, Itoh et al. 2002). The expression of a CRMP2 mutant lacking its microtubule assembly domain inhibits axonal growth and branching in a dominant-negative manner (Fukata, Itoh et al. 2002). CRMP2 can also regulate tubulin transport in the growing axon of hippocampal neurons by linking tubulin and Kinesin-1. CRMP2 binds directly to kinesin light chain 1 and tubulin where it regulates soluble tubulin transport to the growth tip of the axon (Kimura, Watanabe et al. 2005). In contrast to CRMP2, both CRMP3 and CRMP5 have been shown to inhibit microtubule polymerization (Aylsworth, Jiang et al. 2009; Brot, Rogemond et al. 2010). CRMP5 forms a ternary complex with tubulin and MAP2, which can inhibit tubulin polymerization and neurite elongation (Brot, Rogemond et al. 2010). Interestingly, the co-expression of CRMP5 with CRMP2 antagonizes the ability of CRMP2 to promote neurite outgrowth (Brot, Rogemond et al. 2010). CRMP5 can bind microtubules and impair the ability of CRMP2 to transport tubulin and promote microtubule assembly. Therefore, CRMP5 plays a role in regulating neuronal polarity during brain development (Brot, Rogemond et al. 2010). While CRMP4 does bind directly to tubulin, how CRMP4 modulates tubulin and tubulin-based structures remains unknown (Fukata, Itoh et al. 2002; Rembutsu, Soutar et al. 2008).

1.1.1.3.2 F-actin Bundling

The CRMPs have the ability to bind actin. CRMP2 has been localized to actin within the growth cone but its role in regulating actin dynamics remains unknown (Arimura, Ménager et al. 2005). CRMP2 does not bind actin monomers directly and it has been proposed that CRMP2 interacts with Specifically Rac1-Associated protein (Sra-1), which directly interacts with filamentous-actin (F-actin) in growth cones (Arimura, Ménager et al. 2005). CRMP4 can bind directly to F-actin and organize F-actin into bundles (Rosslenbroich, Dai et al. 2005). CRMP4 localizes to F-actin within the lamellipodia of B35 neuroblastoma cells and DRG growth cones. CRMP4 can regulate the actin cytoskeleton, where overexpression of CRMP4 inhibits migration of B35 neuroblastoma cells, while CRMP4 depletion promotes migration (Rosslenbroich, Dai et al. 2005). Recently, CRMP4 has been identified as a metastasis-suppressor in prostate cancer through expression profiling of metastasis-associated proteins (Gao, Pang et al. 2010). CRMP4 expression is inversely associated with lymph node metastasis of prostate cancer. Overexpression of CRMP4 suppresses the invasive ability of prostate cancer cells and strongly inhibits tumor metastasis in an animal model (Gao, Pang et al. 2010). The overexpression of CRMP4 in these tumor cells results in a rounded cellular morphology that is deficient in filopodial protrusions (Gao, Pang et al. 2010). In contrast, in neuronal growth cones, L-CRMP4 overexpression promotes an actin-based phenotype where both filopodial length and branch numbers are increased (Alabed, Pool et al. 2007). Similarly, CRMP5 also localizes to the filopodia of growth cones, where CRMP5 overexpression promotes filopodia and growth cone formation, while CRMP5 knockdown blocks filopodia formation and leads to aberrant growth cone morphology (Hotta, Inatome et al. 2005). These findings demonstrate that CRMPs can regulate the actin cytoskeleton in non-neuronal and neuronal cells, and provide additional evidence for a broader role for CRMPs in cytoskeletal regulation.

1.1.1.3.3 Rho GTPase Modulator

The Rho family of small guanosine triphosphatases (GTPases) are molecular switches that regulate many cellular processes including adhesion, cell cycle progression, gene transcription and actin dynamics (Bishop and Hall 2000). The best-characterized

mammalian Rho GTPases, Rho, Rac and Cdc42 (cell division cycle 42), have all been shown to be important intracellular regulators of the cytoskeleton (Ridley and Hall 1992; Ridley, Paterson et al. 1992; Bishop and Hall 2000). Previous studies have linked extracellular ligands to signaling cascades that activate Rho, Rac or Cdc42 to promote the formation of actin stress fibers, lamellipodia or filopodia, respectively, in non-neuronal cells (Bishop and Hall 2000). Subsequent studies have demonstrated that the Rho GTPases also play key roles in regulating diverse biological processes that are dependent on the actin cytoskeleton such as cell migration, mitosis, cytokinesis, wound healing, nerve regeneration and axon extension (Luo, Jan et al. 1996; Drechsel, Hyman et al. 1997; Luo, Jan et al. 1997; Nobes and Hall 1999; Prokopenko, Saint et al. 2000; Ellezam, Dubreuil et al. 2002; Winton, Dubreuil et al. 2002; Dubreuil, Winton et al. 2003; Benink and Bement 2005; Dubreuil, Marklund et al. 2006; Narumiya and Yasuda 2006). We have previously demonstrated that L-CRMP4 can physically and functionally interact with RhoA to mediate neurite outgrowth inhibition in response to inhibitory CNS myelin (Alabed, Pool et al. 2007; Alabed, Pool et al. 2010). L-CRMP1 is also a negative regulator of Rho signaling since L-CRMP1 can interact with the kinase domain of Rho Kinase (ROCKII), a Rho effector, and inhibit its catalytic activity towards other substrates (Leung, Ng et al. 2002). Further, CRMP1 has been identified as a metastatic and invasion suppressor, where CRMP1 overexpression results in a decrease in Rac activity and increase in Rho activity. Consistent with these findings, CRMP1 knockdown results in an increase in Rac activity and a decrease in Rho activity. As a consequence of this shift in Rho GTPase activity, CRMP1 can promote actin contractility, focal adhesion formation and decrease invasive potential (Mukherjee, DeSouza et al. 2009)

The expression of CRMP2 in N1E-115 neuroblastoma cells can alter cellular morphology in response to active Rho GTPases. Normally, active RhoA signaling results in growth cone collapse and neurite retraction, while active Rac1 signaling leads to cell spreading, membrane ruffling and formation of neurites (Hall, Brown et al. 2001). The overexpression of CRMP2 switches RhoA and Rac1 morphology, where dominant active RhoA promotes neurite outgrowth and dominant active Rac1 induces collapse, in a ROCKII-dependent manner (Hall, Brown et al. 2001). The ability of CRMP2 to switch these responses indicates that CRMP2 is an important regulator of Rho GTPase signaling.

1.1.1.4 Post-translational regulation of CRMPs

1.1.1.4.1 Phosphorylation and Dephosphorylation

Numerous consensus phosphorylation sites, such as casein kinase II (CKII), protein kinase A (PKA), cyclin-dependent kinase (cdk) and MAP kinase (MAPK), were found in the CRMP sequences when they were first identified (Byk, Dobransky et al. 1996; Byk, Ozon et al. 1998). The regulation of CRMP phosphorylation was first demonstrated through NGF differentiation of PC12 cells where NGF treatment resulted in a decrease in the phosphorylated forms of the CRMPs (Byk, Dobransky et al. 1996; Byk, Ozon et al. 1998). Subsequent studies began to identify the kinases and phosphatases responsible for regulating CRMP phosphorylation levels. ROCKII can phosphorylate CRMP2 at Thr-555 in response to LPA-induced growth cone collapse in chick DRGs, and following myelin associated glycoprotein (MAG) or Nogo-66 treatment of rat cerebellar neurons (Arimura, Inagaki et al. 2000; Mimura, Yamagishi et al. 2006). Ca2+/calmodulin–dependent protein kinase II (CaMKII) can also phosphorylate CRMP2 at Thr-555 in response to ischemic neuronal damage (Hou, Jiang et al. 2009). CRMP2 is also phosphorylated at residues Thr-509, Ser-518 and Ser-522, and this phosphorylated form of CRMP2 has been localized to neurofibrillary tangles and plaque neurites in Alzheimer's disease brains (Gu, Hamajima et al. 2000; Cole, Astell et al. 2007). These residues were identified as a consensus site for glycogen synthase kinase-3β (GSK3β) (Yoshimura, Kawano et al. 2005).

GSK3 is a serine/threonine kinase originally identified as a kinase that phosphorylates glycogen synthase during glycogen metabolism. There are two isoforms of GSK3, GSK3α and GSK3β, which are ubiquitously expressed and constitutively active in cells. GSK3 is inactivated by phosphorylation at its amino-terminus serine (serine 21 for α or serine 9 for β) by several protein kinases such as protein kinase B (PKB, also called Akt), MAPK-activated protein kinase-1 (MAPKAP-K1, also called RSK) and p70 ribosomal S6 kinase-1 (Frame and Cohen 2001). Following an initial priming event on Ser-522 that is mediated by cyclin dependent kinase 5 (Cdk5), CRMP2 is sequentially phosphorylated by GSK3β on residues Ser-518, Thr-514, and Thr-509 (Cole, Knebel et al. 2004). These residues are conserved among CRMP1 and CRMP4,

but not CRMP3 (Cole, Causeret et al. 2006). Additionally, CRMP4, but not CRMP1 or CRMP2, can be primed by dual specificity tyrosine phosphorylation regulated kinase 2 (DYRK2) (Cole, Causeret et al. 2006). In GSK3β and GSK3α/β knockout mice, CRMP2 and CRMP4 phospho-Thr-509 levels are almost undetectable in cortex tissues, thus confirming that GSK3β phosphorylates CRMP2 and CRMP4 in vivo (Soutar, Kim et al. 2010). GSK3β phosphorylates CRMP2 at Thr-514 and decreases the ability of CRMP2 to interact with tubulin and promote axon elongation and branching (Yoshimura, Kawano et al. 2005). Intriguingly, overexpression of CRMP2 mutated at its cdk-5 priming site Ser-522 abrogates its ability to promote neurite formation and elongation in the human neuroblastoma cell line SH-SY5Y and in primary hippocampal neurons (Cole, Knebel et al. 2004). Further, the upregulation of protein phosphatase 2A (PP2A) can dephosphorylate CRMP2 to promote axon formation and elongation (Zhu, Zheng et al. 2010). These findings demonstrate that phosphorylation of the CRMPs regulates important physiological functions such as axon outgrowth.

Phosphorylation of CRMP2 inhibits its ability to bind tubulin heterodimers and promote microtubule assembly (Mimura, Yamagishi et al. 2006). Similarly, the ability of CRMP2 to bind tubulin heterodimers, microtubules and Numb is disrupted by phosphorylation by ROCKII (Arimura, Ménager et al. 2005). However, the ability of CRMP2 to bind actin is unaltered by ROCKII phosphorylation (Arimura, Ménager et al. 2005). Stimulation of cerebellar neurons with myelin associated inhibitors lead to the inactivation of GSK3β and the subsequent dephosphorylation of CRMP4 (Alabed, Pool et al. 2010). The decrease in CRMP4 phosphorylation status increases the ability of CRMP4 to complex with RhoA (Alabed, Pool et al. 2010). In one study to identify proteins that bind to CRMP2 and CRMP4 in a phosphorylation-dependent manner, different interacting proteins were identified (Rembutsu, Soutar et al. 2008). CRMP1, CRMP4 and adenine nucleotide translocator-1 (ANT-1) bound to dephosphorylated CRMP2 but not to phosphorylated CRMP2 (Rembutsu, Soutar et al. 2008). CRMP1, CRMP2, ANT-1, -2, and DYRK bound to dephosphorylated CRMP4 but not to phosphorylated CRMP4, while the peptidyl prolyl isomerase Pin1 bound only to phosphorylated CRMP4 (Rembutsu, Soutar et al. 2008). These results show that the

phosphorylation status of the CRMPs modulates their ability to bind to each other and to other interacting proteins.

1.1.1.4.2 Calpain-mediated Cleavage

All of the CRMPs are targeted for cleavage by ischemia-activated calpain following cerebral ischemia by middle cerebral artery occlusion in mice (Jiang, Kappler et al. 2007). Similarly, in an *in vivo* model of traumatic brain injury, CRMP1, CRMP2 and CRMP4 are found cleaved in the rat cortex and hippocampus following cortical impact injury (Zhang, Ottens et al. 2007). The application of NMDA or H_2O_2 to primary cortical neurons *in vitro* also results in calpain-mediated cleavage of all the CRMPs (Kowara, Chen et al. 2005; Bretin, Rogemond et al. 2006; Kowara, Moraleja et al. 2006; Kowara, Moraleja et al. 2008; Liu, Zhou et al. 2009). These studies demonstrate that CRMPs are important targets of activated calpain and that they may play a role in modulating ischemic neuronal death.

Despite the similarities in amino acid identity, it is surprising that calpain cleavage of the CRMPs does not occur at the same location within the protein sequence. CRMP1, CRMP2 and CRMP4 are cleaved by calpain near the carboxy terminus while CRMP3 is cleaved near the amino terminus (Liu, Zhou et al. 2009). The site of cleavage does not, however, determine the physiological consequence of cleavage as over-expression of the cleaved forms of CRMP3 and CRMP4, but not CRMP1 or CRMP2, induces neuronal apoptosis (Liu, Zhou et al. 2009). In particular, the calpain cleavage product of CRMP3 translocates to the nucleus and mediates axonal retraction and neuronal death following glutamate excitotoxicity *in vitro* and cerebral ischemia *in vivo* (Hou, Jiang et al. 2006). After nuclear translocation, the calpain cleavage CRMP3 product can associate with vimentin and cause nuclear condensation. However, this interaction with vimentin is not required for the calpain cleaved CRMP3 to inhibit neurite outgrowth or to promote neuronal death (Aylsworth, Jiang et al. 2009). In contrast, other calpain cleavage products of CRMPs, specifically CRMP2, may be responsible for the increased tolerance to ischemic injury that neurons acquire following an initial insult (Bretin, Rogemond et al. 2006). The calpain cleavage product of CRMP2 can reduce the amount of NR2B NMDA receptor subunit surface expression on neurons following

excitotoxic injury (Bretin, Rogemond et al. 2006). Interestingly, a similar C-terminal processed CRMP2 isoform is also observed during brain development and localizes to the nucleus through a nuclear localization signal (NLS) (Rogemond, Auger et al. 2008). This short CRMP2 isoform inhibits neurite outgrowth in neuroblastoma cells and cortical neurons, whereas full length CRMP2 promotes neurite outgrowth (Rogemond, Auger et al. 2008). This data supports CRMP2 cleavage in neurons as a part of normal brain development, in addition to its role in pathological processes. Together, these findings demonstrate that calpain cleavage of the CRMPs is a regulated process that can lead to different effects depending on the CRMP that is targeted.

1.2 CRMP4 as a Cytoskeletal Regulator during Mitosis and Nerve Regeneration

1.2.1 ROLE OF CRMPs IN MITOSIS

The CRMPs have been implicated in cellular proliferation in non-neuronal cells and have also been identified as metastatic and invasion suppressors in prostate, lung and glial cancer. These observations prompted us to investigate the role of CRMP4 in mitosis.

1.2.1.1 Introduction

The ability of a cell to accurately replicate its DNA (S phase), segregate its chromosomes and divide into two daughters cells (M phase) is a fundamental property that mitotic cells must possess. Failure to do so results in chromosome non-disjunction and aneuploidy (Decordier, Cundari et al. 2008). Therefore, chromosomal alignment and segregation are important well-controlled steps in mitosis.

Mitosis is divided into five main stages: prophase, prometaphase, metaphase, anaphase and telophase (Fig. 2). During prophase, the nuclear envelope breaks down, chromatin condenses into chromosomes, and centrosomes composed of two centrioles form two microtubule organizing centers (MTOC) at the spindle poles. Sister chromatids are attached at the centromere, where two kinetochores form and await for microtubules to bind to them. Microtubules emanating from the MTOC search for and bind kinetochores, where they position chromosomes at the equatorial plane located equidistant from the two centrosomes. Metaphase occurs when all the chromosomes align at the equatorial plane, also known as the metaphase plate. Importantly, for proper

chromosome segregation to occur all chromosomes must be aligned at the metaphase plate. To prevent premature progression to anaphase, a mitotic spindle checkpoint called the spindle assembly checkpoint (SAC) exists to ensure that every kinetochore is bound to a microtubule and that all chromosomes are aligned at the metaphase plate. Once this checkpoint is reached, the cell progress to anaphase, which is further divided into anaphase A and anaphase B. In Anaphase A chromosomes move towards the spindle poles, while during anaphase B the poles separate farther from each other. In telophase, the chromosomes decondense into chromatin, the nuclear envelope reforms and microtubules continue to lengthen and elongate the cell. At the end of telophase, cytokinesis occurs which divides the cell into two daughter cells.

1.2.1.2 The Mitotic Spindle Apparatus

The mitotic spindle machinery is composed of microtubules, MAPs and other regulatory proteins that are responsible for accurate chromosome alignment and segregation. During mitosis, there are two MTOC that form and organize microtubules into two asters that interact in an antiparallel array at the spindle midzone. The microtubule minus end is embedded in the spindle pole while the plus end is directed outwards. These spindle microtubules can either capture sister chromatids by their kinetochores and direct them to the metaphase plate (kinetochore microtubules), interact with microtubules from the other spindle pole (interpolar microtubules), or interact with the cortex (astral microtubules) to help position the spindle poles and the cleavage furrow (Lutz, Hamaguchi et al. 1988; Gundersen 2002; Rodriguez, Schaefer et al. 2003). These microtubule interactions are largely mediated through motor proteins such as kinesin and dynein and other regulatory proteins. Although the majority of actin is associated with the cortex during mitosis, there is some actin that localizes to mitotic spindle microtubules (Silverman-Gavrila and Forer 2000). It has been proposed that the role of this spindle actin, in association with myosin, is to induce tubulin flux from the kinetochore to the spindle pole (Silverman-Gavrila and Forer 2000). Disruption of mitotic spindle machinery results in a dysregulated mitotic spindle that yields misaligned chromosomes. Perturbation of mitotic microtubule dynamics with the microtubule-stabilizing drug taxol results in long astral tubules in cells, along with misaligned chromosomes located at the

ends of these astral tubules (Ault, DeMarco et al. 1991; Jordan, Wendell et al. 1996; Wakefield, Stephens et al. 2003). Depolymerizing microtubules with nocodazole results in a reversible prometaphase arrest (Centonze and Borisy 1991). Together, these findings highlight the importance of dynamic microtubules during mitosis since global stabilization or depolymerization of microtubules leads to defects in chromosomal alignment or mitotic arrest, respectively. Furthermore, the application of actin depolymerization drugs such as latrunculin B and cytochalasin D disrupts spindle actin and reduces tubulin flux from the kinetochore to the spindle pole, while the F-actin stabilization drug jasplakinolide has no effect (Silverman-Gavrila and Forer 2000). The application of a myosin ATPase inhibitor 2,3-butanedione 2-monoxime also results in a similar phenotype. Therefore, spindle actin is composed of stable F-actin and is necessary for the generation of actomyosin forces that induce tubulin flux from the kinetochore to the spindle pole (Silverman-Gavrila and Forer 2000).

1.2.1.3 Regulators of Chromosome Alignment and mitotic progression

1.2.1.3.1 Chromosome Alignment

Proper chromosomal segregation during mitosis requires the coordination of various processes such as accurate chromosome alignment to the metaphase plate, maturation of correct microtubule-kinetochore attachments, correction of erroneous attachments and the silencing of the SAC (Manning, Bakhoum et al. 2010). Microtubules originating from centrosomes undergo a process known as search and capture, where the plus ends of microtubules are highly dynamic and exploratory until they bind to a kinetochore. Once a kinetochore is bound to a microtubule, an increasing number of microtubules also bind to form a kinetochore fiber (McEwen, Heagle et al. 1997; Kapoor and Compton 2002). For normal segregation to occur, a chromosome must bi-orient through the attachment of sister kinetochores with microtubules originating from opposite spindle poles. Incorrect microtubule-kinetochore attachments do occur, such as monotelic, merotelic or syntelic attachments, but correction mechanisms exist to ensure that proper amphitelic attachments (bi-orientation) form. Monotelic attachments, where only one sister kinetochore is attached to microtubules from one spindle pole, are part of the normal progression to bi-orientation. The presence of an unattached kinetochore is a

potent checkpoint signal where levels of mitotic-arrest deficient homologue-2 (MAD2) and BubR1 remain high and maintain the SAC (Cimini and Degrassi 2005; Musacchio and Salmon 2007). The presence of merotelic attachments, where a kinetochore is bound by microtubules from both spindle poles, activates a correction mechanism that is based on Aurora B kinase (Cimini and Degrassi 2005; Musacchio and Salmon 2007). Syntelic attachments, where both kinetochores are bound to microtubules originating from the same spindle pole, are also corrected by an Aurora B kinase mechanism (Tanaka, Rachidi et al. 2002; Cimini and Degrassi 2005; Musacchio and Salmon 2007). Therefore, the progression from metaphase to anaphase in the presence of misaligned or mal-attached chromosomes indicates that a component of correction mechanism is compromised.

The regulation of mitotic spindle dynamics and chromosomal alignment has been shown to be partly regulated by GSK3 (Frame and Cohen 2001; Wakefield, Stephens et al. 2003; Cohen and Goedert 2004; Tighe, Ray-Sinha et al. 2007). Reports that GSK3β plays a role in regulating microtubule dynamics during interphase provide evidence that GSK3 may also regulate spindle microtubules (Ciani, Krylova et al. 2004). GSK3β can decrease microtubule stability through phosphorylation of MAPs such as Tau, MAP1B and MAP2C (Wang, Wu et al. 1998; Goold, Owen et al. 1999; Ciani, Krylova et al. 2004). During mitosis, GSK3 localizes along spindle microtubules and at the centrosomes (Wakefield, Stephens et al. 2003). Repressing GSK3 function with GSK3 inhibitors (lithium chloride, SB-216763, SB-415286, AR-A014418, I-Azakenpaullone or CHIR99021) or GSK3β RNA interference alters spindle morphology through an increase in spindle length and a weakening of the spindle midzone (Wakefield, Stephens et al. 2003; Tighe, Ray-Sinha et al. 2007). GSK3 inhibition also results in defects in chromosomal alignment, where syntelic and monotelic attachments predominate (Tighe, Ray-Sinha et al. 2007). Although GSK3 inhibition delays mitotic progression, anaphase onset eventually occurs in the presence of misaligned chromosomes resulting in chromosome non-disjunction (Tighe, Ray-Sinha et al. 2007). In mouse preimplantation embryos, GSK3 inhibition delays mitotic cell cycle progression and results in defects in chromosome alignment and cytokinesis (Acevedo, Wang et al. 2007). While the importance of GSK3 as a mitotic kinase has been recognized, the physiological substrates that mediate these GSK3-dependent effects during mitosis have yet to be fully identified.

Aurora-A-interacting protein (AIP), a negative regulator of Aurora-A, is a mitotic target of GSK3 (Fumoto, Lee et al. 2008). GSK3 interacts with AIP to regulate the degradation of Aurora A in early mitotic phase. In Chapter 2, we demonstrate that GSK3 regulates mitotic chromosomal alignment through CRMP4.

1.2.1.3.2 Spindle Assembly Checkpoint

Another regulatory mechanism that exists to ensure that proper chromosomal alignment occurs before mitotic progression can continue is the presence of the spindle assembly checkpoint (SAC). The SAC inhibits metaphase progression to anaphase by negatively regulating the anaphase-promoting complex (APC, also known as the cyclosome) through CDC20 inhibition (Musacchio and Salmon 2007). APC is an ubiquitin ligase that targets cyclin B and securin to the proteasome through ubiquitination. The proteolysis of cyclin B inactivates the mitotic kinase CDK1 and activates mitotic progression. Securin is an inhibitor of the protease separase, which cleaves the cohesin complex that binds sister chromatids together (Musacchio and Salmon 2007). The presence of unattached kinetochores during prophase and prometaphase results in high SAC levels that prevent anaphase onset. As chromosomes align at the metaphase plate, the levels of SAC decrease until all of chromosomes are bi-oriented with proper kinetochore microtubule attachments, which result in the inactivation of the checkpoint and the onset of anaphase.

In addition to proper kinetochore microtubule attachments, the SAC also monitors tension between sister kinetochores (Nicklas, Ward et al. 1995; Musacchio and Salmon 2007). Bi-orientation of sister kinetochores results in an increase in kinetochore tension that leads to an increase in kinetochore-to-kinetochore distance and stretching of centromeric chromatin (Nicklas, Ward et al. 1995; Nicklas 1997). However, tension monitoring alone is not sufficient to detect all incorrect attachments since merotelic attachments are attached to opposite spindle poles. Monotelic and syntelic attachments are still detected since they are attached to only one spindle pole and fail to generate enough tension.

1.2.1.3.3 Rho GTPases as Mitotic Regulators

Although the importance of Rho GTPases during the process of cytokinesis has been well recognized for some time, it was believed that they did not participate in mitosis because a Rho inhibitor, C3 exoenzyme, did not inhibit mitosis (Narumiya and Yasuda 2006). Furthermore, it was commonly believed that microtubules and actin participated in separate stages of cell division, mitosis and cytokinesis, respectively (Narumiya and Yasuda 2006). However, several studies now demonstrate that the Rho GTPases do participate in mitosis and that actin-microtubule interactions are important for both mitosis and cytokinesis. The inactivation of all members of the Rho subfamily of GTPases, but not other GTPases, with toxin B from Clostridium difficile arrests cells in prometaphase with disrupted microtubule-kinetochore attachments and also leads to an increase in chromosome misalignment (Yasuda, Oceguera-Yanez et al. 2004). The expression of a dominant negative mutant of Cdc42 (N17-Cdc42) or the depletion of its effector mDia3 phenocopies toxin B treatment. Therefore, it has been proposed that a Cdc42-mDia3 pathway regulates spindle microtubule-kinetochore attachments and mitotic progression (Tatsumoto, Sakata et al. 2003; Narumiya, Oceguera-Yanez et al. 2004; Yasuda, Oceguera-Yanez et al. 2004; Oceguera-Yanez, Kimura et al. 2005; Narumiya and Yasuda 2006). While these studies demonstrate a role for Cdc42 during mitosis, other studies have demonstrated a role for RhoA in regulating microtubule dynamics during mitosis (Narumiya and Yasuda 2006). Lfc, a Rho GEF, associates with microtubules during interphase and on spindle microtubules during mitosis (Benais-Pont, Punn et al. 2003; Bakal, Finan et al. 2005). Neutralization of Lfc with a function-blocking antibody or Lfc depletion with RNA interference results in a decrease in spindle length, increase in chromosome missegregation and an increase in the cells arrested in prophase/prometaphase (Benais-Pont, Punn et al. 2003; Bakal, Finan et al. 2005). Further, neutralization of mDia1 with a function-blocking antibody phenocopies Lfc neutralization/depletion. This supports a model where active RhoA and mDia1 can regulate microtubule attachment to kinetochores and to the cortex, and in turn influence mitotic progression (Kodama, Karakesisoglou et al. 2003; Wen, Eng et al. 2004; Bakal, Finan et al. 2005; Narumiya and Yasuda 2006). Further, it has also been shown that the actomyosin contractility can regulate centrosome separation and positioning after nuclear envelope breakdown and that these events involve ROCK activity (Rosenblatt, Cramer et

al. 2004). Application of latrunculin A, blebbistatin or the ROCK inhibitor Y-27632 alters spindle morphology and increases chromosome misalignment (Rosenblatt, Cramer et al. 2004).

1.2.1.4 Why CRMPs are ideally positioned to regulate mitosis

The assembly and regulation of the mitotic spindle is a critical aspect of mitosis. In Chapter 2, we investigate the role of CRMP4 during mitosis based on previous studies that have demonstrated that (1) CRMPs can interact directly with tubulin and localize to the mitotic spindle (2) CRMP4 can interact directly with actin and promote actin-based phenotypes, (3) CRMP4 can physically and functionally interact with RhoA and (4) CRMP4 is a physiological target of the mitotic kinase GSK3β (Fukata, Itoh et al. 2002; Rosslenbroich, Dai et al. 2005; Cole, Causeret et al. 2006; Alabed, Pool et al. 2007; Rembutsu, Soutar et al. 2008; Alabed, Pool et al. 2010; Soutar, Kim et al. 2010).

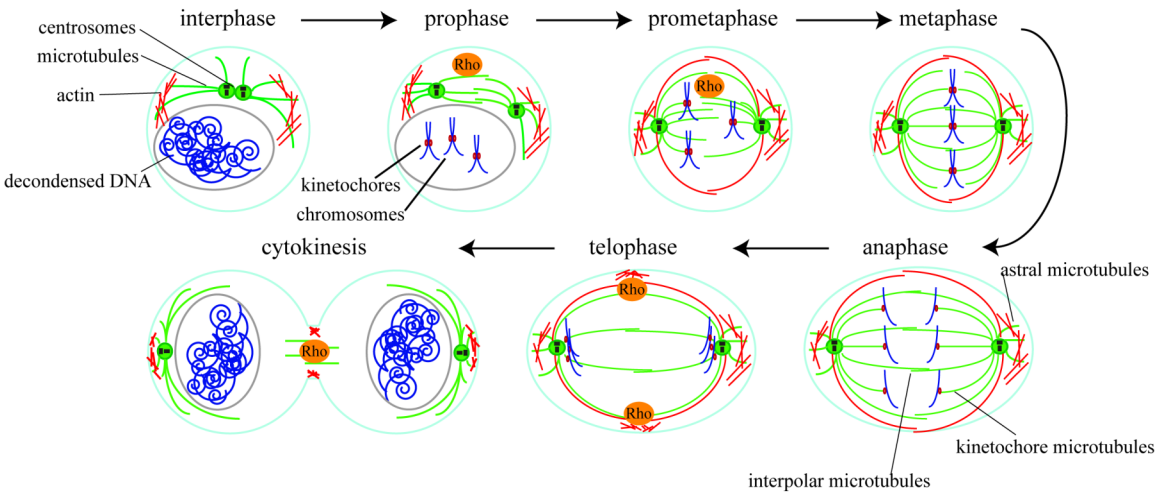

Chapter 1 - Figure 2. Schematic representation of cell division.

Mitosis is divided into five main stages: prophase, prometaphase, metaphase, anaphase and telophase. During mitotic progression, decondensed DNA condense into chromosomes and are positioned to the equatorial by microtubules. This process is also dependent on F-actin since the disruption of spindle actin reduces tubulin flux from the kinetochore to the spindle pole (Silverman-Gavrila and Forer 2000). During prophase and prometaphase, the activation of Rho through the Rho GEF, Lfc, regulates microtubule dynamics (Benais-Pont, Punn et al. 2003; Bakal, Finan et al. 2005). Disruption of Lfc function leads to a decrease in spindle length, an increase in chromosome missegregation and an increase in the cells arrested in prophase/prometaphase (Benais-Pont, Punn et al. 2003; Bakal, Finan et al. 2005).

1.2.2 ROLE OF CRMPs IN NERVE REGENERATION

The CRMPs have been largely characterized in the context of neural development. However, despite their strong expression pattern in the nervous system, not many studies have investigated the roles of CRMPs during nerve regeneration. We have previously identified CRMP4 as key intracellular neuronal protein that mediates neurite outgrowth inhibition in response to myelin and aggrecan (Alabed, Pool et al. 2007). These *in vitro* findings prompted us to further investigate the role of CRMP4 in nerve regeneration.

1.2.2.1 Introduction

The inability of the adult central nervous system (CNS) to regenerate following traumatic injuries, such as spinal cord injury (SCI), stroke and neurodegenerative diseases, results in devastating clinical consequences. Over the past 30 years, much progress has been made in the identification of the molecular components and signaling cascades involved with nerve injury and regeneration. Damage to neurons located in the adult CNS often leads to persistent deficits due to the inability of axons to regenerate and reform functional connections following injury. In contrast to the CNS, neurons located in the PNS can regrow their transected axons over long distances and reform functional synapses. Ramón y Cajal observed that following injury, the terminal ends of axons swelled up and would not regenerate. He proposed that these "dystrophic endballs" no longer had the capacity to regenerate and that the CNS environment was limiting their regenerative potential. Further evidence to support Ramón y Cajal's hypothesis was provided by studies by Aguayo and colleagues, in which they demonstrated that the CNS and PNS environments were quite different in their ability to promote nerve regeneration. They showed that neurons located in the CNS, which normally do not regenerate following injury, have the ability to regenerate their damaged axons into a sciatic nerve graft (Richardson, McGuinness et al. 1980). When a sciatic nerve was grafted to the brain or spinal cord, long distance regeneration was observed into the graft, with the regenerating axons stopping abruptly when they re-encountered the CNS environment (David and Aguayo 1981). Subsequent studies began identifying the molecular components of inhibitory CNS myelin such as Nogo, MAG (Myelin-assciated

glycoprotein), and OMgp (Oligodendrocyte myelin glycoprotein). In addition, the glial scar composed of reactive astrocytes and inhibitory chondroitin sulfate proteogylcans (CSPGs) can form a physical and chemical barrier to regeneration. More recently, embryonic chemorepulsive guidance molecules such as ephrin B3, Sema4D and Netrin-1 are thought to contribute to the inhibition of regeneration (Yiu and He 2006).

Both CSPGs and MAIs contribute to the heterogeneous inhibitory environment found in CNS myelin that limits nerve regeneration. These inhibitory molecules signal through receptor complexes located on the neuronal membrane to mediate myelin inhibition (Yiu and He 2006). Despite the diversity of ligands and receptor complexes, intracellular signaling converges to activate the RhoA pathway to mediate neurite outgrowth inhibition via its effects on the cytoskeleton. One approach to promote nerve regeneration following injury has been to target and neutralize inhibitory molecules in extracellular environment or on the neuronal plasma membrane. An alternative approach has been to inactivate the intracellular molecule RhoA and its downstream effector Rho kinase (Lehmann, Fournier et al. 1999; Winton, Dubreuil et al. 2002; Dubreuil, Winton et al. 2003; Fournier, Takizawa et al. 2003; McKerracher and Higuchi 2006; Lord-Fontaine, Yang et al. 2008). Currently, clinical trials investigating the neuroprotective and neuroregenerative properties of the Rho antagonist, Cethrin®, in patients with thoracic and cervical SCI are underway. However, the ubiquitous expression of RhoA and its involvement in multiple physiological processes in many cells may limit its role as a therapeutic agent due to deleterious side effects. Therefore, to develop a more specific therapeutic agent to promote functional recovery following CNS injury, a greater understanding of the basic mechanisms underlying neuronal injury is needed.

1.2.2.2 Receptor Mechanisms

MAIs are extracellular ligands for receptors located at the neuronal membrane. The MAIs Nogo, MAG and OMgp signal through a tri-partite receptor complex composed of NgR1 (Nogo-66 receptor) (Fournier, GrandPre et al. 2001) or PirB (Paired immunoglobulin-like receptor B) (Atwal, Pinkston-Gosse et al. 2008), LINGO1 (LRR and Ig containing Nogo Receptor interacting protein) (Mi, Lee et al. 2004) and either p75 neurotrophin receptor (p75NTR) (Wang, Kim et al. 2002; Wong, Henley et al. 2002;

Yamashita, Higuchi et al. 2002) or TROY (p75 low affinity neurotrophin receptor or Tumor necrosis factor superfamily member 19 or Taj) (Park, Yiu et al. 2005; Shao, Browning et al. 2005). Other inhibitory molecules such as ephrin-B3, netrin-1 and Sema4D signal through their respective receptors, ephA4, DCC/UNC5 and CD72 (Moreau-Fauvarque, Kumanogoh et al. 2003; Benson, Romero et al. 2005; Löw, Culbertson et al. 2008). CSPGs signal through the neural receptor PTPσ to mediate their inhibitory effects on nerve regeneration (Shen, Tenney et al. 2009).

1.2.2.3 The Growth Cone

During development, neurons project their axons to innervate specific targets. This is a finely tuned process that relies on the ability of the growth cone to integrate information from multiple environmental guidance cues to produce one functional output. The growth cone, a highly motile fan-shaped structure located at the tip of a growing axon, is continually sampling its extracellular environment by extending and retracting its plasma membrane through filopodia and lamellipodia formation and extension. The highly dynamic nature of the growth cone results from specific cytoskeletal changes in actin and microtubules at discrete locations within the growth cone. The peripheral domain of the growth cone is composed primarily of actin-based filopodia and lamellipodia, while the central domain is composed primarily of microtubules. Microtubules originating from the central domain can extend into the peripheral domain, where they play an important role in growth cone steering (Dent, Gupton et al. 2010). The transition domain, located between the peripheral and central domain, is composed of an actin network associated with myosin-2 that generates retrograde actin flow. Receptors located at the growth cone plasma membrane are responsible for generating intracellular signaling cascades activated by extracellular ligand binding. Therefore, extracellular molecules bind to neuronal receptors located at the growth cone to activate intracellular signaling cascades that converge onto proteins that regulate the cytoskeleton and ultimately direct the growth cone to its proper target.

For the regeneration of transected axons to occur following axotomy, the proximal end of the axon must transform into a competent growth cone (Spira, Oren et al. 2003; Sahly, Khoutorsky et al. 2006; Erez, Malkinson et al. 2007; Erez and Spira 2008).

This process requires appropriately controlled microtubule restructuring, vesicle accumulation and actin polymerization (Sahly, Khoutorsky et al. 2006). Perturbation of microtubules with nocodozale inhibits the formation of the microtubule compartment but does not affect actin-based lamellipodia formation. Similarly, inhibition of actin polymerization with cytochalasin D or jasplakinolide disrupts lamellipodia formation but not the microtubule compartment and vesicle accumulation. Thus, while it appears that these processes can occur independently of each other, a competent growth cone does not form and the axon does not regenerate if one of these processes is disrupted (Sahly, Khoutorsky et al. 2006). In the CNS, transected axons form swellings at their axon tips known as retraction bulbs, which are the nongrowing equivalents of growth cones (Ertürk, Hellal et al. 2007). In contrast, in the PNS transected axons readily form growth cones and maintain the capacity to regenerate. These differences in morphology and regenerative capacity have been largely attributed to the underlying microtubule network, where competent growth cones have tightly bundled microtubules and retraction bulbs have a disorganized microtubule network (Ertürk, Hellal et al. 2007). The *in vitro* and *in vivo* administration of pharmacological agents that disrupt microtubules, such as nocodazole, transforms growth cones into retraction bulbs in the PNS following injury. Consistent with these findings, pharmacological agents that stabilize microtubules, such as taxol, prevent transected axon in the CNS from forming retraction bulbs, decrease axonal degeneration and promote neurite outgrowth following injury (Ertürk, Hellal et al. 2007). Therefore, strategies aimed at microtubule stabilization may promote competent growth cone formation and subsequently increase the regenerative capacity of transected axons in the CNS following injury (Hellal, Hurtado et al. 2011).

1.2.2.4 RhoA GTPase and its downstream effectors in nerve regeneration

Following CNS injury, damaged axons are exposed to an unfavorable heterogeneous environment composed of multiple MAIs and inhibitory components of the glial scar. Neutralizing only one of these specific inhibitory components may be limited as a strategy to promote nerve regeneration since multiple layers of inhibition exists. Therefore, targeting an intracellular pathway common to these multiple sources of inhibition could be an effective approach to circumvent the heterogeneous inhibitory

environment at the CNS lesion site. So far, the best-characterized intracellular pathway involves the activation of RhoA and its downstream effector Rho-associated kinase (ROCK) (Jin and Strittmatter 1997; Lehmann, Fournier et al. 1999; Borisoff, Chan et al. 2003; Fournier, Takizawa et al. 2003).

RhoA activation in non-neuronal cells results in the formation of contractile actin-myosin filaments (stress fibers) and associated focal adhesion complexes (Ridley and Hall 1992). In neuronal growth cones, RhoA has been implicated in the rearrangement of the cytoskeleton in response to guidance cues such as Sema4D (Aurandt, Vikis et al. 2002; Perrot, Vazquez-Prado et al. 2002; Swiercz, Kuner et al. 2002). Further, RhoA activation in neuronal cells has been associated with neurite retraction and cell rounding. An increase in RhoA activation is observed in neurons that are plated on an inhibitory myelin substrate (Niederöst, Oertle et al. 2002; Winton, Dubreuil et al. 2002; Fournier, Takizawa et al. 2003). The inactivation of Rho using C3 transferase toxin from Clostridium botulinum, which ADP ribosylates and inactivates RhoA, RhoB and RhoC isoforms, is sufficient to overcome growth inhibition on an inhibitory myelin substrate (Lehmann, Fournier et al. 1999). Since Rho activation in neuronal cell is observed following exposure to most of the inhibitory components of the CNS, it was expected that Rho activation also occurred in neurons following SCI (McKerracher and Higuchi 2006). *In vivo* Rho activation occurs in both white matter and grey matter, where Rho activation is localized to both cell bodies and axons (Madura, Yamashita et al. 2004). Further, *in vivo* Rho activation is also seen through a pull-down assay using the Rho binding domain of Rhotekin in neurons following SCI in both rats and mice (Dubreuil, Winton et al. 2003). In addition to neurons, increased Rho activation following SCI has also been detected in glial cells such as astrocytes and oligodendrocytes (Dubreuil, Winton et al. 2003).

Intriguingly, inhibitory molecules such as CSPGs that do not signal through the NgR1 receptor complex also lead to the intracellular activation of RhoA (Schweigreiter, Walmsley et al. 2004). Further, the application of the RhoA inhibitor C3 transferase or ROCK inhibitors Y-27632 and HA1077 (Fasudil hydrochloride) increase neurite outgrowth on CSPG substrates (Borisoff, Chan et al. 2003; Monnier, Sierra et al. 2003; Lingor, Teusch et al. 2007). Recent evidence supports PKC as a convergent mediator of

RhoA activation following stimulation with either MAIs or CSPGs (Sivasankaran, Pei et al. 2004). EphrinB3 and netrin-1 can also activate RhoA through their receptors, ephA4 and DCC, respectively (Sahin, Greer et al. 2005; Moore, Correia et al. 2008). The convergence of signaling pathways from diverse inhibitory molecules that prevent nerve regeneration supports the strategy to target RhoA activation as a therapeutic treatment for SCI.

1.2.2.4.1 RhoA effectors and Cytoskeleton Remodeling

RhoA activation signals through downstream effectors, such as ROCK, to modulate the cytoskeleton and influence neurite outgrowth. Antagonizing ROCK signaling with the pharmacological inhibitors Y-27632 and HA1077, or with a dominant-negative form of ROCK, attenuates myelin-induced growth cone collapse and neurite outgrowth inhibition (Hara, Takayasu et al. 2000; Dergham, Ellezam et al. 2002; Borisoff, Chan et al. 2003; Fournier, Takizawa et al. 2003; Alabed, Grados-Munro et al. 2006). ROCKII is activated in response to the Nogo and enhances phosphorylation of MLCII, an important signaling component for growth cone collapse and neurite outgrowth inhibition (Alabed, Grados-Munro et al. 2006; Kubo, Endo et al. 2008). Further, following spinal cord injury MLCII is phosphorylated in a ROCK-dependent manner in damaged axons (Kubo, Endo et al. 2008). These findings support an inhibitory signaling cascade whereby RhoA activation promotes ROCK-mediated phosphorylation of MLCII to cause cytoskeletal rearrangements in response to inhibitory molecules.

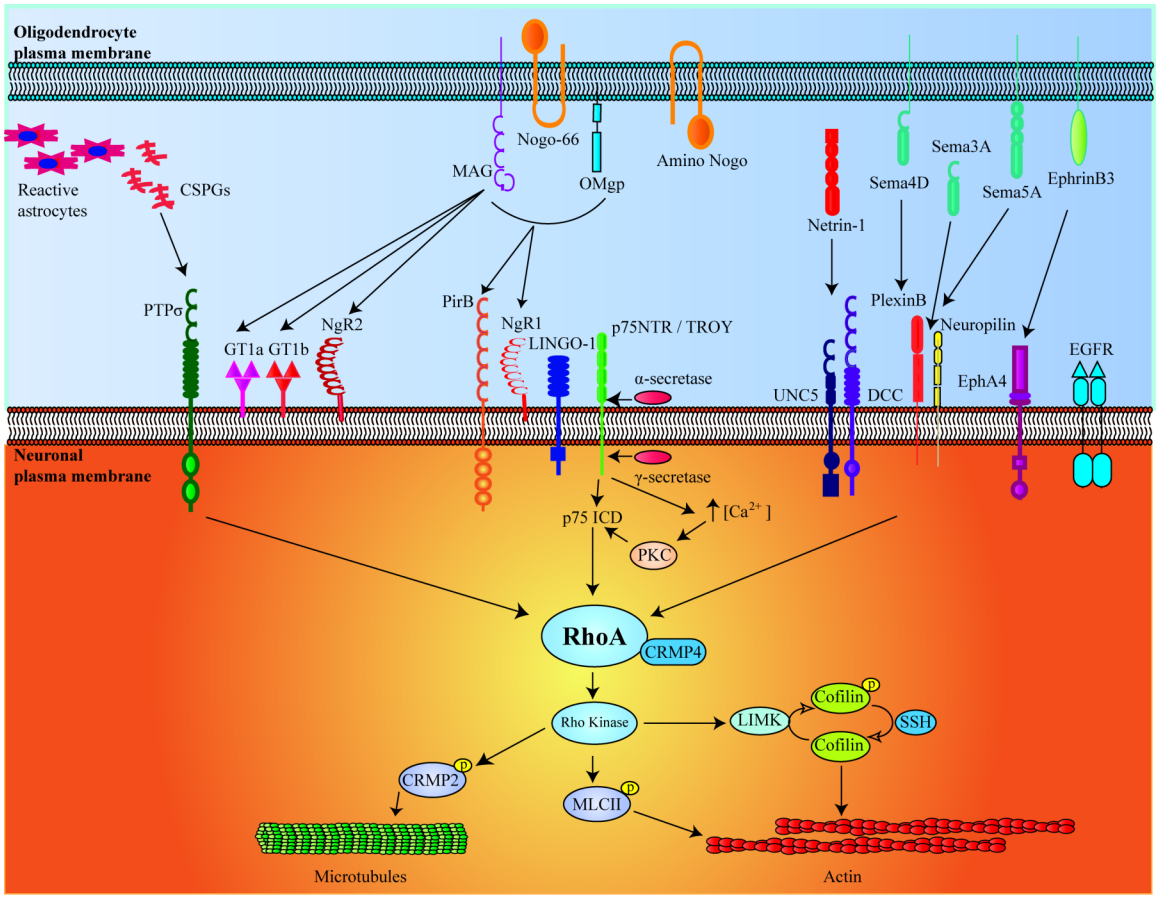

Chapter 1 - Figure 3. Schematic representation of the ligands and receptors that participate in CNS growth inhibition.

Myelin associated inhibitors (MAG, Nogo-66 and OMgp), CSPGs, and other inhibitory molecules (Netrin-1, Sema4D, Sema3A, Sema5A and EphrinB3) signal through receptor complexes at the neuronal plasma membrane to stimulate growth inhibition. Inside neurons, the growth inhibitory signals converge to RhoA, a master switch that regulates the growth cone cytoskeleton in motility. RhoA effectors such as Rho Kinase and CRMP4 are important in mediating these effects. Adapted from *Essentials of Spinal Cord Injury: Targeting Rho inactivation to promote regeneration and treat spinal cord injury: Bench to bedside translational medicine* (In press) by L. McKerracher, M. Fehlings, A.E. Fournier and S. Ong Tone, 2010, NY: Thieme Medical Publishers.

1.2.2.5 The Role of CRMPs in nerve regeneration

Although the role of CRMPs in embryonic development of the nervous system and neuronal polarity has been studied, the role of CRMPs in nerve regeneration is still unknown. In a rat hypoglossal nerve injury model CRMP2a mRNA levels were increased, while CRMP3a and CRMP4a mRNA levels were unchanged following axotomy (Suzuki, Nakagomi et al. 2003). Overexpression of CRMP2 through an adenoviral vector accelerates hypoglossal nerve regeneration following injury. This study demonstrates that CRMP2 has potent neurite elongation activity in an *in vivo* model of PNS injury. The role of CRMP3 in nerve regeneration has not been extensively studied, although the ability of CRMP3 to inhibit microtubule polymerization and neurite outgrowth *in vitro* suggest that CRMP3 is most likely a negative regulator of nerve regeneration. In another PNS injury model, CRMP4 mRNA and protein expression were increased in both adult sciatic motor neurons and DRG neurons that were regenerating following a sciatic nerve lesion (Minturn, Fryer et al. 1995; Jang, Shin et al. 2010). Furthermore, an increase in CRMP4 protein expression is observed in the peripheral axon following the injury (Jang, Shin et al. 2010).

With respect to CNS injury, the CRMP family has also been implicated in the signaling cascade activated in response to MAIs and CSPGs (Mimura, Yamagishi et al. 2006; Alabed, Pool et al. 2007; Alabed, Pool et al. 2010). It has been shown that both *in vitro* treatment of postnatal cerebellar neurons with two components of CNS myelin, MAG and Nogo-66, and *in vivo* spinal cord injury in the adult rat, result in ROCK-dependent phosphorylation of CRMP2 (Mimura, Yamagishi et al. 2006). Further, siRNA-mediated CRMP-2 protein knockdown mimics the inhibitory effect of MAG on neurite outgrowth. Following SCI, microtubule density decreases in a ROCK-dependent manner, which is consistent with CRMP-2 function in promoting microtubule assembly (Mimura, Yamagishi et al. 2006). Consistent with its role in PNS regeneration, overexpression of CRMP2 or a nonphosphorylatable form of CRMP2 in these neurons attenuates their response to these inhibitors *in vitro* (Mimura, Yamagishi et al. 2006). However, whether

overexpression of CRMP2 can promote nerve regeneration in an *in vivo* CNS injury model remains to be investigated.

We have previously demonstrated that L-CRMP4 can physically and functionally interact with RhoA to mediate neurite outgrowth inhibition *in vitro* (Alabed, Pool et al. 2007; Alabed, Pool et al. 2010). Although CRMP4 depletion in DRGs does not affect neurite outgrowth on a permissive laminin coated substrate, CRMP4 depletion does attenuate neurite outgrowth inhibition on CNS myelin (Alabed, Pool et al. 2007). This data demonstrates that RhoA signals through L-CRMP4 to inhibit neurite outgrowth. Further, Nogo66 stimulation increases the RhoA-L-CRMP4 interaction, which is also independent of the nucleotide binding state of RhoA. This suggests that additional upstream signaling pathways other than those leading to RhoA activation may be involved. Blockade of the RhoA-L-CRMP4 interaction with a competitive peptide, C4RIP (CRMP4b-RhoA Inhibitory Peptide), attenuates neurite outgrowth inhibition on both CNS myelin and aggrecan (Alabed, Pool et al. 2007). These findings identify CRMP4 as a convergent regulator of axon outgrowth inhibition, where RhoA-L-CRMP4 pathway activation leads to cytoskeletal rearrangements.

1.2.2.6 Why CRMPs are ideally positioned to regulate nerve regeneration

Following CNS injury, inhibitory extracellular molecules signal through receptor complexes on the injured axon to activate intracellular pathways that inhibit regeneration. These inhibitory pathways largely converge onto the cytoskeleton to prevent growth cone formation and subsequent regenerative axonal outgrowth. While the biological function of CRMPs in an *in vivo* model of regeneration has not been extensively studied, we investigate the role of CRMP4 in nerve regeneration based on (1) the localization of CRMP4 to growth cones, (2) CRMP4 binds directly to tubulin, (3) CRMP4 binds directly to actin and promotes actin-based phenotypes such as filopodial elongation, (4) CRMP4 depletion attenuates neurite outgrowth on myelin, (5) the specific ability of L-CRMP4 to physically and functionally interact with RhoA to mediate neurite outgrowth inhibition in vitro, and (6) the disruption of the L-CRMP4-RhoA interaction with the competitive peptide C4RIP attenuates neurite outgrowth inhibition in response to myelin and aggrecan (Fukata, Itoh et al. 2002; Rosslenbroich, Dai et al. 2005; Cole, Causeret et al.

2006; Alabed, Pool et al. 2007; Rembutsu, Soutar et al. 2008; Alabed, Pool et al. 2010; Soutar, Kim et al. 2010). In Chapters 3 and 4, we investigate CRMP4 function in an *in vivo* preclinical model of CNS nerve regeneration through the development of two versions of C4RIP: (1) an adeno-associated virus encoding C4RIP and (2) a recombinant cell permeable TAT C4RIP protein, respectively.

1.3 THESIS RATIONALE

CRMPs are cytosolic phosphoproteins that have been implicated in various biological processes that include neurite outgrowth, cellular proliferation, cell migration, cell invasion and metastasis. The ability of the CRMPs to participate in these processes has largely been attributed to its role as a cytoskeleton regulator. While all the CRMPs can bind directly to tubulin, and either directly or indirectly to actin, only CRMP4 has been shown to physically and functional bind to RhoA, a key signaling molecule in CNS regeneration and mitosis. Further, this interaction between CRMP4 and RhoA can be regulated by GSK3, a kinase implicated in both mitosis and regeneration. This thesis investigates the role of CRMP4 during mitosis and CNS regeneration. In Chapter 2, we identify CRMP4 as an important regulator of mitotic chromosomal alignment in HeLa cells. We also identify CRMP4 as a physiological substrate of GSK3 and demonstrate the importance of GSK3-dependent phosphorylation of CRMP4 in regulating spindle morphology and mitotic chromosomal alignment. In Chapters 3 and 4, we investigate the role of CRMP4 in CNS regeneration through the administration of a L-CRMP4-RhoA competitive antagonist C4RIP in an *in vivo* preclinical optic nerve injury model in the adult rat. In Chapter 3, we investigate the ability of an adeno-associated virus encoding C4RIP to enhance adult retinal ganglion cell axon regeneration following optic nerve injury. In Chapter 4, we develop a novel method to generate cytosolic recombinant cell permeable TAT fusion proteins and investigate the ability of TAT C4RIP to enhance adult retinal ganglion cell axon regeneration following optic nerve injury.

1.4 REFERENCES

Acevedo, N., X. Wang, et al. (2007). "Glycogen synthase kinase-3 regulation of chromatin segregation and cytokinesis in mouse preimplantation embryos." Mol Reprod Dev **74**(2): 178-188.

Alabed, Y. Z., E. Grados-Munro, et al. (2006). "Neuronal responses to myelin are mediated by rho kinase." J. Neurochem. **96**(6): 1616-1625.

Alabed, Y. Z., M. Pool, et al. (2007). "Identification of CRMP4 as a convergent regulator of axon outgrowth inhibition." Journal of Neuroscience **27**(7): 1702-1711.

Alabed, Y. Z., M. Pool, et al. (2010). "GSK3beta regulates myelin-dependent axon outgrowth inhibition through CRMP4." J. Neurosci. **30**(16): 5635-5643.

Antoine, J. C., J. Honnorat, et al. (1993). "Posterior uveitis, paraneoplastic encephalomyelitis and auto-antibodies reacting with developmental protein of brain and retina." J Neurol Sci **117**(1-2): 215-223.

Arimura, N., N. Inagaki, et al. (2000). "Phosphorylation of collapsin response mediator protein-2 by Rho-kinase. Evidence for two separate signaling pathways for growth cone collapse." J Biol Chem **275**(31): 23973-23980.

Arimura, N., C. Ménager, et al. (2005). "Phosphorylation by Rho kinase regulates CRMP-2 activity in growth cones." Mol Cell Biol **25**(22): 9973-9984.

Atwal, J. K., J. Pinkston-Gosse, et al. (2008). "PirB is a functional receptor for myelin inhibitors of axonal regeneration." Science **322**(5903): 967-970.

Ault, J. G., A. J. DeMarco, et al. (1991). "Studies on the ejection properties of asters: astral microtubule turnover influences the oscillatory behavior and positioning of mono-oriented chromosomes." Journal of Cell Science **99 (Pt 4)**: 701-710.

Aurandt, J., H. G. Vikis, et al. (2002). "The semaphorin receptor plexin-B1 signals through a direct interaction with the Rho-specific nucleotide exchange factor, LARG." Proc Natl Acad Sci USA **99**(19): 12085-12090.

Aylsworth, A., S. X. Jiang, et al. (2009). "Characterization of the role of full-length CRMP3 and its calpain-cleaved product in inhibiting microtubule polymerization and neurite outgrowth." Exp Cell Res **315**(16): 2856-2868.

Bakal, C. J., D. Finan, et al. (2005). "The Rho GTP exchange factor Lfc promotes spindle assembly in early mitosis." Proc Natl Acad Sci USA **102**(27): 9529-9534.

Benais-Pont, G., A. Punn, et al. (2003). "Identification of a tight junction-associated guanine nucleotide exchange factor that activates Rho and regulates paracellular permeability." The Journal of Cell Biology **160**(5): 729-740.

Benink, H. A. and W. M. Bement (2005). "Concentric zones of active RhoA and Cdc42 around single cell wounds." J Cell Biol **168**(3): 429-439.

Benson, M. D., M. I. Romero, et al. (2005). "Ephrin-B3 is a myelin-based inhibitor of neurite outgrowth." Proc Natl Acad Sci USA **102**(30): 10694-10699.

Bishop, A. L. and A. Hall (2000). "Rho GTPases and their effector proteins." Biochem J **348 Pt 2**: 241-255.

Borisoff, J. F., C. C. M. Chan, et al. (2003). "Suppression of Rho-kinase activity promotes axonal growth on inhibitory CNS substrates." Mol Cell Neurosci **22**(3): 405-416.

Bretin, S., S. Reibel, et al. (2005). "Differential expression of CRMP1, CRMP2A, CRMP2B, and CRMP5 in axons or dendrites of distinct neurons in the mouse brain." J Comp Neurol **486**(1): 1-17.

Bretin, S., V. Rogemond, et al. (2006). "Calpain product of WT-CRMP2 reduces the amount of surface NR2B NMDA receptor subunit." Journal of neurochemistry **98**(4): 1252-1265.

Brot, S., V. Rogemond, et al. (2010). "CRMP5 interacts with tubulin to inhibit neurite outgrowth, thereby modulating the function of CRMP2." J Neurosci **30**(32): 10639-10654.

Byk, T., T. Dobransky, et al. (1996). "Identification and molecular characterization of Unc-33-like phosphoprotein (Ulip), a putative mammalian homolog of the axonal guidance-associated unc-33 gene product." J. Neurosci. **16**(2): 688-701.

Byk, T., S. Ozon, et al. (1998). "The Ulip family phosphoproteins--common and specific properties." Eur J Biochem **254**(1): 14-24.

Camdessanché, J.-P., F. Lassablière, et al. (2006). "Expression of the onconeural CV2/CRMP5 antigen in thymus and thymoma." J Neuroimmunol **174**(1-2): 168-173.

Centonze, V. E. and G. G. Borisy (1991). "Pole-to-chromosome movements induced at metaphase: sites of microtubule disassembly." Journal of Cell Science **100 (Pt 1)**: 205-211.

Charrier, E., B. Mosinger, et al. (2006). "Transient alterations in granule cell proliferation, apoptosis and migration in postnatal developing cerebellum of CRMP1-/- mice." Genes Cells **11**(12): 1337-1352.

Charrier, E., S. Reibel, et al. (2003). "Collapsin response mediator proteins (CRMPs): involvement in nervous system development and adult neurodegenerative disorders." Mol Neurobiol **28**(1): 51-64.

Ciani, L., O. Krylova, et al. (2004). "A divergent canonical WNT-signaling pathway regulates microtubule dynamics: dishevelled signals locally to stabilize microtubules." The Journal of Cell Biology **164**(2): 243-253.

Cimini, D. and F. Degrassi (2005). "Aneuploidy: a matter of bad connections." Trends Cell Biol. **15**(8): 442-451.

Cnops, L., B. Van de Plas, et al. (2004). "Age-dependent expression of collapsin response mediator proteins (CRMPs) in cat visual cortex." Eur J Neurosci **19**(8): 2345-2351.

Cohen, P. and M. Goedert (2004). "GSK3 inhibitors: development and therapeutic potential." Nature reviews Drug discovery **3**(6): 479-487.

Cole, A. R., A. Astell, et al. (2007). "Molecular connexions between dementia and diabetes." Neuroscience and biobehavioral reviews **31**(7): 1046-1063.

Cole, A. R., F. Causeret, et al. (2006). "Distinct priming kinases contribute to differential regulation of collapsin response mediator proteins by glycogen synthase kinase-3 in vivo." J. Biol. Chem. **281**(24): 16591-16598.

Cole, A. R., A. Knebel, et al. (2004). "GSK-3 phosphorylation of the Alzheimer epitope within collapsin response mediator proteins regulates axon elongation in primary neurons." J Biol Chem **279**(48): 50176-50180.

Cole, A. R., W. Noble, et al. (2007). "Collapsin response mediator protein-2 hyperphosphorylation is an early event in Alzheimer's disease progression." J Neurochem **103**(3): 1132-1144.
Cross, S. A., D. R. Salomao, et al. (2003). "Paraneoplastic autoimmune optic neuritis with retinitis defined by CRMP-5-IgG." Ann. Neurol. **54**(1): 38-50.
Czech, T., J.-W. Yang, et al. (2004). "Reduction of hippocampal collapsin response mediated protein-2 in patients with mesial temporal lobe epilepsy." Neurochem Res **29**(12): 2189-2196.
David, S. and A. J. Aguayo (1981). "Axonal elongation into peripheral nervous system "bridges" after central nervous system injury in adult rats." Science **214**(4523): 931-933.
Decordier, I., E. Cundari, et al. (2008). "Survival of aneuploid, micronucleated and/or polyploid cells: crosstalk between ploidy control and apoptosis." Mutat Res **651**(1-2): 30-39.
Dent, E. W., S. L. Gupton, et al. (2010). "The Growth Cone Cytoskeleton in Axon Outgrowth and Guidance." Cold Spring Harbor perspectives in biology.
Deo, R. C., E. F. Schmidt, et al. (2004). "Structural bases for CRMP function in plexin-dependent semaphorin3A signaling." EMBO J. **23**(1): 9-22.
Dergham, P., B. Ellezam, et al. (2002). "Rho signaling pathway targeted to promote spinal cord repair." J. Neurosci. **22**(15): 6570-6577.
Drechsel, D. N., A. A. Hyman, et al. (1997). "A requirement for Rho and Cdc42 during cytokinesis in Xenopus embryos." Curr Biol **7**(1): 12-23.
Dubreuil, C. I., N. Marklund, et al. (2006). "Activation of Rho after traumatic brain injury and seizure in rats." Exp Neurol **198**(2): 361-369.
Dubreuil, C. I., M. J. Winton, et al. (2003). "Rho activation patterns after spinal cord injury and the role of activated Rho in apoptosis in the central nervous system." J Cell Biol **162**(2): 233-243.
Ellezam, B., C. Dubreuil, et al. (2002). "Inactivation of intracellular Rho to stimulate axon growth and regeneration." Prog Brain Res **137**: 371-380.
Erez, H., G. Malkinson, et al. (2007). "Formation of microtubule-based traps controls the sorting and concentration of vesicles to restricted sites of regenerating neurons after axotomy." J Cell Biol **176**(4): 497-507.
Erez, H. and M. E. Spira (2008). "Local self-assembly mechanisms underlie the differential transformation of the proximal and distal cut axonal ends into functional and aberrant growth cones." J Comp Neurol **507**(1): 1019-1030.
Ertürk, A., F. Hellal, et al. (2007). "Disorganized microtubules underlie the formation of retraction bulbs and the failure of axonal regeneration." J Neurosci **27**(34): 9169-9180.
Fournier, A. E., T. GrandPre, et al. (2001). "Identification of a receptor mediating Nogo-66 inhibition of axonal regeneration." Nature **409**(6818): 341-346.
Fournier, A. E., B. T. Takizawa, et al. (2003). "Rho kinase inhibition enhances axonal regeneration in the injured CNS." J. Neurosci. **23**(4): 1416-1423.
Frame, S. and P. Cohen (2001). "GSK3 takes centre stage more than 20 years after its discovery." Biochem J **359**(Pt 1): 1-16.

Fukada, M., I. Watakabe, et al. (2000). "Molecular characterization of CRMP5, a novel member of the collapsin response mediator protein family." J Biol Chem **275**(48): 37957-37965.
Fukata, Y., T. J. Itoh, et al. (2002). "CRMP-2 binds to tubulin heterodimers to promote microtubule assembly." Nat Cell Biol **4**(8): 583-591.
Fumoto, K., P.-C. Lee, et al. (2008). "AIP regulates stability of Aurora-A at early mitotic phase coordinately with GSK-3beta." Oncogene **27**(32): 4478-4487.
Gaetano, C., T. Matsuo, et al. (1997). "Identification and characterization of a retinoic acid-regulated human homologue of the unc-33-like phosphoprotein gene (hUlip) from neuroblastoma cells." J Biol Chem **272**(18): 12195-12201.
Gao, X., J. Pang, et al. (2010). "Expression profiling identifies new function of collapsin response mediator protein 4 as a metastasis-suppressor in prostate cancer." Oncogene **29**(32): 4555-4566.
Geschwind, D. H., G. M. Kelly, et al. (1996). "Identification and characterization of novel developmentally regulated proteins in rat spinal cord." Brain Res Dev Brain Res **97**(1): 62-75.
Good, P. F., D. Alapat, et al. (2004). "A role for semaphorin 3A signaling in the degeneration of hippocampal neurons during Alzheimer's disease." Journal of neurochemistry **91**(3): 716-736.
Goold, R. G., R. Owen, et al. (1999). "Glycogen synthase kinase 3beta phosphorylation of microtubule-associated protein 1B regulates the stability of microtubules in growth cones." Journal of Cell Science **112 (Pt 19)**: 3373-3384.
Goshima, Y., F. Nakamura, et al. (1995). "Collapsin-induced growth cone collapse mediated by an intracellular protein related to UNC-33." Nature **376**(6540): 509-514.
Gu, Y., N. Hamajima, et al. (2000). "Neurofibrillary tangle-associated collapsin response mediator protein-2 (CRMP-2) is highly phosphorylated on Thr-509, Ser-518, and Ser-522." Biochemistry **39**(15): 4267-4275.
Gu, Y. and Y. Ihara (2000). "Evidence that collapsin response mediator protein-2 is involved in the dynamics of microtubules." J Biol Chem **275**(24): 17917-17920.
Gundersen, G. G. (2002). "Evolutionary conservation of microtubule-capture mechanisms." Nat Rev Mol Cell Biol **3**(4): 296-304.
Hall, C., M. Brown, et al. (2001). "Collapsin response mediator protein switches RhoA and Rac1 morphology in N1E-115 neuroblastoma cells and is regulated by Rho kinase." J Biol Chem **276**(46): 43482-43486.
Hara, M., M. Takayasu, et al. (2000). "Protein kinase inhibition by fasudil hydrochloride promotes neurological recovery after spinal cord injury in rats." J Neurosurg **93**(1 Suppl): 94-101.
Hedgecock, E. M., J. G. Culotti, et al. (1985). "Axonal guidance mutants of Caenorhabditis elegans identified by filling sensory neurons with fluorescein dyes." Developmental Biology **111**(1): 158-170.
Hellal, F., A. Hurtado, et al. (2011). "Microtubule Stabilization Reduces Scarring and Causes Axon Regeneration After Spinal Cord Injury." Science (New York, NY).
Honnorat, J., S. Cartalat-Carel, et al. (2009). "Onco-neural antibodies and tumour type determine survival and neurological symptoms in paraneoplastic neurological

syndromes with Hu or CV2/CRMP5 antibodies." J Neurol Neurosurg Psychiatr **80**(4): 412-416.
Hotta, A., R. Inatome, et al. (2005). "Critical role of collapsin response mediator protein-associated molecule CRAM for filopodia and growth cone development in neurons." Mol Biol Cell **16**(1): 32-39.
Hou, S., S. Jiang, et al. (2009). "CaMKII phosphorylates collapsin response mediator protein 2 and modulates axonal damage during glutamate excitotoxicity." J Neurochem.
Hou, S. T., S. X. Jiang, et al. (2006). "Calpain-cleaved collapsin response mediator protein-3 induces neuronal death after glutamate toxicity and cerebral ischemia." J. Neurosci. **26**(8): 2241-2249.
Inagaki, N., K. Chihara, et al. (2001). "CRMP-2 induces axons in cultured hippocampal neurons." Nat. Neurosci. **4**(8): 781-782.
Inatome, R., T. Tsujimura, et al. (2000). "Identification of CRAM, a novel unc-33 gene family protein that associates with CRMP3 and protein-tyrosine kinase(s) in the developing rat brain." J Biol Chem **275**(35): 27291-27302.
Jang, S. Y., Y. K. Shin, et al. (2010). "Injury-induced CRMP4 expression in adult sensory neurons; a possible target gene for ciliary neurotrophic factor." Neuroscience letters **485**(1): 37-42.
Jiang, S. X., J. Kappler, et al. (2007). "Calpain cleavage of collapsin response mediator proteins in ischemic mouse brain." Eur J Neurosci **26**(4): 801-809.
Jin, Z. and S. M. Strittmatter (1997). "Rac1 mediates collapsin-1-induced growth cone collapse." J Neurosci **17**(16): 6256-6263.
Jordan, M. A., K. Wendell, et al. (1996). "Mitotic block induced in HeLa cells by low concentrations of paclitaxel (Taxol) results in abnormal mitotic exit and apoptotic cell death." Cancer Res **56**(4): 816-825.
Kapoor, T. M. and D. A. Compton (2002). "Searching for the middle ground: mechanisms of chromosome alignment during mitosis." J Cell Biol **157**(4): 551-556.
Kimura, T., H. Watanabe, et al. (2005). "Tubulin and CRMP-2 complex is transported via Kinesin-1." J Neurochem **93**(6): 1371-1382.
Knudsen, A., G. Bredholt, et al. (2007). "Antibodies to CRMP3-4 associated with limbic encephalitis and thymoma." Clin Exp Immunol **149**(1): 16-22.
Kodama, A., I. Karakesisoglou, et al. (2003). "ACF7: an essential integrator of microtubule dynamics." Cell **115**(3): 343-354.
Kowara, R., Q. Chen, et al. (2005). "Calpain-mediated truncation of dihydropyrimidinase-like 3 protein (DPYSL3) in response to NMDA and H2O2 toxicity." Journal of neurochemistry **95**(2): 466-474.
Kowara, R., K. L. Moraleja, et al. (2006). "Involvement of nitric oxide synthase and ROS-mediated activation of L-type voltage-gated Ca2+ channels in NMDA-induced DPYSL3 degradation." Brain Res. **1119**(1): 40-49.
Kowara, R., K. L. Moraleja, et al. (2008). "PLA(2) signaling is involved in calpain-mediated degradation of synaptic dihydropyrimidinase-like 3 protein in response to NMDA excitotoxicity." Neurosci Lett **430**(3): 197-202.
Kubo, T., M. Endo, et al. (2008). "Myosin IIA is required for neurite outgrowth inhibition produced by repulsive guidance molecule." J. Neurochem. **105**(1): 113-126.

Lehmann, M., A. Fournier, et al. (1999). "Inactivation of Rho signaling pathway promotes CNS axon regeneration." J Neurosci **19**(17): 7537-7547.
Leung, T., Y. Ng, et al. (2002). "p80 ROKalpha binding protein is a novel splice variant of CRMP-1 which associates with CRMP-2 and modulates RhoA-induced neuronal morphology." FEBS Lett **532**(3): 445-449.
Lingor, P., N. Teusch, et al. (2007). "Inhibition of Rho kinase (ROCK) increases neurite outgrowth on chondroitin sulphate proteoglycan in vitro and axonal regeneration in the adult optic nerve in vivo." J Neurochem **103**(1): 181-189.
Liu, P.-C., Z.-J. Yang, et al. (2003). "Induction of CRMP-4 in striatum of adult rat after transient brain ischemia." Acta Pharmacol Sin **24**(12): 1205-1211.
Liu, W., X.-W. Zhou, et al. (2009). "Calpain-truncated CRMP-3 and -4 contribute to potassium deprivation-induced apoptosis of cerebellar granule neurons." Proteomics **9**(14): 3712-3728.
Liu, Z. and L. J. Martin (2003). "Olfactory bulb core is a rich source of neural progenitor and stem cells in adult rodent and human." J. Comp. Neurol. **459**(4): 368-391.
Lord-Fontaine, S., F. Yang, et al. (2008). "Local inhibition of Rho signaling by cell-permeable recombinant protein BA-210 prevents secondary damage and promotes functional recovery following acute spinal cord injury." J Neurotrauma **25**(11): 1309-1322.
Löw, K., M. Culbertson, et al. (2008). "Netrin-1 is a novel myelin-associated inhibitor to axon growth." J. Neurosci. **28**(5): 1099-1108.
Luo, L., L. Jan, et al. (1996). "Small GTPases in axon outgrowth." Perspect Dev Neurobiol **4**(2-3): 199-204.
Luo, L., L. Y. Jan, et al. (1997). "Rho family GTP-binding proteins in growth cone signalling." Curr. Opin. Neurobiol. **7**(1): 81-86.
Lutz, D. A., Y. Hamaguchi, et al. (1988). "Micromanipulation studies of the asymmetric positioning of the maturation spindle in Chaetopterus sp. oocytes: I. Anchorage of the spindle to the cortex and migration of a displaced spindle." Cell Motil. Cytoskeleton **11**(2): 83-96.
Madura, T., T. Yamashita, et al. (2004). "Activation of Rho in the injured axons following spinal cord injury." EMBO Rep **5**(4): 412-417.
Manning, A. L., S. F. Bakhoum, et al. (2010). "CLASP1, astrin and Kif2b form a molecular switch that regulates kinetochore-microtubule dynamics to promote mitotic progression and fidelity." EMBO J. **29**(20): 3531-3543.
Margolin, E., A. Flint, et al. (2008). "High-titer collapsin response-mediating protein-associated (CRMP-5) paraneoplastic optic neuropathy and Vitritis as the only clinical manifestations in a patient with small cell lung carcinoma." Journal of neuro-ophthalmology : the official journal of the North American Neuro-Ophthalmology Society **28**(1): 17-22.
McEwen, B. F., A. B. Heagle, et al. (1997). "Kinetochore fiber maturation in PtK1 cells and its implications for the mechanisms of chromosome congression and anaphase onset." J Cell Biol **137**(7): 1567-1580.
McKerracher, L. and H. Higuchi (2006). "Targeting Rho to stimulate repair after spinal cord injury." J Neurotrauma **23**(3-4): 309-317.
Mi, S., X. Lee, et al. (2004). "LINGO-1 is a component of the Nogo-66 receptor/p75 signaling complex." Nat. Neurosci. **7**(3): 221-228.

Mimura, F., S. Yamagishi, et al. (2006). "Myelin-associated glycoprotein inhibits microtubule assembly by a Rho-kinase-dependent mechanism." J. Biol. Chem. **281**(23): 15970-15979.

Minturn, J. E., H. J. Fryer, et al. (1995). "TOAD-64, a gene expressed early in neuronal differentiation in the rat, is related to unc-33, a C. elegans gene involved in axon outgrowth." J Neurosci **15**(10): 6757-6766.

Minturn, J. E., D. H. Geschwind, et al. (1995). "Early postmitotic neurons transiently express TOAD-64, a neural specific protein." J. Comp. Neurol. **355**(3): 369-379.

Monnier, P. P., A. Sierra, et al. (2003). "The Rho/ROCK pathway mediates neurite growth-inhibitory activity associated with the chondroitin sulfate proteoglycans of the CNS glial scar." Mol Cell Neurosci **22**(3): 319-330.

Moore, S. W., J. P. Correia, et al. (2008). "Rho inhibition recruits DCC to the neuronal plasma membrane and enhances axon chemoattraction to netrin 1." Development **135**(17): 2855-2864.

Moreau-Fauvarque, C., A. Kumanogoh, et al. (2003). "The transmembrane semaphorin Sema4D/CD100, an inhibitor of axonal growth, is expressed on oligodendrocytes and upregulated after CNS lesion." J Neurosci **23**(27): 9229-9239.

Mukherjee, J., L. V. DeSouza, et al. (2009). "Loss of collapsin response mediator Protein1, as detected by iTRAQ analysis, promotes invasion of human gliomas expressing mutant EGFRvIII." Cancer Res **69**(22): 8545-8554.

Musacchio, A. and E. D. Salmon (2007). "The spindle-assembly checkpoint in space and time." Nat Rev Mol Cell Biol **8**(5): 379-393.

Nacher, J., D. R. Rosell, et al. (2000). "Widespread expression of rat collapsin response-mediated protein 4 in the telencephalon and other areas of the adult rat central nervous system." J. Comp. Neurol. **424**(4): 628-639.

Narumiya, S., F. Oceguera-Yanez, et al. (2004). "A new look at Rho GTPases in cell cycle: role in kinetochore-microtubule attachment." Cell Cycle **3**(7): 855-857.

Narumiya, S. and S. Yasuda (2006). "Rho GTPases in animal cell mitosis." Curr Opin Cell Biol **18**(2): 199-205.

Nicklas, R. B. (1997). "How cells get the right chromosomes." Science **275**(5300): 632-637.

Nicklas, R. B., S. C. Ward, et al. (1995). "Kinetochore chemistry is sensitive to tension and may link mitotic forces to a cell cycle checkpoint." J Cell Biol **130**(4): 929-939.

Niederöst, B., T. Oertle, et al. (2002). "Nogo-A and myelin-associated glycoprotein mediate neurite growth inhibition by antagonistic regulation of RhoA and Rac1." J Neurosci **22**(23): 10368-10376.

Nobes, C. D. and A. Hall (1999). "Rho GTPases control polarity, protrusion, and adhesion during cell movement." J Cell Biol **144**(6): 1235-1244.

Oceguera-Yanez, F., K. Kimura, et al. (2005). "Ect2 and MgcRacGAP regulate the activation and function of Cdc42 in mitosis." J Cell Biol **168**(2): 221-232.

Pan, S., Y. Chao, et al. (2009). "Long form collapsin response mediator protein-1 (LCRMP-1) expression is associated with clinical outcome and lymph node metastasis in non-small cell lung cancer patients." Lung Cancer.

Park, J. B., G. Yiu, et al. (2005). "A TNF receptor family member, TROY, is a coreceptor with Nogo receptor in mediating the inhibitory activity of myelin inhibitors." Neuron **45**(3): 345-351.

Perrot, V., J. Vazquez-Prado, et al. (2002). "Plexin B regulates Rho through the guanine nucleotide exchange factors leukemia-associated Rho GEF (LARG) and PDZ-RhoGEF." J. Biol. Chem. **277**(45): 43115-43120.

Prokopenko, S. N., R. Saint, et al. (2000). "Untying the Gordian knot of cytokinesis. Role of small G proteins and their regulators." J Cell Biol **148**(5): 843-848.

Quach, T. T., A.-M. Duchemin, et al. (2004). "Involvement of collapsin response mediator proteins in the neurite extension induced by neurotrophins in dorsal root ganglion neurons." Mol Cell Neurosci **25**(3): 433-443.

Quach, T. T., G. Massicotte, et al. (2008). "CRMP3 is required for hippocampal CA1 dendritic organization and plasticity." FASEB J **22**(2): 401-409.

Quach, T. T., B. Mosinger, et al. (2000). "Collapsin response mediator protein-3/unc-33-like protein-4 gene: organization, chromosomal mapping and expression in the developing mouse brain." Gene **242**(1-2): 175-182.

Quinn, C. C., E. Chen, et al. (2003). "TUC-4b, a novel TUC family variant, regulates neurite outgrowth and associates with vesicles in the growth cone." J. Neurosci. **23**(7): 2815-2823.

Quinn, C. C., G. E. Gray, et al. (1999). "A family of proteins implicated in axon guidance and outgrowth." J Neurobiol **41**(1): 158-164.

Rembutsu, M., M. P. M. Soutar, et al. (2008). "Novel procedure to investigate the effect of phosphorylation on protein complex formation in vitro and in cells." Biochemistry **47**(7): 2153-2161.

Ricard, D., B. Stankoff, et al. (2000). "Differential expression of collapsin response mediator proteins (CRMP/ULIP) in subsets of oligodendrocytes in the postnatal rodent brain." Mol. Cell. Neurosci. **16**(4): 324-337.

Richardson, P. M., U. M. McGuinness, et al. (1980). "Axons from CNS neurons regenerate into PNS grafts." Nature **284**(5753): 264-265.

Ridley, A. J. and A. Hall (1992). "The small GTP-binding protein rho regulates the assembly of focal adhesions and actin stress fibers in response to growth factors." Cell **70**(3): 389-399.

Ridley, A. J., H. F. Paterson, et al. (1992). "The small GTP-binding protein rac regulates growth factor-induced membrane ruffling." Cell **70**(3): 401-410.

Rodriguez, O. C., A. W. Schaefer, et al. (2003). "Conserved microtubule-actin interactions in cell movement and morphogenesis." Nat. Cell Biol. **5**(7): 599-609.

Rogemond, V., C. Auger, et al. (2008). "Processing and nuclear localization of CRMP2 during brain development induce neurite outgrowth inhibition." J. Biol. Chem. **283**(21): 14751-14761.

Rosenblatt, J., L. P. Cramer, et al. (2004). "Myosin II-dependent cortical movement is required for centrosome separation and positioning during mitotic spindle assembly." Cell **117**(3): 361-372.

Rosslenbroich, V., L. Dai, et al. (2005). "Collapsin response mediator protein-4 regulates F-actin bundling." Exp. Cell Res. **310**(2): 434-444.

Sahin, M., P. L. Greer, et al. (2005). "Eph-dependent tyrosine phosphorylation of ephexin1 modulates growth cone collapse." Neuron **46**(2): 191-204.

Sahly, I., A. Khoutorsky, et al. (2006). "On-line confocal imaging of the events leading to structural dedifferentiation of an axonal segment into a growth cone after axotomy." J Comp Neurol **494**(5): 705-720.

Schweigreiter, R., A. R. Walmsley, et al. (2004). "Versican V2 and the central inhibitory domain of Nogo-A inhibit neurite growth via p75NTR/NgR-independent pathways that converge at RhoA." Mol Cell Neurosci **27**(2): 163-174.

Shao, Z., J. L. Browning, et al. (2005). "TAJ/TROY, an orphan TNF receptor family member, binds Nogo-66 receptor 1 and regulates axonal regeneration." Neuron **45**(3): 353-359.

Shen, Y., A. Tenney, et al. (2009). "PTP{sigma} Is a Receptor for Chondroitin Sulfate Proteoglycan, an Inhibitor of Neural Regeneration." Science.

Shih, J.-Y., Y.-C. G. Lee, et al. (2003). "Collapsin response mediator protein-1: a novel invasion-suppressor gene." Clin Exp Metastasis **20**(1): 69-76.

Shih, J. Y., S. C. Yang, et al. (2001). "Collapsin response mediator protein-1 and the invasion and metastasis of cancer cells." J Natl Cancer Inst **93**(18): 1392-1400.

Siddiqui, S. S. and J. G. Culotti (1991). "Examination of neurons in wild type and mutants of Caenorhabditis elegans using antibodies to horseradish peroxidase." Journal of Neurogenetics **7**(4): 193-211.

Silverman-Gavrila, R. V. and A. Forer (2000). "Evidence that actin and myosin are involved in the poleward flux of tubulin in metaphase kinetochore microtubules of crane-fly spermatocytes." J Cell Sci **113 (Pt 4)**: 597-609.

Sivasankaran, R., J. Pei, et al. (2004). "PKC mediates inhibitory effects of myelin and chondroitin sulfate proteoglycans on axonal regeneration." Nat. Neurosci. **7**(3): 261-268.

Soutar, M. P. M., W.-Y. Kim, et al. (2010). "Evidence that Glycogen Synthase Kinase-3 isoforms have distinct substrate preference in the brain." Journal of neurochemistry.

Spira, M. E., R. Oren, et al. (2003). "Critical calpain-dependent ultrastructural alterations underlie the transformation of an axonal segment into a growth cone after axotomy of cultured Aplysia neurons." J Comp Neurol **457**(3): 293-312.

Su, K.-Y., W.-L. Chien, et al. (2007). "Mice deficient in collapsin response mediator protein-1 exhibit impaired long-term potentiation and impaired spatial learning and memory." J. Neurosci. **27**(10): 2513-2524.

Suzuki, Y., S. Nakagomi, et al. (2003). "Collapsin response mediator protein-2 accelerates axon regeneration of nerve-injured motor neurons of rat." Journal of neurochemistry **86**(4): 1042-1050.

Swiercz, J. M., R. Kuner, et al. (2002). "Plexin-B1 directly interacts with PDZ-RhoGEF/LARG to regulate RhoA and growth cone morphology." Neuron **35**(1): 51-63.

Tahimic, C. G. T., N. Tomimatsu, et al. (2006). "Evidence for a role of Collapsin response mediator protein-2 in signaling pathways that regulate the proliferation of non-neuronal cells." Biochem. Biophys. Res. Commun. **340**(4): 1244-1250.

Takahashi, T., F. Nakamura, et al. (1998). "Semaphorins A and E act as antagonists of neuropilin-1 and agonists of neuropilin-2 receptors." Nat. Neurosci. **1**(6): 487-493.

Tanaka, T. U., N. Rachidi, et al. (2002). "Evidence that the Ipl1-Sli15 (Aurora kinase-INCENP) complex promotes chromosome bi-orientation by altering kinetochore-spindle pole connections." Cell **108**(3): 317-329.

Tatsumoto, T., H. Sakata, et al. (2003). "Potential roles of the nucleotide exchange factor ECT2 and Cdc42 GTPase in spindle assembly in Xenopus egg cell-free extracts." J Cell Biochem **90**(5): 892-900.

Thambisetty, M. R., C. R. Scherzer, et al. (2001). "Paraneoplastic optic neuropathy and cerebellar ataxia with small cell carcinoma of the lung." Journal of neuro-ophthalmology : the official journal of the North American Neuro-Ophthalmology Society **21**(3): 164-167.

Tighe, A., A. Ray-Sinha, et al. (2007). "GSK-3 inhibitors induce chromosome instability." BMC Cell Biol **8**: 34.

Uchida, Y., T. Ohshima, et al. (2005). "Semaphorin3A signalling is mediated via sequential Cdk5 and GSK3beta phosphorylation of CRMP2: implication of common phosphorylating mechanism underlying axon guidance and Alzheimer's disease." Genes Cells **10**(2): 165-179.

Vincent, P., Y. Collette, et al. (2005). "A role for the neuronal protein collapsin response mediator protein 2 in T lymphocyte polarization and migration." J Immunol **175**(11): 7650-7660.

Vuaillat, Varrin-Doyer, et al. (2007). "High CRMP2 expression in peripheral T lymphocytes is associated with recruitment to the brain during virus-induced neuroinflammation." J Neuroimmunol.

Wakefield, J. G., D. J. Stephens, et al. (2003). "A role for glycogen synthase kinase-3 in mitotic spindle dynamics and chromosome alignment." J Cell Sci **116**(Pt 4): 637-646.

Wang, J. Z., Q. Wu, et al. (1998). "Tau is phosphorylated by GSK-3 at several sites found in Alzheimer disease and its biological activity markedly inhibited only after it is prephosphorylated by A-kinase." FEBS Lett **436**(1): 28-34.

Wang, K. C., J. A. Kim, et al. (2002). "P75 interacts with the Nogo receptor as a co-receptor for Nogo, MAG and OMgp." Nature **420**(6911): 74-78.

Wang, L. H. and S. M. Strittmatter (1996). "A family of rat CRMP genes is differentially expressed in the nervous system." J Neurosci **16**(19): 6197-6207.

Wang, L. H. and S. M. Strittmatter (1997). "Brain CRMP forms heterotetramers similar to liver dihydropyrimidinase." J Neurochem **69**(6): 2261-2269.

Wen, Y., C. H. Eng, et al. (2004). "EB1 and APC bind to mDia to stabilize microtubules downstream of Rho and promote cell migration." Nat. Cell Biol. **6**(9): 820-830.

Winton, M. J., C. I. Dubreuil, et al. (2002). "Characterization of new cell permeable C3-like proteins that inactivate Rho and stimulate neurite outgrowth on inhibitory substrates." J Biol Chem **277**(36): 32820-32829.

Wong, S. T., J. R. Henley, et al. (2002). "A p75(NTR) and Nogo receptor complex mediates repulsive signaling by myelin-associated glycoprotein." Nat. Neurosci. **5**(12): 1302-1308.

Wu, C.-C., H.-C. Chen, et al. (2008). "Identification of collapsin response mediator protein-2 as a potential marker of colorectal carcinoma by comparative analysis of cancer cell secretomes." Proteomics **8**(2): 316-332.

Yamashita, N., Y. Uchida, et al. (2006). "Collapsin response mediator protein 1 mediates reelin signaling in cortical neuronal migration." J. Neurosci. **26**(51): 13357-13362.

Yamashita, T., H. Higuchi, et al. (2002). "The p75 receptor transduces the signal from myelin-associated glycoprotein to Rho." J. Cell Biol. **157**(4): 565-570.

Yasuda, S., F. Oceguera-Yanez, et al. (2004). "Cdc42 and mDia3 regulate microtubule attachment to kinetochores." Nature **428**(6984): 767-771.

Yiu, G. and Z. He (2006). "Glial inhibition of CNS axon regeneration." Nat Rev Neurosci **7**(8): 617-627.

Yoshimura, T., N. Arimura, et al. (2006). "Ras regulates neuronal polarity via the PI3-kinase/Akt/GSK-3beta/CRMP-2 pathway." Biochem. Biophys. Res. Commun. **340**(1): 62-68.

Yoshimura, T., Y. Kawano, et al. (2005). "GSK-3beta regulates phosphorylation of CRMP-2 and neuronal polarity." Cell **120**(1): 137-149.

Yuasa-Kawada, J., R. Suzuki, et al. (2003). "Axonal morphogenesis controlled by antagonistic roles of two CRMP subtypes in microtubule organization." Eur J Neurosci **17**(11): 2329-2343.

Zhang, Z., A. K. Ottens, et al. (2007). "Calpain-mediated collapsin response mediator protein-1, -2, and -4 proteolysis after neurotoxic and traumatic brain injury." J. Neurotrauma **24**(3): 460-472.

Zhu, L.-Q., H.-Y. Zheng, et al. (2010). "Protein phosphatase 2A facilitates axonogenesis by dephosphorylating CRMP2." J. Neurosci. **30**(10): 3839-3848.

CHAPTER 2

2 GSK3 REGULATES MITOTIC CHROMOSOMAL ALIGNMENT THROUGH CRMP4

PLoS ONE, 2010, 5(12):e14345

Title:

GSK3 Regulates Mitotic Chromosomal Alignment through CRMP4

Authors and Affiliations:

Stephan Ong Tone[1], Bama Dayanandan[2], Alyson E. Fournier[1*], Craig A. Mandato[2*]

[*]Equal Contribution

[1]Department of Neurology and Neurosurgery, Montreal Neurological Institute, Montreal, Quebec, Canada
[2]Department of Anatomy and Cell Biology, McGill University, Montreal, Quebec, Canada

Address Correspondence to:

Craig Mandato
Department of Anatomy and Cell Biology
McGill University
3640 Rue University
Montreal, Quebec
H3A 2B2
craig.mandato@mcgill.ca

Or

Alyson Fournier
Department of Neurology and Neurosurgery
Montreal Neurological Institute
3801 Rue University
Montreal, Quebec
H3A 2B4
alyson.fournier@mcgill.ca

Keywords: GSK3 / CRMP / chromosome misalignment / mitosis

2.1 PREFACE

In Chapter 1, we discuss the importance of the cytoskeleton and cytoskeleton regulators during mitosis. We also identify some key properties about CRMPs, specifically CRMP4, that support a model in which they play a broader role in biological processes that rely on cytoskeleton rearrangements. CRMPs can interact directly with tubulin and localize to the mitotic spindle, and CRMP4 can interact directly with actin and promote actin-based phenotypes. We have also previously shown that CRMP4 can physically and functionally interact with RhoA, an important mitotic regulator. Additionally, CRMP4 is a physiological target of the mitotic kinase GSK3β. Based on this published data, we investigated the role of CRMP4 during mitosis.

2.2 ABSTRACT

2.2.1 Background

Glycogen Synthase Kinase 3 (GSK3) has been implicated in regulating chromosomal alignment and mitotic progression but the physiological substrates mediating these GSK3-dependent effects have not been identified. Collapsin Response Mediator Protein 4 (CRMP4) is a cytosolic phosphoprotein known to regulate cytoskeletal dynamics and is a known physiological substrate of GSK3. In this study, we investigate the role of CRMP4 during mitosis.

2.2.2 Methodology and Principal Findings

Here we demonstrate that during mitosis CRMP4 phosphorylation is regulated in a GSK3-dependent manner. We show that CRMP4 localizes to spindle microtubules during mitosis and loss of CRMP4 disrupts chromosomal alignment and mitotic progression. The effect of CRMP4 on chromosomal alignment is dependent on phosphorylation by GSK3 identifying CRMP4 as a critical GSK3 substrate during mitotic progression. We also provide mechanistic data demonstrating that CRMP4 regulates spindle microtubules consistent with its known role in the regulation of the microtubule cytoskeleton.

2.2.3 Conclusion and Significance

Our findings identify CRMP4 as a key physiological substrate of GSK3 in regulating chromosomal alignment and mitotic progression through its effect on spindle microtubules.

2.3 INTRODUCTION

Chromosomal alignment and segregation are important well-controlled steps in mitosis. This process is largely regulated by the mitotic spindle where microtubules and microtubule binding proteins capture condensed chromosomes by their kinetochores and direct them to the metaphase plate. Understanding the molecular mechanisms responsible for regulating the process of chromosomal alignment is important because failure to accurately segregate chromosomes results in chromosome non-disjunction and aneuploidy (Decordier, Cundari et al. 2008).

Glycogen Synthase Kinase 3 (GSK3) is a serine/threonine kinase originally identified as a kinase that phosphorylates glycogen synthase during glycogen metabolism. There are two isoforms of GSK3, GSK3α and GSK3β, which are ubiquitously expressed and constitutively active in cells. GSK3 is inactivated by phosphorylation at its amino-terminus serine (serine 21 for α or serine 9 for β) by several protein kinases such as protein kinase B (PKB, also called Akt), MAPK-activated protein kinase-1 (MAPKAP-K1, also called RSK) and p70 ribosomal S6 kinase-1 (Frame and Cohen 2001). GSK3 has been implicated in a diverse range of cellular functions including the regulation of mitotic spindle dynamics and chromosomal alignment (Frame and Cohen 2001; Wakefield, Stephens et al. 2003; Cohen and Goedert 2004; Tighe, Ray-Sinha et al. 2007).

Reports that GSK3β plays a role in regulating microtubule dynamics during interphase provide evidence that GSK3 may regulate spindle microtubules (Ciani, Krylova et al. 2004). GSK3β can phosphorylate microtubule-associated proteins (MAPs) such as Tau, MAP1B and MAP2C resulting in decreased microtubule stability (Wang, Wu et al. 1998; Goold, Owen et al. 1999; Ciani, Krylova et al. 2004). Repressing GSK3 function with GSK3 inhibitors or GSK3β RNAi alters spindle morphology, increases defects in chromosomal alignment, and subsequently delays mitotic progression (Wakefield, Stephens et al. 2003; Tighe, Ray-Sinha et al. 2007). Although the importance of GSK3 as a mitotic kinase has been recognized, the physiological substrates that mediate the GSK3-dependent effects during mitosis have yet to be identified.

Collapsin Response Mediator Proteins (CRMPs) are cytosolic phosphoproteins that are highly expressed in the nervous system during development (Goshima,

Nakamura et al. 1995; Wang and Strittmatter 1996; Gaetano, Matsuo et al. 1997; Byk, Ozon et al. 1998; Quinn, Gray et al. 1999; Quach, Duchemin et al. 2004). The CRMP family is composed of five family members (CRMP1-5) in vertebrates (Goshima, Nakamura et al. 1995; Minturn, Fryer et al. 1995; Byk, Dobransky et al. 1996; Gaetano, Matsuo et al. 1997; Inatome, Tsujimura et al. 2000). Each CRMP allele produces two transcripts that differ in their amino terminal domains producing a long (L-CRMP) and short (S-CRMP) isoforms that have been alternatively referred to as 'a' and 'b' isoforms (Quinn, Chen et al. 2003; Yuasa-Kawada, Suzuki et al. 2003; Alabed, Pool et al. 2007; Pan, Chao et al. 2009). The CRMPs have been implicated in regulating axon path finding and neurite outgrowth (Hedgecock, Culotti et al. 1985; Goshima, Nakamura et al. 1995; Minturn, Fryer et al. 1995; Quinn, Gray et al. 1999; Quinn, Chen et al. 2003; Yoshimura, Arimura et al. 2005; Alabed, Pool et al. 2007). Although the CRMPs have not been directly implicated in mitosis, previous studies have shown that CRMP1 and CRMP2 localize to the mitotic spindle (Gu and Ihara 2000; Shih, Yang et al. 2001; Arimura, Ménager et al. 2005). CRMP1-4 bind to tubulin heterodimers and microtubules, while CRMP4 has been shown to promote F-actin bundling (Fukata, Itoh et al. 2002; Rosslenbroich, Dai et al. 2005; Alabed, Pool et al. 2007). Further, CRMP4, but not other CRMP family members, binds to RhoA, an important regulator of cell cycle progression and cytokinesis (Glotzer 2001; Narumiya and Yasuda 2006; Alabed, Pool et al. 2007). These observations suggest that CRMPs, particularly CRMP4, may play a role in regulating microtubule dynamics during mitosis.

In this study, we investigate the role of CRMP4, a known physiological substrate of GSK3, during mitosis (Cole, Knebel et al. 2004; Cole, Causeret et al. 2006). We identify CRMP4 as a GSK3 substrate that regulates chromosomal alignment during mitosis.

2.4 *MATERIALS AND METHODS*

2.4.1 Cell Culture

HeLa cells (ATCC; catalogue number CCL-2) were grown in DMEM (Invitrogen, Burlington, Ontario) supplemented with 10% FBS (HyClone, Logan, UT) and were maintained in 5% CO_2 at 37 °C. Cells were synchronized using a double thymidine block as previously described (Yüce, Piekny et al. 2005). In brief, HeLa cells (~45% confluency) were grown in 2.5 mM thymidine for 18-24 hours, released for 12-13 hours, and grown in 2.5 mM thymidine for 12-13 hours. The cells were released from the second block and fixed 9 hours later for immunofluorescence microscopy when most of the cells were in metaphase. For immunoblotting, HeLa cells were collected at different time intervals following release from the second block. In some experiments, HeLa cells were blocked with 1 uM nocodazole for 16 hours.

2.4.2 Plasmids and antibodies

The L-CRMP4-WT-V5 construct was described previously (Alabed, Pool et al. 2007). L-CRMP4-AAA-V5 was generated using site-directed mutagenesis (Thr622, Thr627, Ser631) (Stratagene, La Jolla, CA). CRMP4 antibody to the antigen YDGPVFDLTTTPK (as per (Minturn, Geschwind et al. 1995)) and phosphospecific CRMP4 antibody to the antigen FDLTT(pT)PKGGTPAGC (where pT is phosphothreonine) were generously provided by Biogen Idec (Cambridge, MA). Antiserum was affinity purified on an antigen-Sepharose column or was affinity purified by depleting antibodies that recognize unphosphorylated CRMP4 on a non-phosphorylated peptide column followed by selecting phospho-specific antibodies on a phosphopeptide antigen column. Other antibodies that were used: mouse α-tubulin (Sigma-Aldrich, Oakville, ON), sheep anti-tubulin (Cytoskeleton, Denver, CO), mouse BubR1 (BD Bioscience, MD), mouse and rabbit V5 (Sigma-Aldrich), mouse GAPDH (ABCAM, Cambridge, MA), rabbit phospho-Threonine (Sigma-Aldrich), and sheep phospho-CRMP2 (pT509/514) (generously provided by Dr. Calum Sutherland, Neurosciences Institute, University of Dundee). The sheep phospho-CRMP2 (pT509/514) antibody recognizes CRMP2 phosphorylated at its Thr509 and Thr514, which are known GSK3 sites (Cole, Knebel et al. 2004). The following secondary antibodies were used:

goat anti-rabbit Alexa Fluor 488, goat anti-rabbit Alexa Fluor 568, goat anti-sheep Alexa Fluor 546, goat anti-human Alexa Fluor 647, goat anti-mouse Alexa Fluor 647 (Invitrogen); goat anti-rabbit-HRP, goat anti-mouse-HRP and goat anti-sheep-HRP (Sigma-Aldrich); goat anti-rabbit IRDye 800CW and goat anti-mouse IRDye 800CW (LI-COR Biosciences).

2.4.3 Pharmacological inhibitors

GSK3 inhibitors were used at the following concentrations: 10 uM SB-216763 (Sigma-Aldrich) and 2 uM CT-99021 (generously provided by Dr. Rodolfo Marquez, School of Life Sciences, University of Dundee). For inhibitor experiments, the drugs were added for 90 minutes 7.5 hours after release from the second thymidine block. Control treatments with solvent (DMSO) were performed in parallel.

2.4.4 RNAi

Fluorescently tagged siRNA duplexes were designed to knockdown human CRMP4 (both long "L" and short "S" isoforms) protein expression: sense 5' Alexa 488 GUG UUG AUG ACG UAC GUU ATT 3', antisense 5' UAA CGU ACG UCA UCA ACA CTT 3' (Invitrogen). CRMP4 siRNA was transfected into HeLa cells using LipofectAMINE 2000 according to the manufacturer's instructions (Invitrogen). Control cells were transfected with non-targeting control siRNA (Dharmacon, Colorado, USA). HeLa cells were incubated with the transfection mixture for 5 hours after which the media was replaced with fresh growth medium.

2.4.5 Flow Cytometry

HeLa cells were transfected with CRMP4 siRNA and synchronized by double thymidine block. HeLa cells were collected at different time intervals after the second thymidine block by trypsinizing the cells off the culture dish and fixing them in ice-cold ethanol. HeLa cells were resuspended in propidium iodide and analyzed using a FACScan at the McGill Flow Cytometry Facility.

2.4.6 Immunoblot

HeLa cells were washed twice with ice cold PBS and lysed in complete HEPES RIPA buffer (20 mM HEPES, 150 mM NaCl, 0.5% sodium deoxycholate, 0.1% SDS, 1% Triton X-100, 1 mM Na_3VO_4, 5 mM NaF, 1X protease inhibitors (Roche Diagnostics,

Laval, Quebec), 100 nM Calyculin A (Cell Signaling Technology, Danvers, MA)). For experiments requiring plasmid transfection, HeLa cell were grown to subconfluence and transfected with Effectene according to manufacturer's instructions (Qiagen, Mississauga, ON). Lysates were separated by SDS-PAGE and immunoblotted with phospho-CRMP4, CRMP4 and GAPDH antibodies.

2.4.7 Immunoprecipitation

Transfected lysates were precleared with protein A/G-agarose (Santa Cruz Biotechnology, Santa Cruz, CA) and subjected to immunoprecipitation with V5-agarose (Sigma-Aldrich). After washing three times with ice-cold lysis buffer, bound protein was eluted with SDS and immunoblotted with anti-V5, phospho-CRMP4, phospho-CRMP2 (pT509/514) or phospho-Threonine antibodies. Briefly, either L-CRMP1-V5 or S-CRMP2-V5 was immunoprecipitated with V5-agarose and immunoblotted with a phospho-Threonine antibody or phospho-CRMP2 (pT509/514), respectively. In another experiment, either L-CRMP4-WT-V5 or L-CRMP4-AAA-V5 was immunoprecipitated with V5-agarose and immunoblotted with phospho-CRMP4 antibody.

2.4.8 Immunofluorescence

HeLa cells were briefly washed in extraction buffer (Microtubule Stabilization Buffer (MTSB): 100 mM PIPES pH 6.8, 1 mM EGTA, 5 mM $MgCl_2$), incubated with MTSB / 0.05% Triton X-100 for 2 minutes at room temperature, and fixed with 2% paraformaldehyde (PFA) / 0.02% Triton X-100 / 0.05 mM Taxol in MTSB for 1 hour at room temperature. HeLa cells were incubated with Image-iT FX signal enhancer (Invitrogen) for 30 minutes at room temperature and blocked in 5% BSA / 0.2% Triton X-100 in PBS for 30 minutes at room temperature. Primary antibodies were diluted in 0.5% BSA in PBS for 3 hours at room temperature. Secondary antibodies were diluted in 0.5% BSA in PBS for 1 hour at room temperature. Actin was visualized with an Alexa Fluor 568 phalloidin (Invitrogen) and DNA was stained using DAPI (Invitrogen) or Hoechst 33342 (Invitrogen). Cover slips were mounted using PermaFluor (Thermo Scientific, Rockford, IL) and images were acquired with a Zeiss Axiovert 200 using a 63X or 100X oil objective.

2.4.9 Chromosome Alignment Scoring

HeLa cells were transfected with CRMP4 siRNA or control siRNA, synchronized by double thymidine block and fixed 9 hours following the second block in 4% PFA / 20% sucrose in PBS for 30 minutes at room temperature. In rescue experiments, L-CRMP4-WT-V5 or L-CRMP4-AAA-V5 was co-transfected with the siRNA duplexes. In some experiments, the GSK3 inhibitor SB-216763 was added to the cells 7.5 hours following the second thymidine block for 90 minutes. HeLa cells were permeabilized with 0.2% Triton X-100 in PBS for 4 minutes and blocked with 5% BSA in PBS for 30 minutes. HeLa cells were incubated with a rabbit anti-V5 antibody followed by a goat anti-rabbit AlexaFluor 568. DNA was visualized with Hoechst 33342. Coverslips were mounted using Fluoromount-G (SouthernBiotech, Birmingham, AL). CRMP4 siRNA-transfected cells were identified by virtue of the fluorescent tag and only cells in metaphase were scored. HeLa cells with at least one misaligned chromosome were scored as abnormal metaphase. At least 100 cells were scored per experiment.

2.4.10 Live Time-Lapse Microscopy

For time-lapse analysis, HeLa cells were cultured on 35 mm glass bottom dishes (MatTek Co., Ashland, MA) and transfected with an mcherry Histone H3 construct (generously provided by Dr. Paul Maddox, Université de Montreal) and either control or CRMP4 siRNA. Microscopy was performed on Zeiss Axiovert 200 using a 20X objective equipped with an automated stage and an environmental control chamber, which maintained the cells at 37˚C and 5% CO_2. Nuclear envelope breakdown (NEB) was defined as the point when prophase chromatin lost a smooth, linear periphery, and the time of anaphase onset was defined to be the first frame where coordinated pole wards movement was observed (Tighe, Ray-Sinha et al. 2007).

2.4.11 Morphometric analysis of mitotic spindles

For pole to pole distance measurements, tubulin fluorescence intensities were measured from one end of the cell to the other end along the spindle axis using ImageJ, and when plotted as a function of spindle position, the tubulin intensity gave two peaks corresponding to the spindle poles (Fig. S3) (Tighe, Ray-Sinha et al. 2007). For spindle width measurements, the two lateral edges of the mitotic spindle were identified by tubulin fluorescence and the distance between them was measured using ImageJ. For pole

to pole distance and spindle width measurements, at least 3 independent experiments were performed with at least 20 cells per condition measured in each experiment.

2.4.12 Cold Stability Assay

Cold stability assay was performed as previously described (Jeffery, Urquhart et al. 2010). Briefly, HeLa cells were incubated with ice cold media for 10 minutes before fixation and immunostaining for α-tubulin. For quantification of average tubulin intensity at the mitotic spindle, images were acquired at the same exposure and mitotic spindles were traced using ImageJ. For average tubulin intensity measurements at the mitotic spindle, at least 3 independent experiments were performed with at least 19 cells per condition measured in each experiment.

2.5 RESULTS

2.5.1 CRMP4 localizes to spindle microtubules during mitosis

Previous studies have shown that CRMP1 and CRMP2 localize to the mitotic spindle (Gu and Ihara 2000; Shih, Yang et al. 2001; Arimura, Ménager et al. 2005). Although CRMP4 has been shown to bind to tubulin and F-actin, CRMP4 localization throughout the mitotic cycle has not been investigated (Fukata, Itoh et al. 2002; Rosslenbroich, Dai et al. 2005). To investigate CRMP4 localization during mitosis we double stained HeLa cells with CRMP4 and α-tubulin antibodies. We established the specificity of the CRMP4 antibody by immunostaining HeLa cells that were depleted of CRMP4 and observed a reduction in the immunoreactivity at the mitotic spindle (Fig. 1). Throughout the different stages of mitosis we observed CRMP4 co-localizing with microtubules (Fig. 1). During interphase, CRMP4 was primarily associated with microtubules located in the perinuclear region of the cell but was also associated along actin stress fibers. Further, we observed CRMP4 localization to actin structures such as the cleavage furrow and the cortex. As the cells entered mitosis and progressed from prometaphase to metaphase, CRMP4 localized along spindle microtubules. CRMP4 remained localized with microtubules throughout anaphase and telophase, and strongly co-localized with microtubules associated with the mid-body.

2.5.2 CRMP4 influences chromosomal alignment and mitotic progression

The presence of CRMP4 along the mitotic spindle raises the possibility that CRMP4 regulates mitotic microtubules. To investigate the role of CRMP4 during mitosis we used RNA interference to knockdown CRMP4 protein expression in HeLa cells and followed the mitotic progression of these cells following synchronization with a double thymidine block. Introduction of CRMP4 siRNA robustly inhibited CRMP4 protein expression while a control siRNA had no effect (Fig. 2A). To examine chromosomal alignment, we fixed and stained the cells with Hoechst 33342 to visualize DNA 9 hours following the second thymidine block when the majority of cells were in metaphase. We frequently observed CRMP4 siRNA-transfected mitotic cells with abnormal metaphase plates that were characterized by at least one misaligned chromosome (Fig. 2B). CRMP4 knockdown resulted in a significant increase in the percentage of cells with abnormal

metaphase (Fig. 2C). We confirmed that the increase in abnormal metaphase could be attributed to the targeted repression of CRMP4 by rescuing the phenotype with an siRNA-resistant wild type rat CRMP4 construct (L-CRMP4-WT-V5) (Fig. 2C). These results demonstrate that CRMP4 plays an important role in the proper alignment of chromosomes during mitosis.

A similar abnormal metaphase phenotype has been reported as a result of GSK3 inhibition (Wakefield, Stephens et al. 2003; Tighe, Ray-Sinha et al. 2007). Consistent with previous reports, we find that approximately 40% of cells treated with the GSK3 inhibitor SB-216763 exhibited misaligned chromosomes (Wakefield, Stephens et al. 2003; Tighe, Ray-Sinha et al. 2007), very similar to the severity of effects observed with CRMP4 loss of function (Fig. 2C). In addition, a delay in mitotic entry and exit has also been described with GSK inhibition and has been attributed to an increase in time taken for cells to align their chromosomes and progress from prophase to metaphase (Tighe, Ray-Sinha et al. 2007), thus we investigated if CRMP4 knockdown would affect the rate of mitotic progression. We transfected HeLa cells with a fluorescently tagged mcherry Histone H3 and either control (Fig. 3A and Video S1) or CRMP4 siRNA (Fig. 3B and Video S2) and visualized mitotic progression by time-lapse microscopy. 48 hours following transfection, we measured the time from nuclear envelope breakdown (NEB) to anaphase onset. The average time taken for control siRNA treated cells to progress through NEB to anaphase was 38 minutes, while CRMP4 siRNA treated cells took an average of 47 minutes (Fig. 3C) indicating that CRMP4 regulates the rate of mitotic progression. Although the phenotype we observed with CRMP4 protein knockdown was equal in severity to that seen with GSK3 inhibition (Fig. 2C), cells depleted of CRMP4 protein eventually aligned all their chromosomes and progressed through mitosis. This finding suggests that CRMP4 regulates accurate chromosomal alignment, but in its absence, compensatory mechanisms are activated to ensure that the cell does not initiate anaphase with misaligned chromosomes.

Consistent with previous reports we found that the release of synchronized HeLa cells into SB-216763 resulted in an observable delay in mitotic progression by flow cytometry (Fig. S1) (Tighe, Ray-Sinha et al. 2007). We did not detect a similar delay in mitotic progression in CRMP4 siRNA treated cells by flow cytometry, likely because

hourly collection of cells fails to detect short mitotic delays (Fig. 3C). The severe effect of GSK3 inhibition on mitotic progression compared to CRMP4 knockdown suggests that additional GSK3 substrates affect mitotic progression.

2.5.3 CRMP4 depletion yields monopolar syntelic attachments and reduces cold stable microtubules

It has been previously demonstrated that GSK3 inhibitor-treated cells delay chromosomal alignment largely due to their inability to perfectly bi-orient all their chromosomes (Tighe, Ray-Sinha et al. 2007). More specifically, monopolar syntelic attachments predominate in GSK3 inhibitor-treated cells (Tighe, Ray-Sinha et al. 2007). To determine if a similar phenotype was observed following CRMP4 depletion, we transfected HeLa cells with CRMP4 siRNA and immunostained for α-tubulin and the kinetochore protein BubR1. Both GSK3 inhibition and CRMP4 depletion resulted in the presence of monopolar syntelic attachments in HeLa cells, where both sister kinetochores were attached to the same spindle pole (Fig. 4). Thus, both GSK3 inhibition and CRMP4 depletion affected the ability of a cell to perfectly bi-orient all of its chromosomes.

The presence of monopolar syntelic attachments, and the increase in chromosomal misalignment following CRMP4 depletion suggest that spindle microtubule stability is affected. To assess spindle microtubule stability in CRMP4 depleted cells, we performed a cold stability assay, which disintegrates mitotic spindle structures over time except for spindle microtubules that are stably attached to kinetochores (Lampson and Kapoor 2005; Jeffery, Urquhart et al. 2010). While CRMP4 depletion or GSK3 inhibition had no effect on the average tubulin intensity at the mitotic spindle at 0 minutes exposure (Fig. 5A), we observed a significant reduction in cold stable microtubules following a 10 minute exposure to ice cold media (Fig. 5B). These findings indicate that both GSK3 and CRMP4 regulate spindle microtubule attachment to kinetochores.

2.5.4 CRMP4 is phosphorylated in a GSK3-dependent manner during mitosis

Previous studies have identified CRMP4 as a physiological substrate of GSK3 (Cole, Knebel et al. 2004; Cole, Causeret et al. 2006). Following an initial priming event that may be mediated by either cyclin dependent kinase 5 (Cdk5) or dual specificity tyrosine phosphorylation regulated kinase 2 (DYRK2), L-CRMP4 is sequentially phosphorylated by GSK3β on residues Ser631, Thr627 and Thr622 (Cole, Knebel et al.

2004). We generated a phospho-specific antibody recognizing pThr622 of L-CRMP4 (pThr509 of S-CRMP4) (Cole, Knebel et al. 2004) to detect CRMP4 that has been primed and fully phosphorylated by GSK3. To investigate CRMP4 phosphorylation throughout mitosis we synchronized HeLa cells using a double thymidine block, collected the cells at different time intervals, and immunoblotted with phospho-CRMP4 antibody. Lysates from synchronized cells showed an increase in CRMP4 phosphorylation from 7 hours to 11 hours following release from the second block (Fig. 6A). This time interval corresponds to when the majority of synchronized HeLa cells are undergoing mitosis (Fig. S1). Furthermore, as the synchronized cells progressed through mitosis and returned to interphase, the levels of phosphorylated CRMP4 decreased to similar levels seen in unsynchronized cells. The phospho-CRMP4 doublet that appears corresponds to distinct phospho-species of the long isoform of CRMP4 (Fig. S2A and S2B). The increase in phosphorylated CRMP4 was also observed in HeLa cells blocked with nocodazole for 16 hours (Fig. 6C and Fig. S2A). A rat CRMP4 triple alanine substitution mutant (L-CRMP4-AAA-V5) for the three carboxy terminal phospho-residues targeted by GSK3β (Thr622, Thr627, Ser631) fails to undergo phosphorylation in response to nocodazole establishing the specificity of the antibody for phospho-CRMP4 (Fig. S2C).

To investigate if GSK3 is the kinase responsible for CRMP4 phosphorylation during mitosis, we synchronized HeLa cells with a double thymidine block and released them into thymidine-free media for 7.5 hours followed by a 90-minute incubation with a GSK3 inhibitor. Two GSK3 inhibitors were used at concentrations previously shown to inhibit GSK3 activity: SB-216763 (10 uM) or CT-99021 (2 uM) (Wakefield, Stephens et al. 2003; Bain, Plater et al. 2007; Tighe, Ray-Sinha et al. 2007). SB-216763 and CT-99021 both attenuated CRMP4 phosphorylation following cellular synchronization and release with a double thymidine block or with nocodazole (Fig. 6B and 6C). Although CRMP4 phosphorylation was reduced in the presence of GSK3 inhibitors, the phospho-signal was not completely abrogated raising the possibility that additional kinases contribute to CRMP4 phosphorylation during mitosis.

To determine if other CRMP family members may be similarly regulated, we examined the phosphorylation profile of CRMP1 and CRMP2, known GSK3 substrates, during mitosis (Cole, Causeret et al. 2006). Following cellular synchronization and

release, we did not observe any changes in threonine phosphorylation levels of CRMP1 (Fig. 6D) or CRMP2 phosphorylation at their GSK3 sites (Fig. 6E and 6F). This suggests that although several CRMPs localize to the mitotic spindle, CRMP4 may be specifically regulated by GSK3 during mitosis.

2.5.5 Chromosomal alignment during mitosis is phospho-CRMP4-dependent

To localize phosphorylated CRMP4 in mitotic HeLa cells, we immunostained dividing cells with phospho-CRMP4 antibody. We established the specificity of the phospho-CRMP4 antibody by immunostaining HeLa cells that were depleted of CRMP4 or exposed to the GSK3 inhibitor SB-216763 and observed a reduction in the pCRMP4 signal compared to control cells (Fig. 7). Phosphorylated CRMP4 localized to both the cortex adjacent to the spindle poles and to the spindle microtubules in metaphase (Fig. 7). During anaphase and telophase, phosphorylated CRMP4 also localized to microtubules and to the cortex and cleavage furrow located between the two dividing cells (Fig. 7). The phospho-CRMP4 localization pattern is consistent with previous reports that have shown GSK3 localization to the spindle microtubules of mitotic HeLa cells (Wakefield, Stephens et al. 2003). Additionally, inactivated phosphorylated GSK3 was concentrated at the centrosomes and not along the spindle microtubules (Wakefield, Stephens et al. 2003). This localization pattern provides indirect evidence that GSK3 associated with the spindle microtubules is active.

To determine the importance of CRMP4 phosphorylation in chromosomal alignment, we depleted endogenous CRMP4 protein using CRMP4 siRNA, and assessed whether a CRMP4 mutant that is not phosphorylated by GSK3β, L-CRMP4-AAA-V5, could rescue the chromosomal misalignment phenotype. As shown previously (Fig. 2C) rat L-CRMP4-WT-V5 rescues the chromosomal misalignment phenotype in CRMP4-depleted cells; however rat L-CRMP4-AAA-V5 fails to mediate rescue (Fig. 8). This result demonstrates that CRMP4 phosphorylation is necessary for proper chromosomal alignment during mitosis.

2.5.6 CRMP4 regulates spindle morphology

CRMP proteins are known to affect microtubule polymerization raising the possibility that the role of phospho-CRMP4 may be to regulate spindle microtubules. To

investigate if phosphorylation altered the ability of CRMP4 to associate with spindle microtubules, we transfected HeLa cells with either L-CRMP4-WT-V5 or L-CRMP4-AAA-V5 and immunostained for V5, α-tubulin and DNA. Only wild type CRMP4 localized to the spindle microtubules during metaphase, while the CRMP4 phospho-mutant was observed throughout the cytoplasm (Fig. 9A) indicating that an important role for CRMP4 phosphorylation is to localize CRMP4 to the spindle microtubules. To further investigate the role of GSK3-dependent phosphorylation of CRMP4 during mitosis, we treated HeLa cells with SB-216763 for 90 minutes and immunostained for CRMP4. We observed a significant reduction of CRMP4 signal at the spindle microtubules in SB-216763 treated HeLa cells compared to DMSO treated cells (Fig. 9B and 9C). This finding is consistent with our data showing that CRMP4 phosphorylation was reduced in the presence of GSK3 inhibitors (Fig. 6B and 6C) but was not completely abrogated.

We investigated the role of CRMP4 in regulating spindle morphology by transfecting HeLa cells with control or CRMP4 siRNA, fixing and immunostaining for α-tubulin. We performed a morphometric analysis of the mitotic spindle by measuring spindle length (pole to pole distance) and spindle width 9 hours following release from a double thymidine block (Fig. 10A -10C), as described previously with GSK3 inhibitors (Tighe, Ray-Sinha et al. 2007). While siRNA-mediated CRMP4 knockdown had no effect on spindle width (Fig. 10C), we did observe a significant decrease in the pole to pole distance compared to control treated cells (Fig. 10A and 10B). In CRMP4 siRNA-treated cells, L-CRMP4-WT-V5 but not L-CRMP4-AAA-V5 rescued the spindle morphology phenotype (Fig. 10A and 10B). This finding and the inability of L-CRMP4-AAA-V5 to localize to spindle microtubules (Fig. 9A) indicate that phosphorylated CRMP4 regulates spindle morphology.

2.6 DISCUSSION

2.6.1 Identification of CRMP4 as a regulator of mitotic chromosomal alignment

Herein, we identify CRMP4 as a regulator of chromosomal alignment during mitosis. We show that CRMP4 localizes to spindle microtubules and demonstrate that CRMP4 loss of function leads to defects in chromosomal alignment during mitosis and delays in mitotic progression. We provide evidence that CRMP4 is phosphorylated during mitosis in a GSK3-dependent manner and demonstrate that CRMP4 phosphorylation by GSK3 regulates chromosomal alignment. Further, we show that CRMP4 loss of function yields monopolar syntelic attachments, reduces cold stable microtubules, and alters spindle morphology. These findings identify CRMP4 as a downstream regulator of GSK3-dependent chromosomal alignment during mitosis.

2.6.2 CRMP4 mechanism of action in regulating chromosomal alignment

The proteins that regulate microtubules during mitosis have not been fully elucidated and our findings indicate that CRMP4 plays such a role. CRMP1-4 bind to tubulin and CRMP1, 2 and 4 localize to the mitotic spindle (Shih, Yang et al. 2001; Fukata, Itoh et al. 2002); however our data demonstrating that the phosphorylation status of CRMP4 at its GSK3 sites, but not CRMP1 or CRMP2, is regulated through the mitotic cycle suggests that CRMP4 plays a unique role downstream of GSK3 during mitosis. These observations raise the possibility that CRMP1 and CRMP2 recruitment to the mitotic spindle is regulated through a GSK3-independent mechanism.

We demonstrate that CRMP4 localizes along spindle microtubules in HeLa cells, and that CRMP4 depletion results in chromosomal misalignment, mitotic delay, monopolar syntelic attachments, a reduction in cold stable microtubules and a decrease in spindle length. These findings provide evidence for an important role for CRMP4 in organizing microtubules during mitosis. Moreover, since microtubule dynamics are the major determinants of metaphase spindle length, CRMP4 may have a role in regulating microtubule dynamics (Goshima, Wollman et al. 2005). Specifically, the decrease in spindle length observed with CRMP4 depletion suggests that CRMP4 may be involved with microtubule stabilization since RNAi-depletion of proteins that promote microtubule stabilization such EB1, Minispindles [Dis1/XMAP215/TOG], and Mast/Orbit [CLASP]

result in a shorten metaphasic spindle (Goshima, Wollman et al. 2005). In contrast, RNAi-depletion of proteins that promote microtubule depolymerization such as Kinesin-8 and Kinesin-13 result in a longer metaphasic spindle (Goshima, Wollman et al. 2005).

L-CRMP4-WT-V5, but not L-CRMP4-AAA-V5, localizes to microtubules at the mitotic spindle, rescues chromosomal misalignment and the altered spindle morphology phenotype seen in CRMP4-depleted cells. We generated a rat CRMP4 triple glutamic acid substitution mutant (L-CRMP4-EEE-V5) for the three carboxy terminal phospho-residues targeted by GSK3β (Thr622, Thr627, Ser631) and find that it does not rescue the misalignment phenotype observed with GSK3 inhibition (data not shown); however, we believe that the L-CRMP4-EEE-V5 mutant does not function as a phospho-mimetic based on published results demonstrating that an S-D mutation on a CRMP2 and CRMP4 priming residue (S522) does not mimic phosphorylation (Cole, Knebel et al. 2004). These findings support a model in which CRMP4 phosphorylation at its GSK3 sites plays an important role in regulating spindle microtubules during mitosis.

Our findings that CRMP4 depletion reduces cold stable microtubules and yields monopolar syntelic attachments suggest that CRMP4 is involved in the regulation of stable microtubule-kinetochore attachments. However, the observation that CRMP4 depleted cells have an organized metaphasic plate and eventually progress through mitosis with all their chromosomes aligned indicates that stable microtubule-kinetochore attachments do occur. Therefore the unstable microtubule-kinetochore attachment phenotype we observed is most likely a transient one, whereby compensatory mechanisms, such as Aurora B kinase activation, can eliminate microtubule-kinetochore attachments that do not generate tension and thereby ensure that the cell does not progress through mitosis with misaligned chromosomes (Tanaka, Rachidi et al. 2002; Dewar, Tanaka et al. 2004; Lampson, Renduchitala et al. 2004; Maure, Kitamura et al. 2007).

CRMP4 can also promote an actin-based phenotype. Overexpression of CRMP4 results in the extension of filopodia and neurite branches in neurons (Alabed, Pool et al. 2007). Similarly, CRMP4 can bundle F-actin filaments in B35 neuroblastoma cells (Rosslenbroich, Dai et al. 2005). The ability of CRMP4 to modulate the actin cytoskeleton raises the possibility that CRMP4 plays an additional role in regulating

actomyosin-based events during mitosis. Interestingly, we do observe localization of pT622 CRMP4 at the cortex during anaphase and telophase in areas that have been associated with actin structures, such as the cleavage furrow. However, the role of CRMP4 in modulating these actin-based events during mitosis remains to be investigated.

2.6.3 The role of CRMP4 phosphorylation during mitosis

The ability of L-CRMP4-WT-V5 but not L-CRMP4-AAA-V5 to rescue the chromosomal misalignment phenotype and the altered spindle morphology phenotype resulting from CRMP4 loss of function indicates that the function of CRMP4 in mitosis is highly dependent on its phosphorylation status. Transient phosphorylation/dephosphorylation of proteins is often critical for the recruitment and release of binding partners. This raises the possibility that CRMP4 may also regulate the complement of proteins associated with the microtubule machinery over the course of the mitotic cycle. CRMP4 binds to RhoA in a phospho-dependent fashion and this interaction is disrupted by CRMP4 phosphorylation by GSK3β (Alabed, Pool et al. 2007; Alabed, Pool et al. 2010). An interesting possibility is that CRMP4 may recruit RhoA to the microtubule machinery and that CRMP4 phosphorylation may result in the local release of RhoA for binding to the microtubule machinery during the mitotic cycle. Further, the ability of CRMP4 to bundle F-actin and its localization to the cleavage furrow suggests that the role of CRMP4 during mitosis may not be limited to regulating spindle microtubules.

2.6.4 GSK3 as a regulator of chromosomal alignment and mitotic progression

Previous studies have reported that GSK3 inhibition results in a delay in mitotic exit, and this phenotype has been largely attributed to chromosomal alignment defects (Wakefield, Stephens et al. 2003; Tighe, Ray-Sinha et al. 2007). Our finding that CRMP4 loss of function results in a delay in mitotic progression is consistent with our hypothesis that GSK3 regulates chromosomal alignment through CRMP4. However, the more severe effects observed with GSK3 inhibition on mitotic progression and spindle morphology suggests that, in addition to CRMP4, there are other downstream effectors of GSK3 that are involved with these processes.

Several other MAPs identified as GSK3 substrates are candidates for regulating additional aspects of microtubule dynamics during mitosis. GSK3 can phosphorylate Tau, MAP1B and MAP2C, all of which result in a decreased ability to stabilize microtubules (Lovestone, Hartley et al. 1996; Wang, Wu et al. 1998; Goold, Owen et al. 1999). Both CLIP-associated protein (CLASP) 2 and Adenomatous Polposis Coli (APC) are phosphorylated by GSK3, which alters their ability to bind and stabilize the distal end of microtubules (Akhmanova, Hoogenraad et al. 2001; Kaplan, Burds et al. 2001; Watanabe, Noritake et al. 2009). Further, mutations that eliminate the microtubule-binding domain of APC result in defective chromosomal segregation (Kaplan, Burds et al. 2001).

GSK3 can also target substrates other than MAPs that likely contribute to GSK3-dependent effects on mitotic progression. There is evidence that GSK3 positively regulates protein levels of Aurora A, a mitotic kinase that has been implicated in the centrosome cycle, spindle assembly, chromosomal segregation and mitotic progression (Meraldi, Honda et al. 2004; Marumoto, Zhang et al. 2005; Fumoto, Lee et al. 2008). Further, GSK3 can phosphorylate cyclin dependent kinases (Cdks), which control cell cycle progression in response to mitogenic signals (Diehl, Cheng et al. 1998; Massagué 2004; Pizarro, Folch et al. 2008). Therefore, the delay in mitotic progression seen with GSK3 inhibition may not be fully attributed to defects in chromosomal alignment but rather the dysregulation of mitotic complexes that control cell cycle progression.

2.7 ACKNOWLEDGEMENTS

The authors would like to thank Dr. Rodolfo Marquez (School of Life Sciences, University of Dundee) and Dr. Calum Sutherland (Neurosciences Institute, University of Dundee) for generously providing CT-99021 and phospho-CRMP2 (pT509/514) antibody, respectively. The authors would also like to thank Dr. Paul Maddox for generously providing the mcherry Histone H3 construct (Université de Montreal) and for comments and suggestions on this manuscript. The authors would also like to thank Dr. Madeline Pool for comments and suggestions on this manuscript.

2.8 REFERENCES

Akhmanova, A., C. C. Hoogenraad, et al. (2001). "Clasps are CLIP-115 and -170 associating proteins involved in the regional regulation of microtubule dynamics in motile fibroblasts." Cell **104**(6): 923-935.

Alabed, Y. Z., M. Pool, et al. (2007). "Identification of CRMP4 as a convergent regulator of axon outgrowth inhibition." Journal of Neuroscience **27**(7): 1702-1711.

Alabed, Y. Z., M. Pool, et al. (2010). "GSK3beta regulates myelin-dependent axon outgrowth inhibition through CRMP4." J. Neurosci. **30**(16): 5635-5643.

Arimura, N., C. Ménager, et al. (2005). "Phosphorylation by Rho kinase regulates CRMP-2 activity in growth cones." Mol Cell Biol **25**(22): 9973-9984.

Bain, J., L. Plater, et al. (2007). "The selectivity of protein kinase inhibitors: a further update." Biochem J **408**(3): 297-315.

Byk, T., T. Dobransky, et al. (1996). "Identification and molecular characterization of Unc-33-like phosphoprotein (Ulip), a putative mammalian homolog of the axonal guidance-associated unc-33 gene product." J Neurosci **16**(2): 688-701.

Byk, T., S. Ozon, et al. (1998). "The Ulip family phosphoproteins--common and specific properties." Eur J Biochem **254**(1): 14-24.

Ciani, L., O. Krylova, et al. (2004). "A divergent canonical WNT-signaling pathway regulates microtubule dynamics: dishevelled signals locally to stabilize microtubules." The Journal of Cell Biology **164**(2): 243-253.

Cohen, P. and M. Goedert (2004). "GSK3 inhibitors: development and therapeutic potential." Nature reviews Drug discovery **3**(6): 479-487.

Cole, A. R., F. Causeret, et al. (2006). "Distinct priming kinases contribute to differential regulation of collapsin response mediator proteins by glycogen synthase kinase-3 in vivo." J Biol Chem **281**(24): 16591-16598.

Cole, A. R., A. Knebel, et al. (2004). "GSK-3 phosphorylation of the Alzheimer epitope within collapsin response mediator proteins regulates axon elongation in primary neurons." J Biol Chem **279**(48): 50176-50180.

Decordier, I., E. Cundari, et al. (2008). "Survival of aneuploid, micronucleated and/or polyploid cells: crosstalk between ploidy control and apoptosis." Mutat Res **651**(1-2): 30-39.

Dewar, H., K. Tanaka, et al. (2004). "Tension between two kinetochores suffices for their bi-orientation on the mitotic spindle." Nature **428**(6978): 93-97.

Diehl, J. A., M. Cheng, et al. (1998). "Glycogen synthase kinase-3beta regulates cyclin D1 proteolysis and subcellular localization." Genes Dev **12**(22): 3499-3511.

Frame, S. and P. Cohen (2001). "GSK3 takes centre stage more than 20 years after its discovery." Biochem J **359**(Pt 1): 1-16.

Fukata, Y., T. J. Itoh, et al. (2002). "CRMP-2 binds to tubulin heterodimers to promote microtubule assembly." Nat. Cell Biol. **4**(8): 583-591.

Fumoto, K., P. C. Lee, et al. (2008). "AIP regulates stability of Aurora-A at early mitotic phase coordinately with GSK-3beta." Oncogene **27**(32): 4478-4487.

Gaetano, C., T. Matsuo, et al. (1997). "Identification and characterization of a retinoic acid-regulated human homologue of the unc-33-like phosphoprotein gene (hUlip) from neuroblastoma cells." J Biol Chem **272**(18): 12195-12201.

Glotzer, M. (2001). "Animal cell cytokinesis." Annu Rev Cell Dev Biol **17**: 351-386.

Goold, R. G., R. Owen, et al. (1999). "Glycogen synthase kinase 3beta phosphorylation of microtubule-associated protein 1B regulates the stability of microtubules in growth cones." Journal of Cell Science **112 (Pt 19)**: 3373-3384.

Goshima, G., R. Wollman, et al. (2005). "Length control of the metaphase spindle." Curr Biol **15**(22): 1979-1988.

Goshima, Y., F. Nakamura, et al. (1995). "Collapsin-induced growth cone collapse mediated by an intracellular protein related to UNC-33." Nature **376**(6540): 509-514.

Gu, Y. and Y. Ihara (2000). "Evidence that collapsin response mediator protein-2 is involved in the dynamics of microtubules." J Biol Chem **275**(24): 17917-17920.

Hedgecock, E. M., J. G. Culotti, et al. (1985). "Axonal guidance mutants of Caenorhabditis elegans identified by filling sensory neurons with fluorescein dyes." Dev Biol **111**(1): 158-170.

Inatome, R., T. Tsujimura, et al. (2000). "Identification of CRAM, a novel unc-33 gene family protein that associates with CRMP3 and protein-tyrosine kinase(s) in the developing rat brain." J Biol Chem **275**(35): 27291-27302.

Jeffery, J. M., A. J. Urquhart, et al. (2010). "Centrobin regulates the assembly of functional mitotic spindles." Oncogene **29**(18): 2649-2658.

Kaplan, K. B., A. A. Burds, et al. (2001). "A role for the Adenomatous Polyposis Coli protein in chromosome segregation." Nat. Cell Biol. **3**(4): 429-432.

Lampson, M. A. and T. M. Kapoor (2005). "The human mitotic checkpoint protein BubR1 regulates chromosome-spindle attachments." Nat Cell Biol **7**(1): 93-98.

Lampson, M. A., K. Renduchitala, et al. (2004). "Correcting improper chromosome-spindle attachments during cell division." Nat Cell Biol **6**(3): 232-237.

Lovestone, S., C. L. Hartley, et al. (1996). "Phosphorylation of tau by glycogen synthase kinase-3 beta in intact mammalian cells: the effects on the organization and stability of microtubules." Neuroscience **73**(4): 1145-1157.

Marumoto, T., D. Zhang, et al. (2005). "Aurora-A - a guardian of poles." Nat Rev Cancer **5**(1): 42-50.

Massagué, J. (2004). "G1 cell-cycle control and cancer." Nature **432**(7015): 298-306.

Maure, J.-F., E. Kitamura, et al. (2007). "Mps1 kinase promotes sister-kinetochore bi-orientation by a tension-dependent mechanism." Curr Biol **17**(24): 2175-2182.

Meraldi, P., R. Honda, et al. (2004). "Aurora kinases link chromosome segregation and cell division to cancer susceptibility." Curr Opin Genet Dev **14**(1): 29-36.

Minturn, J. E., H. J. Fryer, et al. (1995). "TOAD-64, a gene expressed early in neuronal differentiation in the rat, is related to unc-33, a C. elegans gene involved in axon outgrowth." J Neurosci **15**(10): 6757-6766.

Minturn, J. E., D. H. Geschwind, et al. (1995). "Early postmitotic neurons transiently express TOAD-64, a neural specific protein." J Comp Neurol **355**(3): 369-379.

Narumiya, S. and S. Yasuda (2006). "Rho GTPases in animal cell mitosis." Current Opinion in Cell Biology **18**(2): 199-205.

Pan, S., Y. Chao, et al. (2009). "Long form collapsin response mediator protein-1 (LCRMP-1) expression is associated with clinical outcome and lymph node metastasis in non-small cell lung cancer patients." Lung Cancer.

Pizarro, J. G., J. Folch, et al. (2008). "A molecular study of pathways involved in the inhibition of cell proliferation in neuroblastoma B65 cells by the GSK-3 inhibitors lithium and SB-415286." J Cell Mol Med.

Quach, T. T., A.-M. Duchemin, et al. (2004). "Involvement of collapsin response mediator proteins in the neurite extension induced by neurotrophins in dorsal root ganglion neurons." Mol Cell Neurosci **25**(3): 433-443.

Quinn, C. C., E. Chen, et al. (2003). "TUC-4b, a novel TUC family variant, regulates neurite outgrowth and associates with vesicles in the growth cone." Journal of Neuroscience **23**(7): 2815-2823.

Quinn, C. C., G. E. Gray, et al. (1999). "A family of proteins implicated in axon guidance and outgrowth." J Neurobiol **41**(1): 158-164.

Rosslenbroich, V., L. Dai, et al. (2005). "Collapsin response mediator protein-4 regulates F-actin bundling." Experimental Cell Research **310**(2): 434-444.

Shih, J. Y., S. C. Yang, et al. (2001). "Collapsin response mediator protein-1 and the invasion and metastasis of cancer cells." J Natl Cancer Inst **93**(18): 1392-1400.

Tanaka, T. U., N. Rachidi, et al. (2002). "Evidence that the Ipl1-Sli15 (Aurora kinase-INCENP) complex promotes chromosome bi-orientation by altering kinetochore-spindle pole connections." Cell **108**(3): 317-329.

Tighe, A., A. Ray-Sinha, et al. (2007). "GSK-3 inhibitors induce chromosome instability." BMC Cell Biol **8**: 34.

Wakefield, J., D. Stephens, et al. (2003). "A role for glycogen synthase kinase-3 in mitotic spindle dynamics and chromosome alignment." Journal of Cell Science **116**(4): 637-646.

Wang, J. Z., Q. Wu, et al. (1998). "Tau is phosphorylated by GSK-3 at several sites found in Alzheimer disease and its biological activity markedly inhibited only after it is prephosphorylated by A-kinase." FEBS Lett **436**(1): 28-34.

Wang, L. H. and S. M. Strittmatter (1996). "A family of rat CRMP genes is differentially expressed in the nervous system." J Neurosci **16**(19): 6197-6207.

Watanabe, T., J. Noritake, et al. (2009). "Phosphorylation of CLASP2 by GSK-3{beta} regulates its interaction with IQGAP1, EB1 and microtubules." Journal of Cell Science **122**(Pt 16): 2969-2979.

Yoshimura, T., N. Arimura, et al. (2005). "Ras regulates neuronal polarity via the PI3-kinase/Akt/GSK-3β/CRMP-2 pathway." Biochemical and Biophysical Research Communications: 7.

Yuasa-Kawada, J., R. Suzuki, et al. (2003). "Axonal morphogenesis controlled by antagonistic roles of two CRMP subtypes in microtubule organization." Eur J Neurosci **17**(11): 2329-2343.

Yüce, O., A. Piekny, et al. (2005). "An ECT2-centralspindlin complex regulates the localization and function of RhoA." The Journal of Cell Biology **170**(4): 571-582.

Chapter 2 - Figure 1. CRMP4 localizes with spindle microtubules during mitosis.

Immunofluorescence detection of CRMP4, α-tubulin, and DNA in mitotic HeLa cells. HeLa cells were permeabilized with a cytosolic extraction buffer prior to fixation with 4% PFA. CRMP4 associates with microtubules throughout mitosis. Immunofluorescence detection of CRMP4 was markedly reduced in HeLa cells transfected with CRMP4 siRNA. Bar, 10 um.

FIGURE 1

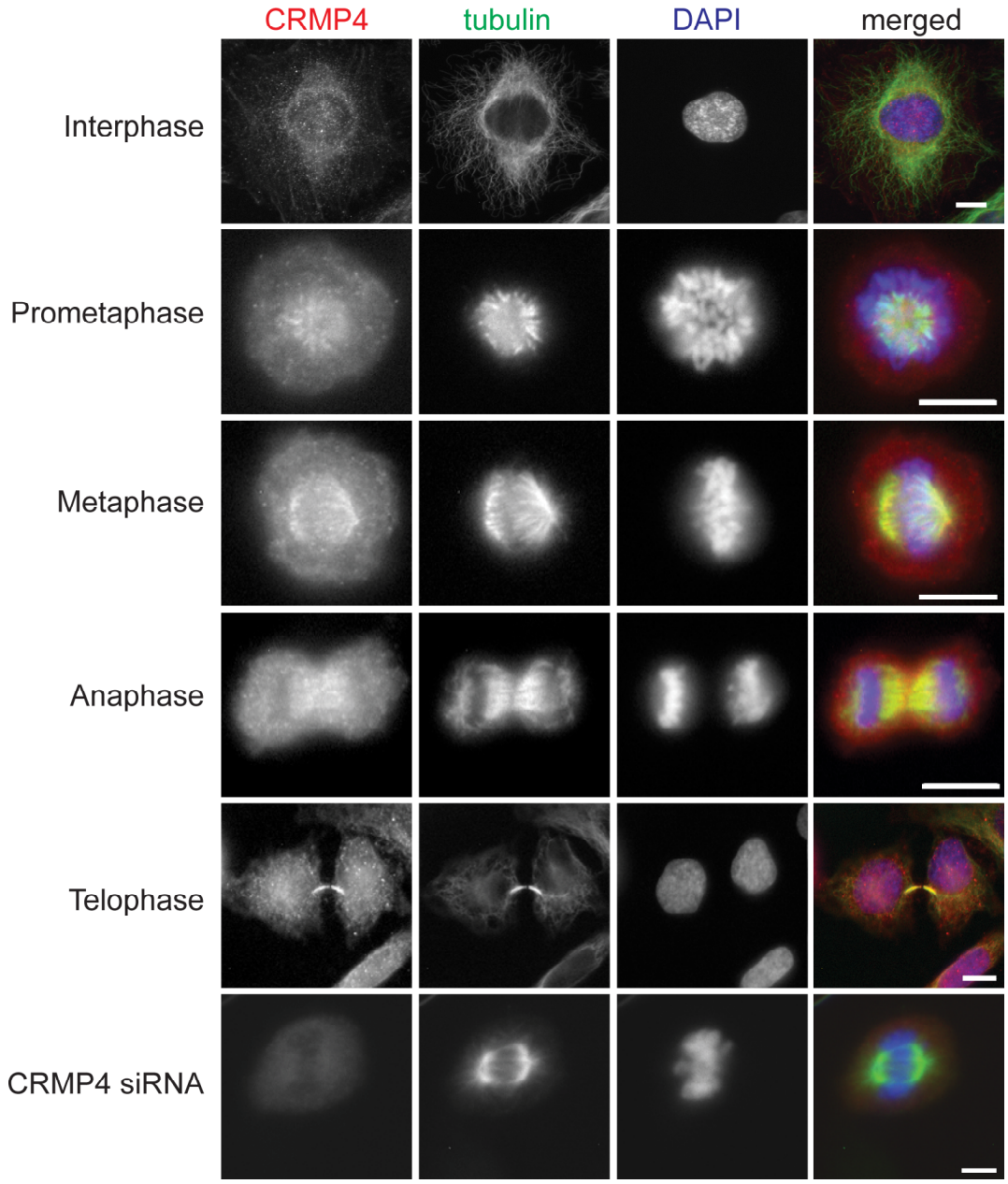
CRMP4
tubulin
DAPI
merged
Interphase
Prometaphase
Metaphase
Anaphase
Telophase
CRMP4 siRNA

Chapter 2 - Figure 2. siRNA-mediated knockdown of CRMP4 leads to chromosomal misalignment.

(A) HeLa cells transfected with CRMP4 siRNA, control siRNA or treated with SB-216763 (10 uM) were immunoblotted with a CRMP4 antibody. CRMP4 siRNA transfection results in a reduction of CRMP4 protein expression. (B) Synchronized HeLa cells were stained with Hoechst 33342 to visualize DNA. HeLa cells with misaligned chromosomes (arrows) were scored as abnormal metaphase. Only cells in metaphase were scored. Representative images of HeLa cells with normal and abnormal metaphase plates are shown. Bar, 10 um. (C) HeLa cells were transfected with either CRMP4 siRNA or control siRNA and were synchronized by double thymidine block. HeLa cells were released into thymidine-free culture medium and fixed 9 hours later, when a large proportion of cells were in metaphase. siRNA-mediated knockdown of CRMP4 resulted in an increase in the percentage of cells with abnormal metaphase (n=3, **$p<0.01$ Student's *t* test compared to control siRNA). Co-transfection of HeLa cells with CRMP4 siRNA and a CRMP4 siRNA-resistant wild type rat L-CRMP4 construct (L-CRMP4-WT-V5) rescued the abnormal metaphase phenotype (n=3, **$p<0.01$, Student's *t* test compared to CRMP4 siRNA; n=3, ns = non significant $p>0.05$, Student's *t* test compared to control siRNA). For experiments with the GSK3 inhibitor, SB-216763 (10 uM) was added 7.5 hours following release into thymidine-free media and fixed 90 minutes later. Inhibition of GSK3 with SB-216763 resulted in an increase in the percentage of abnormal metaphase cells (n=3, **$p<0.01$, Student's *t* test compared to DMSO). n=3 refers to 3 independent experiments where at least 100 cells were scored per experiment.

FIGURE 2

A

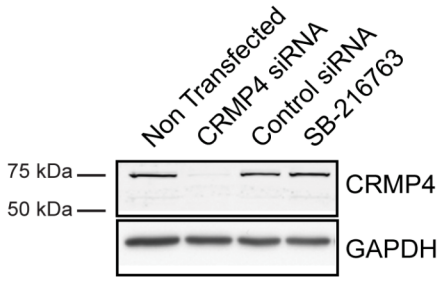
Non Transfected
CRMP4 siRNA
Control siRNA
SB-216763
75 kDa
50 kDa
CRMP4
GAPDH

B

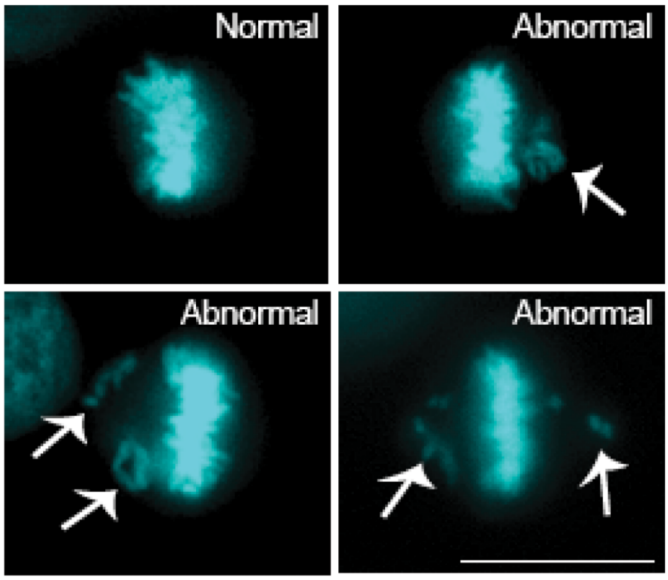
Normal
Abnormal
Abnormal
Abnormal

C

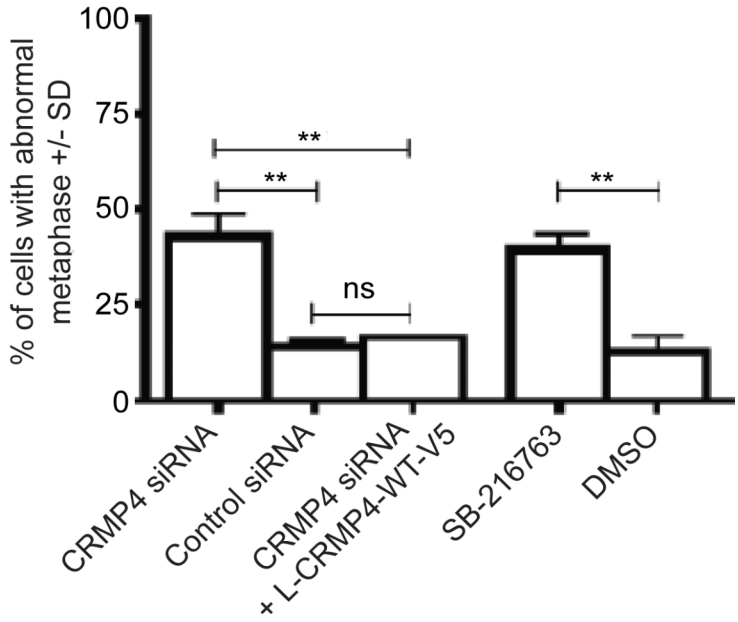
% of cells with abnormal metaphase +/- SD
100
75
50
25
0
**
**
ns
**
CRMP4 siRNA
Control siRNA
CRMP4 siRNA + L-CRMP4-WT-V5
SB-216763
DMSO

Chapter 2 - Figure 3. siRNA-mediated knockdown of CRMP4 leads to a delay in mitotic progression.

HeLa cells transfected with a fluorescently tagged mcherry Histone H3 plasmid and either control or CRMP4 siRNA were analyzed by time-lapse microscopy. **(**A) Images from a time-lapse movie showing a control cell that undergoes normal mitosis. (B) Images from a time-lapse movie showing a CRMP4 siRNA treated cell that delays anaphase onset until the misaligned chromosome (arrow) aligns to the metaphasic plate. Time intervals are indicated in hours and minutes (0:00), where 0:00 corresponds to nuclear envelope breakdown (NEB). Bar, 10 um. (C) Scatter dot plot measuring the time interval from NEB to anaphase onset in control and CRMP4 siRNA treated groups for 71 cells and 157 cells, respectively. CRMP4 siRNA treated cells delayed anaphase onset until all their chromosomes were aligned to the metaphasic plate (***$p<0.0001$, Student's *t* test compared to control siRNA).

FIGURE 3

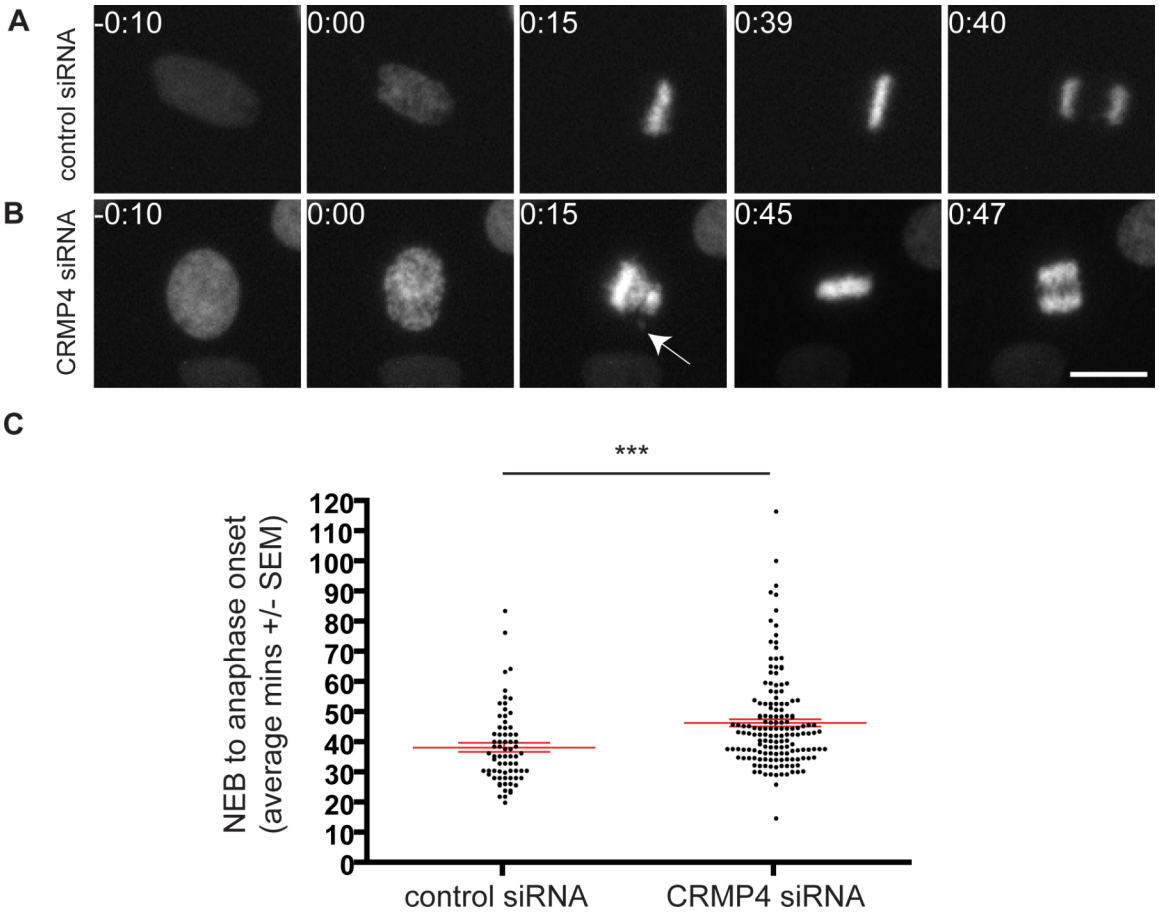
A
control siRNA
-0:10
0:00
0:15
0:39
0:40
B
CRMP4 siRNA
-0:10
0:00
0:15
0:45
0:47
C
***
NEB to anaphase onset
(average mins +/- SEM)
120
110
100
90
80
70
60
50
40
30
20
10
0
control siRNA
CRMP4 siRNA

Chapter 2 - Figure 4. CRMP4 depletion yields monopolar syntelic attachments.

HeLa cells transfected with either control siRNA or CRMP4 siRNA for 48 hours, or treated with SB-216763 (10uM) for 90 minutes were immunostained for α-tubulin (red), BubR1 (green) and DNA. Boxes outline either normal microtubule-kinetochore attachment (top panel) or abnormal monopolar syntelic attachments (middle and bottom panels). Bar, 10 um.

FIGURE 4

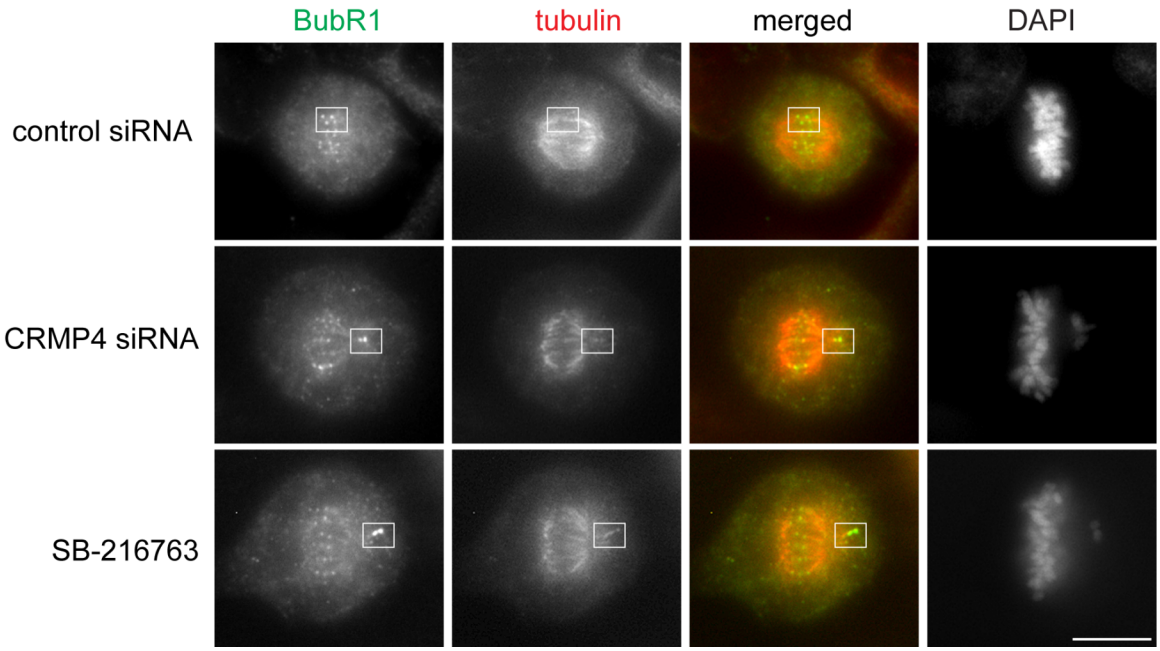
BubR1
tubulin
merged
DAPI
control siRNA
CRMP4 siRNA
SB-216763

Chapter 2 - Figure 5. CRMP4 depletion reduces cold stable microtubules.

(A) HeLa cells transfected with either control siRNA or CRMP4 siRNA for 48 hours, or treated with SB-216763 (10uM) for 90 minutes, were immunostained for α-tubulin (red) and DNA (blue). Bar, 5 um. Quantification of average tubulin intensity at the mitotic spindle (n=3, ns = non significant $p>0.05$, one sample *t* test compared to control siRNA.) (B) HeLa cells transfected with either control siRNA or CRMP4 siRNA for 48 hours, or treated with SB-216763 (10uM) for 90 minutes, were incubated with ice cold media for 10 minutes and immunostained for α-tubulin (red) and DNA (blue). Bar, 5 um. Quantification of average tubulin intensity at the mitotic spindle following incubation with ice cold media for 10 mins. Both CRMP4 depletion (n=3, $**p<0.01$, one sample *t* test compared to control siRNA) and incubation with SB-216763 (n=3, $*p<0.05$, one sample *t* test compared to control siRNA) resulted in a reduction in the average tubulin intensity at the mitotic spindle. n=3 refers to 3 independent experiments where at least 19 cells were analyzed in each experiment.

FIGURE 5

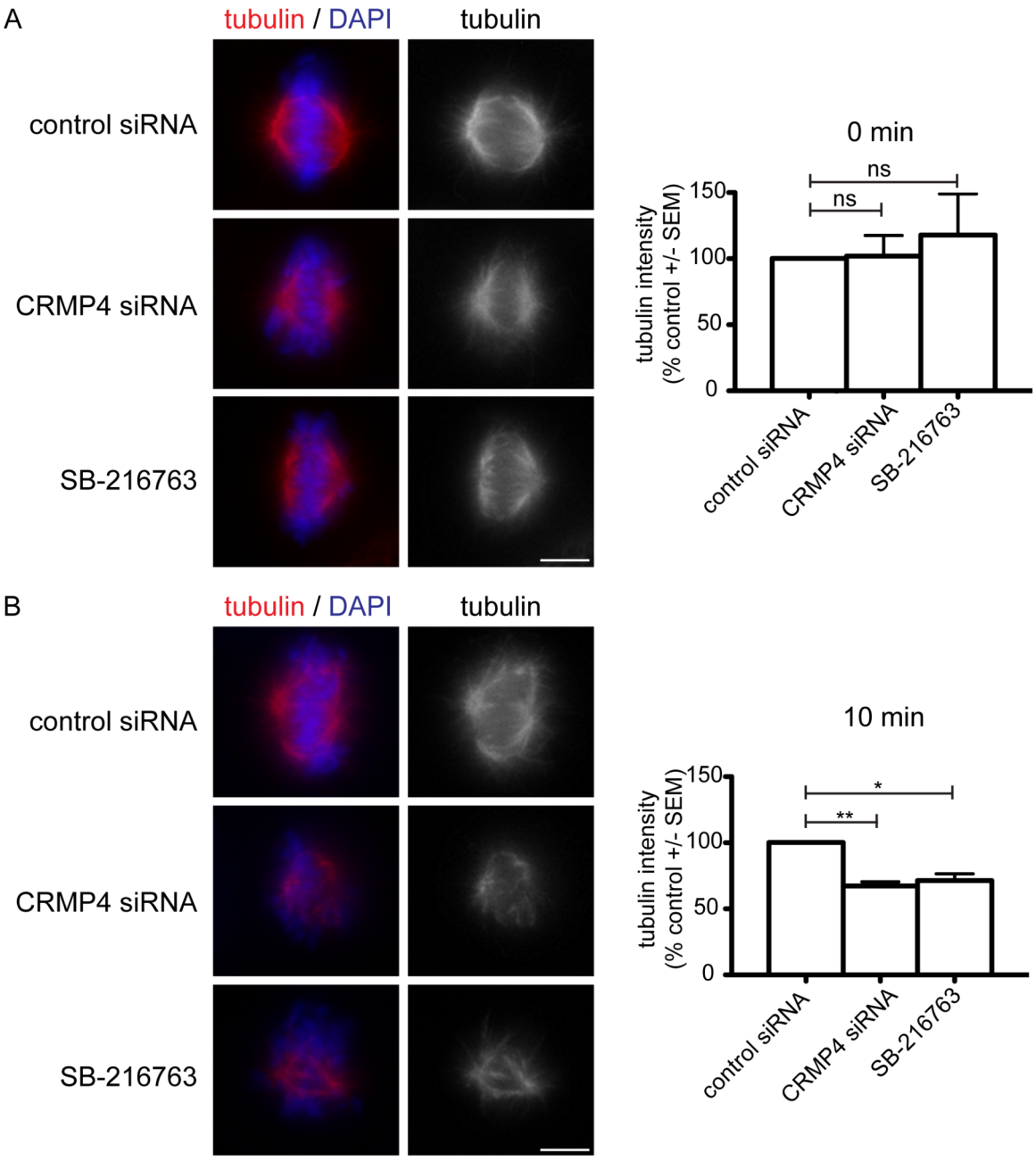
A
tubulin / DAPI
tubulin
control siRNA
CRMP4 siRNA
SB-216763
0 min
ns
ns
tubulin intensity
(% control +/- SEM)
150
100
50
0
control siRNA
CRMP4 siRNA
SB-216763
B
tubulin / DAPI
tubulin
control siRNA
CRMP4 siRNA
SB-216763
10 min
*
**
tubulin intensity
(% control +/- SEM)
150
100
50
0
control siRNA
CRMP4 siRNA
SB-216763

Chapter 2 - Figure 6. GSK3-dependent phosphorylation of CRMP4 during mitosis.

(A) HeLa cells were synchronized by double thymidine block, released into thymidine-free media and collected at different time intervals (number indicates hours post-release). Lysates were immunoblotted for pCRMP4 and total CRMP4. CRMP4 is phosphorylated throughout mitotic progression and is dephosphorylated as the cells complete mitosis. We observed that the majority of synchronized HeLa cells were in metaphase between 9-10 hours following release from the second thymidine block. By 12 hours, the majority of cells had completed mitosis. (B) HeLa cells were synchronized by double thymidine block, released into thymidine-free media for 7.5 hours, and were incubated with either SB-216763 (10 uM) or CT-99021 (2 uM) for 90 minutes. Immunoblot of lysates with a pCRMP4 or CRMP4 antibody showed that GSK3 inhibition with either SB-216763 or CT-99021 reduced the amount of pCRMP4 compared to DMSO treatment. (C) HeLa cells were synchronized with nocodazole (1 uM) for 14.5 hours after which either SB-216763 (10 uM) or CT-99021 (2 uM) was added for 90 minutes. Immunoblot of lysates with a pCRMP4 or CRMP4 antibody show that GSK3 inhibition with either SB-216763 or CT-99021 reduced the amount of pCRMP4 compared to DMSO treatment. (D) HeLa cells were transfected with L-CRMP1-V5 and either blocked with nocodazole for 16 hours or treated with calyculin for 30 mins. L-CRMP1-V5 was immunoprecipitated from lysates and immunoblotted with a pThreonine antibody. CRMP1 phospho-threonine levels did not increase following nocodazole treatment, while calyculin treatment did increase phospho-threonine levels. (E) HeLa cells were transfected with S-CRMP2-V5 and either blocked with nocodazole for 16 hours or treated with calyculin for 30 mins. S-CRMP2-V5 was immunoprecipitated from lysates and immunoblotted with a pCRMP2 (pThr509/514) antibody. Phospho-CRMP2 levels did not increase following nocodazole treatment, while calyculin treatment did increase phospho-CRMP2 levels. Input lysates were immunoblotted for pCRMP4 and CRMP4. (F) Lysates from HeLa cells synchronized by double thymidine block were immunoblotted for pCRMP4, CRMP4, pCRMP2 (pThr509/514) and GAPDH. Endogenous phospho-CRMP2 levels were unchanged throughout mitosis but increased with calyculin treatment.

FIGURE 6

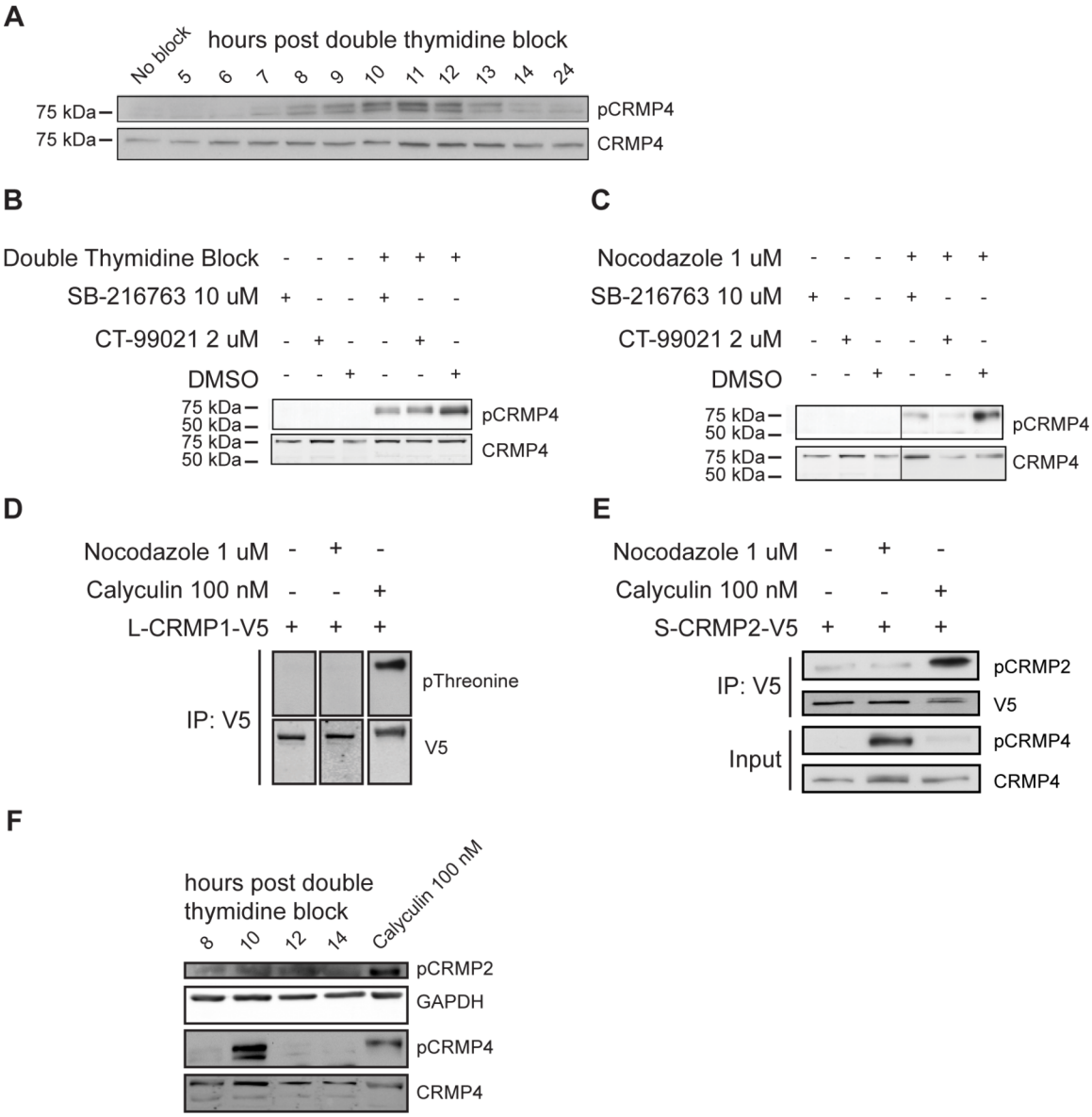
A
hours post double thymidine block
No block
5
6
7
8
9
10
11
12
13
14
24
75 kDa
75 kDa
pCRMP4
CRMP4
B
Double Thymidine Block - - - + + +
SB-216763 10 uM + - - + - -
CT-99021 2 uM - + - - + -
DMSO - - + - - +
75 kDa
50 kDa
75 kDa
50 kDa
pCRMP4
CRMP4
C
Nocodazole 1 uM - - - + + +
SB-216763 10 uM + - - + - -
CT-99021 2 uM - + - - + -
DMSO - - + - - +
75 kDa
50 kDa
75 kDa
50 kDa
pCRMP4
CRMP4
D
Nocodazole 1 uM - + -
Calyculin 100 nM - - +
L-CRMP1-V5 + + +
IP: V5
pThreonine
V5
E
Nocodazole 1 uM - + -
Calyculin 100 nM - - +
S-CRMP2-V5 + + +
IP: V5
pCRMP2
V5
Input
pCRMP4
CRMP4
F
hours post double thymidine block
8
10
12
14
Calyculin 100 nM
pCRMP2
GAPDH
pCRMP4
CRMP4

Chapter 2 - Figure 7. Phosphorylated CRMP4 localizes with the mitotic apparatus.

Immunofluorescence detection of pCRMP4, α-tubulin, and DNA in mitotic HeLa cells. Phosphorylated CRMP4 accumulates both at the cortex adjacent to the spindle poles and spindle microtubules during metaphase. Immunofluorescence detection of pCRMP4 is reduced in HeLa cells treated with the GSK3 inhibitor SB-216763 (10 uM) for 90 mins or transfected with CRMP4 siRNA. Bar, 10 um.

FIGURE 7

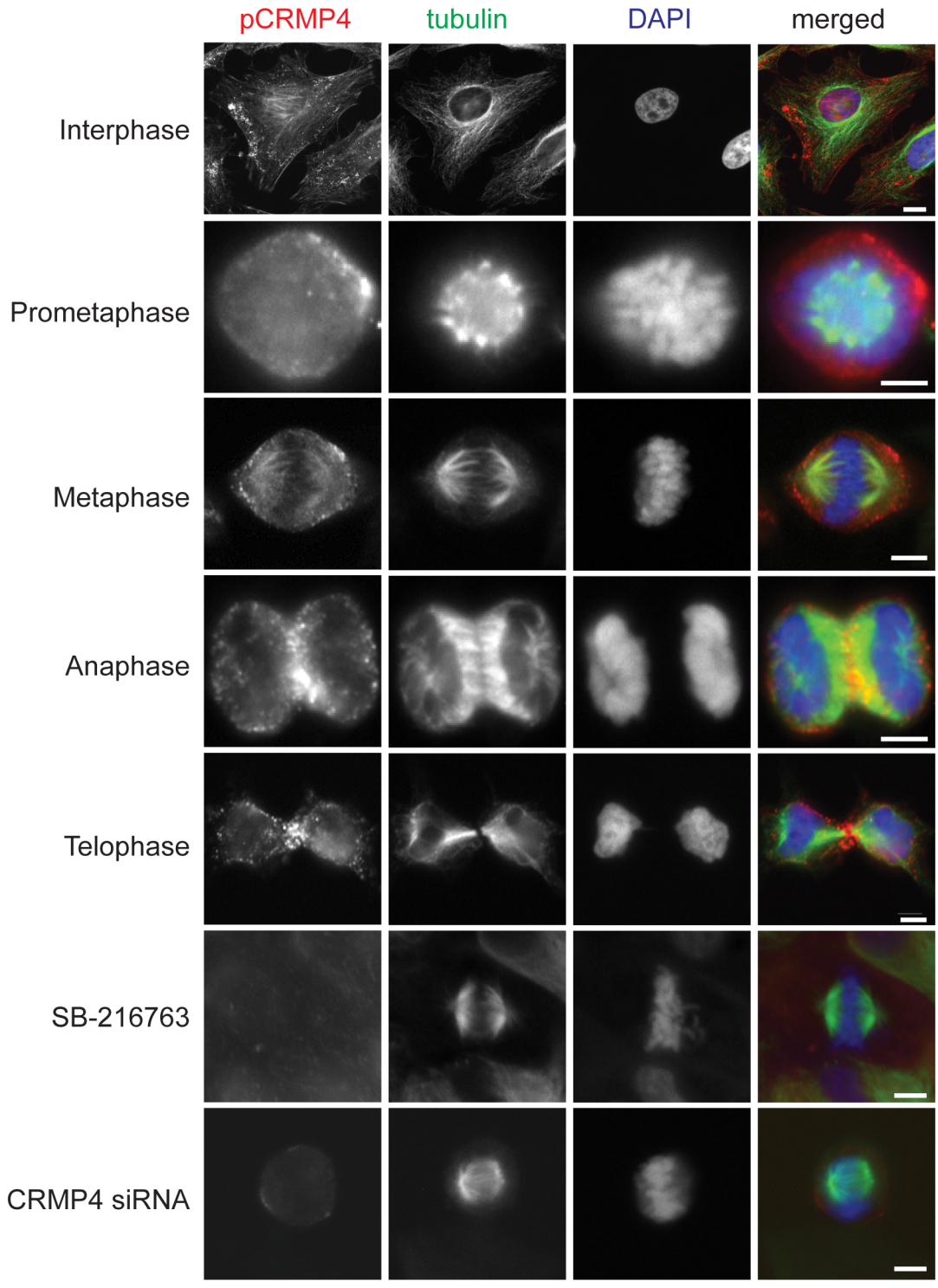
pCRMP4
tubulin
DAPI
merged
Interphase
Prometaphase
Metaphase
Anaphase
Telophase
SB-216763
CRMP4 siRNA

Chapter 2 - Figure 8. Chromosomal alignment during mitosis is phospho-CRMP4-dependent.

Overexpression of L-CRMP4-WT-V5 rescued the abnormal metaphase phenotype observed with CRMP4 knockdown (n=3, one way ANOVA, post-hoc Bonferroni test, ***$p<0.001$ compared CRMP4 siRNA) while overexpression of the CRMP4 mutant L-CRMP4-AAA-V5 fails to rescue the phenotype (n=3, one way ANOVA, post-hoc Bonferonni test, ns = non significant $p>0.05$ compared to CRMP4 siRNA). n=3 refers to 3 independent experiments where at least 100 cells were scored per experiment.

FIGURE 8

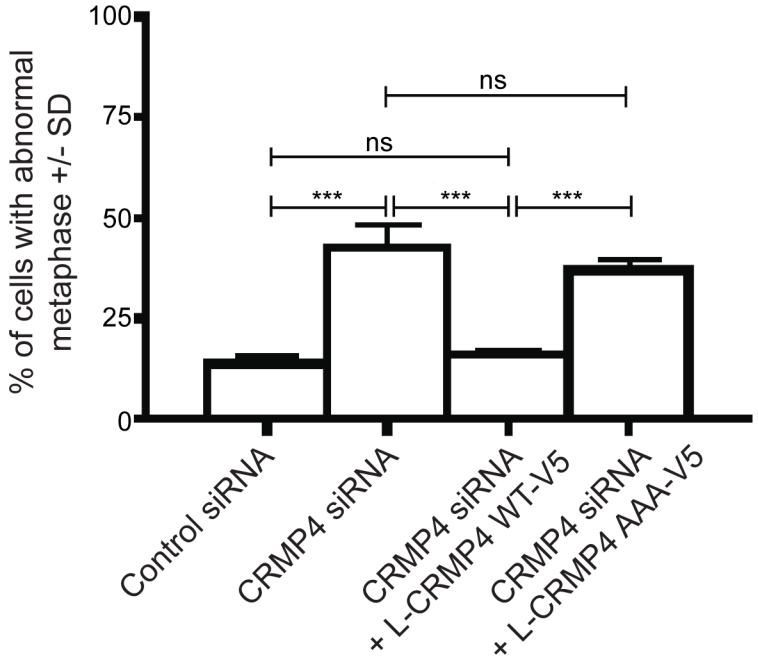
% of cells with abnormal metaphase +/- SD
100
75
50
25
0
ns
ns
***
***
***
Control siRNA
CRMP4 siRNA
CRMP4 siRNA + L-CRMP4 WT-V5
CRMP4 siRNA + L-CRMP4 AAA-V5

Chapter 2 - Figure 9. CRMP4 localization to the mitotic spindle is phospho-dependent.

(A) HeLa cells were transfected with either L-CRMP4-WT-V5 or L-CRMP4-AAA-V5. Immunofluorescence was used to detect V5, α-tubulin, and DNA in HeLa cells in metaphase. HeLa cells were permeabilized with a cytosolic extraction buffer prior to fixation. L-CRMP4-WT-V5 localizes along the spindle microtubules while L-CRMP4-AAA-V5 does not. Bar, 10 um. (B) HeLa cells were incubated with either 10 uM SB-216763 or DMSO for 90 minutes prior to fixation and immunostaining for CRMP4. Bar, 10 um. (C) Quantification of CRMP4 intensity at the mitotic spindle shows a decrease in CRMP4 intensity in SB-216763 treated HeLa cells (n=3, *$p<0.05$, Student's *t* test compared to DMSO). n=3 refers to 3 independent experiments where at least 20 cells were analyzed per experiment.

FIGURE 9

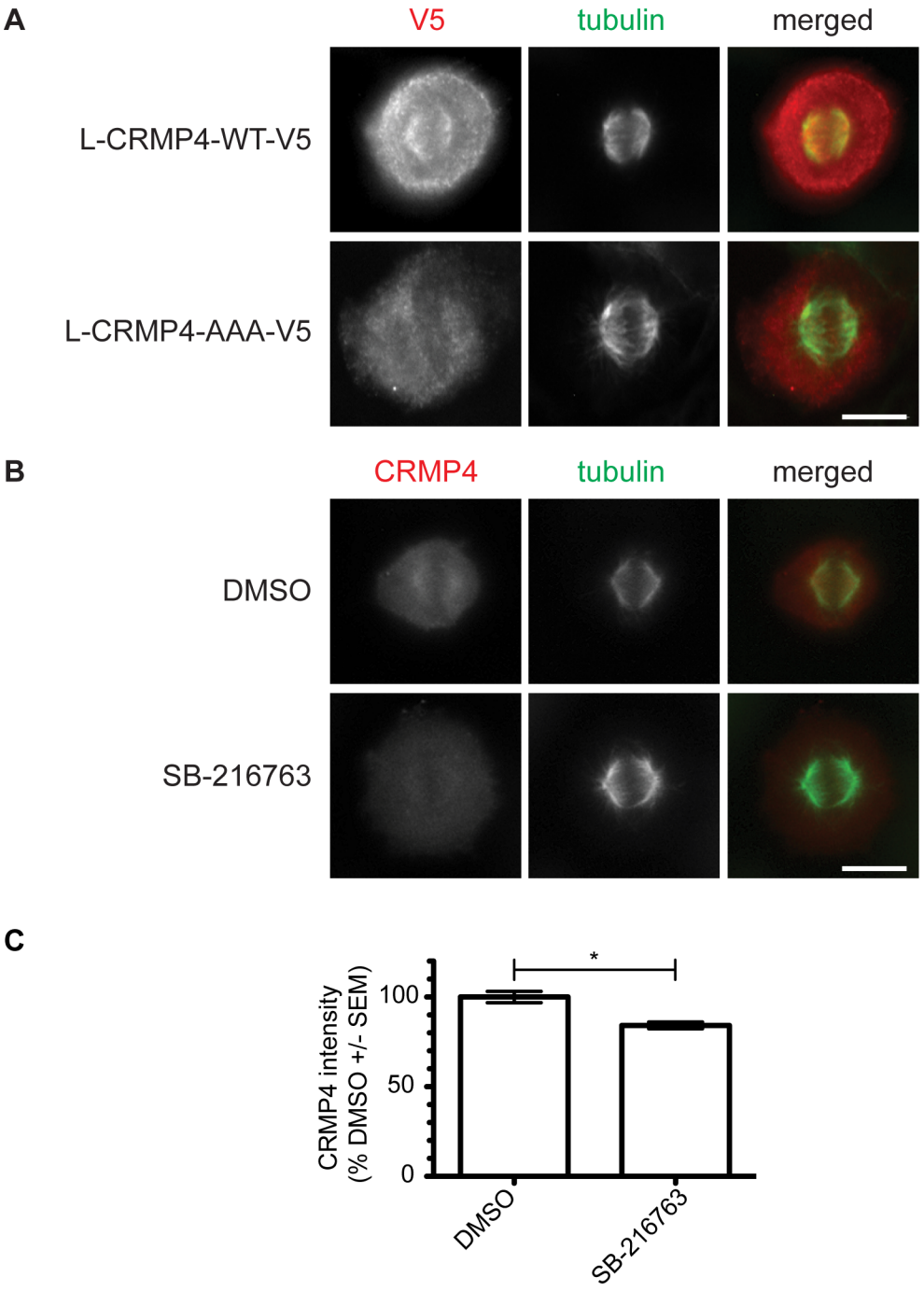
A
V5
tubulin
merged
L-CRMP4-WT-V5
L-CRMP4-AAA-V5
B
CRMP4
tubulin
merged
DMSO
SB-216763
C
CRMP4 intensity
(% DMSO +/- SEM)
100
50
0
*
DMSO
SB-216763

Chapter 2 - Figure 10. siRNA-mediated knockdown of CRMP4 alters spindle morphology.

(A) HeLa cells were transfected with either control or CRMP4 siRNA, and for rescue experiments were co-transfected with either L-CRMP4-WT-V5 or L-CRMP4-AAA-V5. In some experiments, HeLa cells were treated with SB-216763 (10 um) for 90 mins. HeLa cells were permeabilized with a cytosolic extraction buffer prior to fixation with 4% PFA and immunofluorescence detection of α-tubulin and DNA. Bar, 10 um. (B) Bar graph plotting pole to pole distance. HeLa cells transfected with CRMP4 siRNA had a shorter pole to pole distance (n=3, **p=0.0059, Student's *t* test compared to control siRNA). Co-transfection with a L-CRMP4-WT-V5 construct rescued the shorter pole to pole distance phenotype (n=3, **p=0.0069, Student's *t* test compared to CRMP4 siRNA) while a L-CRMP4-AAA-V5 construct did not rescue (n=3, ns=non significant p>0.05, Student's *t* test compared to CRMP4 siRNA). HeLa cells treated with SB-216763 (10 uM) for 90 mins resulted in a shorter pole to pole distance (n=3, ***p<0.0001, Student's *t* test compared to control siRNA; n=3, *p=0.0322, Student's *t* test compared to CRMP4 siRNA). (C) Bar graph plotting spindle width. HeLa cells transfected with either control siRNA, CRMP4 siRNA or treated with SB-216763 did not show any differences in spindle width (n=3, ns=non significant p>0.05, Student's *t* test compared to control siRNA). n=3 refers to 3 independent experiments where at least 20 cells were analyzed per experiment.

FIGURE 10

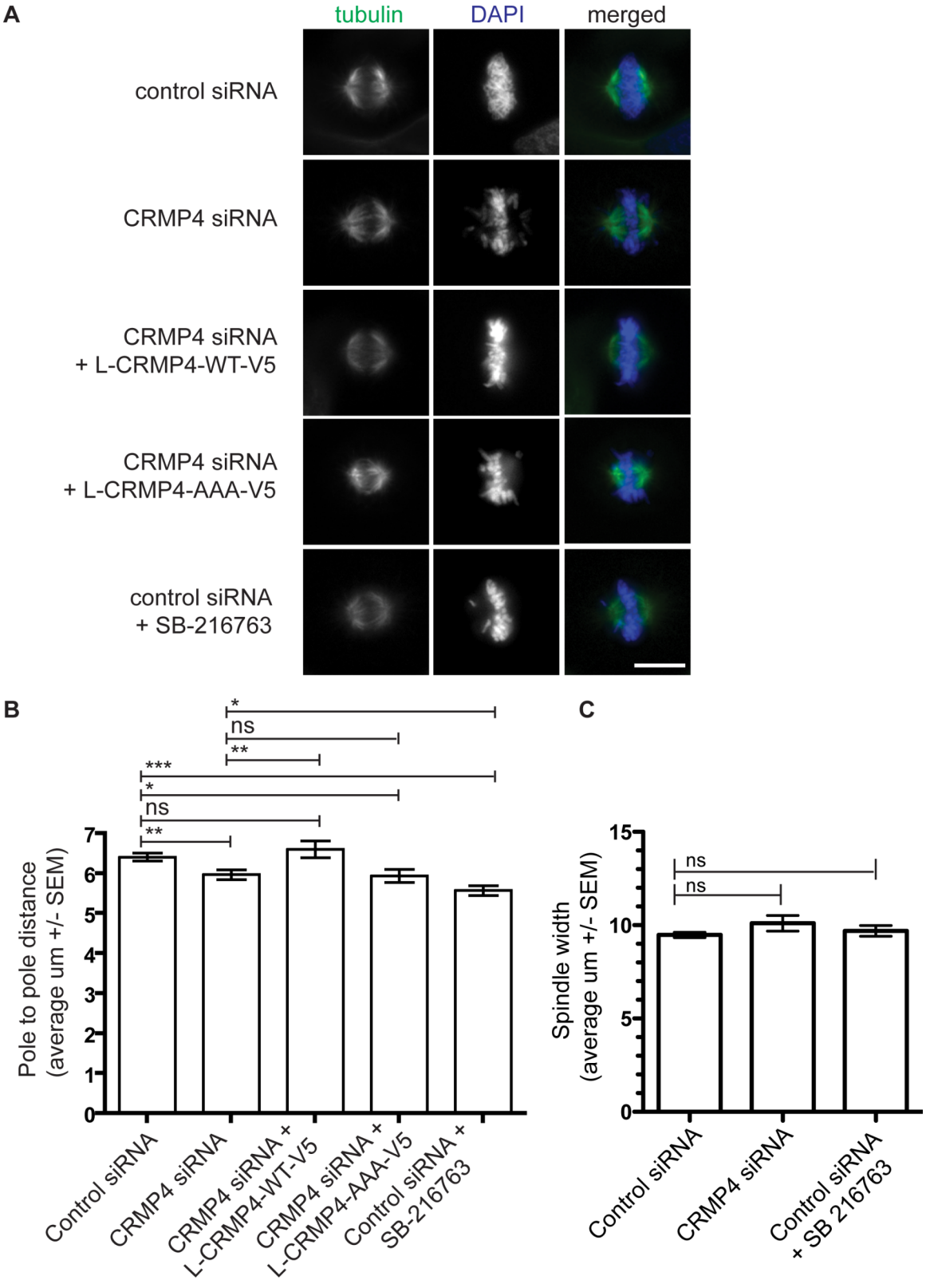
A
tubulin
DAPI
merged
control siRNA
CRMP4 siRNA
CRMP4 siRNA
+ L-CRMP4-WT-V5
CRMP4 siRNA
+ L-CRMP4-AAA-V5
control siRNA
+ SB-216763
B
Pole to pole distance
(average um +/- SEM)
0
1
2
3
4
5
6
7
*
ns
**
***
*
ns
**
Control siRNA
CRMP4 siRNA
CRMP4 siRNA +
L-CRMP4-WT-V5
CRMP4 siRNA +
L-CRMP4-AAA-V5
Control siRNA +
SB-216763
C
Spindle width
(average um +/- SEM)
0
5
10
15
ns
ns
Control siRNA
CRMP4 siRNA
Control siRNA
+ SB 216763

Chapter 2 - Figure S 1. GSK3 inhibition delays mitotic exit.

Flow cytometry graphs of double thymidine block synchronized HeLa cells transfected with CRMP4 siRNA or transfection reagent alone. HeLa cells were collected at different time intervals following release into thymidine-free media (upper and middle panels) or media containing SB-216763 (10 uM) (lower panels). Knockdown of CRMP4 protein expression did not delay mitotic entry or exit, while treatment with SB-216763 resulted in a delay in mitotic progression. M2= 2n peak, M4= 4n peak.

FIGURE S1

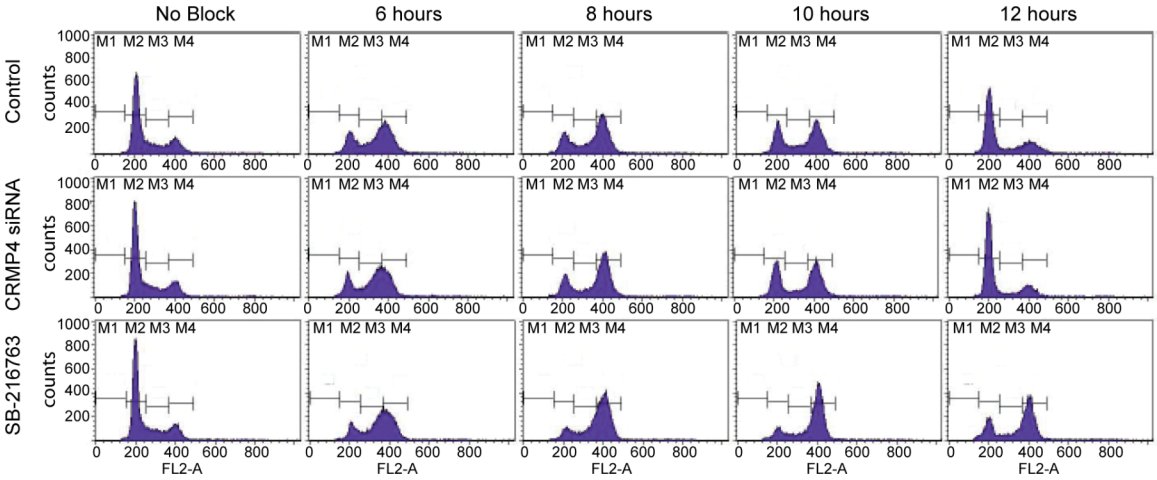
No Block
6 hours
8 hours
10 hours
12 hours
Control
CRMP4 siRNA
SB-216763
counts
M1 M2 M3 M4
FL2-A

Chapter 2 - Figure S 2. Phosphorylation of L-CRMP4 during mitosis.

(A) An increase in L-CRMP4 phosphorylation at the Thr622 residue was observed with pT622 CRMP4 antibody in nocodazole blocked HeLa cell lysates. The phospho doublet band was also detected with a CRMP4 antibody, however the upper band was faint compared to the lower band. Overexpression of L-CRMP4-V5 or S-CRMP4-V5 in HeLa cells reveals that the majority of endogenous CRMP4 is L-CRMP4. (B) Lysates from HeLa cells transfected with either control or CRMP4 siRNA, and synchronized with a double thymidine block, were probed with either pT622 CRMP4, CRMP4 or GAPDH. (C) HeLa cells were transfected with pcDNA V5, L-CRMP4 WT-V5, or L-CRMP4 AAA-V5 and were blocked with nocodazole (1 uM) for 16 hours. V5 was immunoprecipitated from the lysates and immunoblotted with pCRMP4 or V5 antibodies. The pCRMP4 antibody did not recognize L-CRMP4 AAA-V5.

FIGURE S2

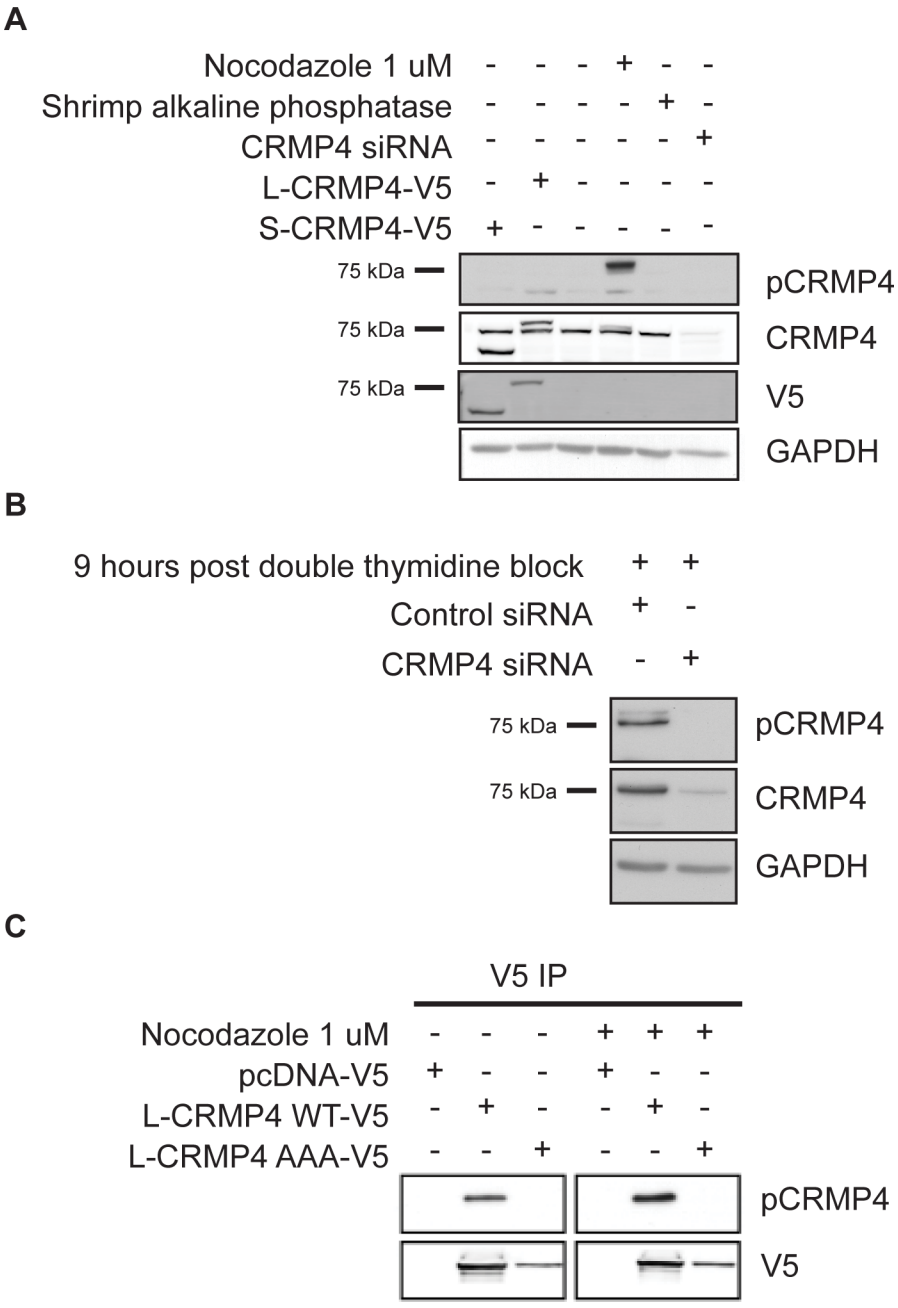
A
Nocodazole 1 uM - - - + - -
Shrimp alkaline phosphatase - - - - + -
CRMP4 siRNA - - - - - +
L-CRMP4-V5 - + - - - -
S-CRMP4-V5 + - - - - -
75 kDa
pCRMP4
75 kDa
CRMP4
75 kDa
V5
GAPDH
B
9 hours post double thymidine block + +
Control siRNA + -
CRMP4 siRNA - +
75 kDa
pCRMP4
75 kDa
CRMP4
GAPDH
C
V5 IP
Nocodazole 1 uM - - - + + +
pcDNA-V5 + - - + - -
L-CRMP4 WT-V5 - + - - + -
L-CRMP4 AAA-V5 - - + - - +
pCRMP4
V5

Chapter 2 - Figure S 3. Representative line scan of pole to pole distance measurements.

For pole to pole distance measurements, tubulin fluorescence intensities were measured from one end of the cell to the other end along the spindle axis using ImageJ, and when plotted as a function of spindle position, the tubulin intensity gave two peaks corresponding to the spindle poles.

FIGURE S3

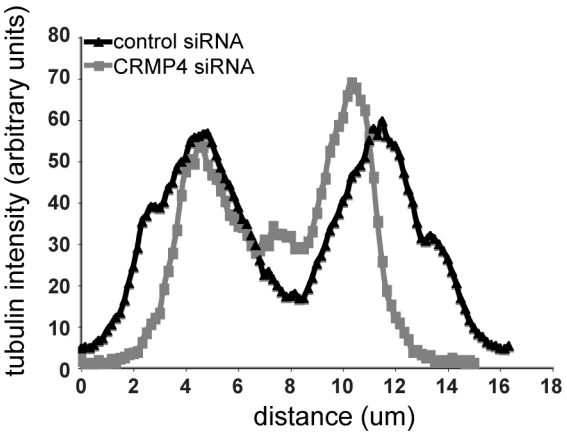
control siRNA
CRMP4 siRNA
tubulin intensity (arbitrary units)
distance (um)
0
10
20
30
40
50
60
70
80
0
2
4
6
8
10
12
14
16
18

CHAPTER 3

3 ADENO-ASSOCIATED VIRUS-MEDIATED DELIVERY OF C4RIP AS A THERAPEUTIC AGENT TO PROMOTE CNS REGENERATION

3.1 PREFACE

Following central nervous system (CNS) injury, myelin associated inhibitors (MAIs) and chondroitin sulfate proteoglycans (CSPGs) signal through receptor complexes located on damaged axons to activate the intracellular protein RhoA. RhoA activation results in neuronal cytoskeleton rearrangements that lead to the inhibition of nerve regeneration. The RhoA effector proteins that mediate these events are not well characterized. We have previously identified CRMP4 as a RhoA-interacting protein that mediates neurite outgrowth inhibition in response to myelin. Antagonizing RhoA-L-CRMP4 interactions with a competitive antagonist C4RIP attenuates neurite outgrowth inhibition in dorsal root ganglion neurons *in vitro*. The aim of this study was to investigate the role of CRMP4 in CNS regeneration in an *in vivo* preclinical model of CNS injury. We evaluate the ability of adeno-associated virus-mediated expression of C4RIP to promote retinal ganglion cell neuronal survival and axon regeneration following an optic nerve injury in the adult rat.

3.2 ABSTRACT

MAIs and CSPGs signal through receptor complexes located on the neuronal plasma membrane to activate the intracellular protein RhoA. RhoA pathway antagonists promote neuronal survival and regeneration following CNS injury, however side effects may limit their therapeutic application because RhoA is ubiquitously expressed and regulates multiple cellular processes including cell division, cell migration and dendritic spine morphology (Riento and Ridley 2003). In an attempt to identify more specific therapeutic targets to promote CNS regeneration following injury, we have previously identified CRMP4 as a RhoA interacting protein that mediates neurite outgrowth inhibition in dorsal root ganglion neurons (DRGs) *in vitro*. Through a structure function analysis we identified a fragment of CRMP4, C4RIP (CRMP4b-RhoA Inhibitory Peptide) that antagonizes RhoA-L-CRMP4 interactions and promotes neurite outgrowth inhibition of DRGs on inhibitory substrates *in vitro*. Here, we evaluate the ability of adeno-associated virus (AAV)-mediated expression of C4RIP to promote retinal ganglion cell (RGC) neuronal survival and axon regeneration following an optic nerve injury in the adult rat. We demonstrate that CRMP4 is expressed in adult RGCs and AAV serotype 2 directs selective C4RIP transgene expression in adult RGCs. However, AAV C4RIP does not promote RGC neuronal survival or axon regeneration following optic nerve injury even if RGCs are in an active growth state. Analysis of C4RIP retinal expression levels by immunoblot suggests that C4RIP expression is insufficient for it to act as a competitive antagonist to RhoA-L-CRMP4 interactions. We discuss strategies for future studies focusing on increasing C4RIP levels in RGCs to promote axon regeneration following optic nerve injury.

3.3 INTRODUCTION

CNS neurons fail to spontaneously regenerate following injury, in part due to the expression of inhibitory molecules including MAIs and CSPGs in the glial scar (Yiu and He 2006). MAIs and CSPGs signal through distinct receptor complexes but the inhibitory signals converge to activate the cytosolic protein RhoA and its downstream effector Rho-associated kinase (ROCK) (Jin and Strittmatter 1997; Lehmann, Fournier et al. 1999; Borisoff, Chan et al. 2003; Fournier, Takizawa et al. 2003). Although RhoA antagonists promote neuronal survival and regeneration *in vitro* and *in vivo* (Lehmann, Fournier et al. 1999; Dergham, Ellezam et al. 2002; Winton, Dubreuil et al. 2002; Dubreuil, Winton et al. 2003; Fournier, Takizawa et al. 2003; Monnier, Sierra et al. 2003; Fischer, Petkova et al. 2004; Bertrand, Winton et al. 2005; Bertrand, Di Polo et al. 2007; Lord-Fontaine, Yang et al. 2008), the widespread roles of RhoA in multiple cellular processes and cell types may limit its potential as a therapeutic target (Riento and Ridley 2003). In an attempt to discover more specific therapeutic targets to promote nerve regeneration, our lab previously identified the cytosolic phosphoprotein L-CRMP4 (Long-Collapsin Response Mediator Protein 4, previously referred to as CRMP4b) as a protein that physically and functionally interacts with RhoA to mediate neurite outgrowth inhibition (Alabed, Pool et al. 2007).

CRMPs are cytosolic phosphoproteins that are highly expressed in the nervous system during development and play widespread roles in migration and axonal growth (Goshima, Nakamura et al. 1995; Wang and Strittmatter 1996; Gaetano, Matsuo et al. 1997; Byk, Ozon et al. 1998; Quinn, Gray et al. 1999; Quach, Duchemin et al. 2004). The CRMPs are homologs of UNC-33, a protein originally identified in *Caenorhabditis elegans* to be important for axon extension and guidance (Hedgecock, Culotti et al. 1985; Siddiqui and Culotti 1991). The CRMP family is composed of five family members (CRMP1-5) in vertebrates (Goshima, Nakamura et al. 1995; Minturn, Fryer et al. 1995; Byk, Dobransky et al. 1996; Gaetano, Matsuo et al. 1997; Wang and Strittmatter 1997; Inatome, Tsujimura et al. 2000; Quinn, Chen et al. 2003). Each CRMP allele produces two transcripts that differ in their amino terminal domains producing long (L-CRMP) and

short (S-CRMP) isoforms that have been alternatively referred to as ‘a’ and ‘b’ isoforms (Quinn, Chen et al. 2003; Yuasa-Kawada, Suzuki et al. 2003; Alabed, Pool et al. 2007; Pan, Chao et al. 2009; Alabed, Pool et al. 2010).

The role of CRMP4 in the nerve regeneration has not been extensively studied. In a rat hypoglossal nerve injury model CRMP4a mRNA levels are unchanged following axotomy (Suzuki, Nakagomi et al. 2003). CRMP4 mRNA and protein expression are increased in both adult sciatic motor neurons and DRG neurons that are regenerating following a sciatic nerve lesion (Minturn, Fryer et al. 1995; Jang, Shin et al. 2010). Furthermore, an increase in CRMP4 protein expression is observed in the peripheral axon following the injury (Jang, Shin et al. 2010). With respect to CRMP4 function in CNS inhibition, we have previously demonstrated that L-CRMP4 can physically and functionally interact with RhoA to mediate neurite outgrowth inhibition *in vitro* (Alabed, Pool et al. 2007; Alabed, Pool et al. 2010). CRMP4 depletion in DRGs promotes neurite outgrowth on inhibitory CNS myelin (Alabed, Pool et al. 2007). Further, blockade of the RhoA-L-CRMP4 interaction with a competitive peptide, C4RIP (CRMP4b-RhoA Inhibitory Peptide), attenuates neurite outgrowth inhibition on both CNS myelin and aggrecan (Fig. 1) (Alabed, Pool et al. 2007). These findings identify CRMP4 as a convergent regular of axon outgrowth inhibition. However, the biological function of CRMP4 in an *in vivo* model of regeneration has not been extensively studied. The objective of this study is to evaluate the therapeutic potential of C4RIP to promote CNS nerve regeneration in a preclinical adult rat optic nerve injury model. We have developed an adeno-associated virus (AAV) containing C4RIP as a potential therapeutic agent to promote axon regeneration following CNS injury.

3.4 MATERIALS AND METHODS

3.4.1 Recombinant Adeno-Associated Virus Serotype 2 vector

C4RIP-V5 cDNA was amplified by PCR from pcDNA 3.1 C4RIP-V5 (Alabed, Pool et al. 2007) using the following primers: 5' GCCAAGCTTGCTTGAACCATGG CTTCG 3', and 5' GCCAAGCTTTCAATGGT GATGGTGATGATG 3'. The amplified C4RIP-V5 PCR product was digested with HindIII and inserted into the HindIII site downstream of the hybrid chick β-actin/CMV enhancer promoter in the plasmid pXX-UF12, which is derived from pTR-UF5 (Zolotukhin, Potter et al. 1996). The plasmid pXX-UF12 contains AAV terminal repeats, a simian virus 40 polyadenylation sequence and an internal ribosomal entry site (IRES) driven GFP. Vectors were packaged, concentrated and titered as previously described (Hauswirth, Lewin et al. 2000).

3.4.2 Intraocular Injection of Viral Vectors

All animal procedures followed guidelines from the Canadian Council of Animal Care. Surgeries were performed on female Sprague-Dawley rats (180g-200g) under general gas anesthesia (2-3% isofluorane mixed in oxygen, 0.8 L/min). The conjunctiva was dissected away until the sclera was reached. A small puncture wound was made in the superior quadrant through the sclera just temporal to the episcleral vein using a 30-gauge needle. Intraocular injections of the viral vectors (5 μl) into the vitreous space of the left eye were performed using a fine glass tube attached to a 10 μl-Hamilton syringe. The tip of the needle was inserted through the small puncture wound in the sclera at a 45º angle, with the tip of the needle pointed towards the optic nerve head (Fig. 2A). This route of administration avoided injury to the lens and iris, which have been shown to promote RGC survival and regeneration (Leon, Yin et al. 2000). The injection was performed over 1 minute, after which the needle was held in place for approximately 2 minutes before slowly removing the needle. The puncture wound was sealed with surgical glue (Indermill, Tyco Health Care, Montreal, Quebec). Further surgical procedures were performed 3-4 week after the administration of viral vectors to allow AAV-mediated transgene

expression levels to plateau. It has been proposed that the delay in AAV-mediated transgene expression *in vivo* is due to the need to convert single-stranded viral DNA to a double-strand prior to active transcription (Ferrari, Samulski et al. 1996).

3.4.3 Retrograde labeling and RGC survival

RGCs were retrogradely labeled through the application of 2% FluoroGold (Fluoro-chrome, Englewood, CO) in 0.9% NaCl containing 10% DMSO to both superior colliculi (Fig. 2B). Seven day following the application of FluoroGold, the left optic nerve was axotomized 0.5-1 mm from the back of the eye, with care to avoid injury to the ophthalmic artery. Fourteen days later, the rats were intracardially perfused with 4% paraformaldehyde (PFA) in 0.1 M phosphate buffer (PB, pH=7.2), and retinal flat mounts were prepared as described previously (Pernet, Hauswirth et al. 2005). FluoroGold-labeled neurons were counted in 12 standard retinal areas as described previously (Cheng, Sapieha et al. 2002; Pernet, Hauswirth et al. 2005; Bertrand, Di Polo et al. 2007). Data analysis was performed using Prism by using Student's *t* test.

3.4.4 Forcep Crush Injury, Lens Injury and Immnohistochemistry

The lacrymal glands and extra-ocular muscles were resected to expose the optic nerve. The epineurium was cut along the long axis of the optic nerve and the optic nerve was crushed approximately 2 mm from the back of the eye with an angled jeweler's forcep (Dumont #5) for 10 seconds (Fig. 2C). For a microcrush lesion, a 10-0 pt suture was tied around the optic nerve approximately 2 mm from the back of the eye, kept in place for 1 minute and removed (Fig. 2C). Optic nerve injury was visualized by the clearance of the crush site and the retinal vascular integrity was evaluated by fundoscopic examination. Rats with impaired vascular integrity were excluded from the study. In some cases, we performed a lens injury by puncturing the sclera about 2 mm above the optic nerve head with a 30 gauge needle to intentionally damage to posterior surface of the lens (Fig. 2D). We immediately visualized the lens injury through the cornea and observed a cataract form within a week of the injury. Thirteen days later, an intraocular injection of 5 μl of 1% cholera toxin beta-subunit (CTβ) (Sigma, Oakville, ON) in phosphate-buffered

saline (PBS) through the same puncture wound was performed to anterogradely label regenerating axons. 24 hours later, rats were intracardially perfused with 4% PFA 0.1 M PB and their left eye and optic nerve was removed. The anterior part of the eye and the lens were dissected away, and the eye cup and optic nerve were fixed for an additional 2 hours at 4 ºC. The eye cup and optic nerve were cyroprotected in 30 % sucrose in PBS overnight at 4 ºC, and embedded in OCT (optimal cutting temperature) compound (Tissue-Tek, Miles Laboratories, Elkhart, IN) and frozen in 2-methylbutane on dry ice. Cryosections (14 μm for optic nerves and 16 μm for retinas) were collected on Superfrost slides (Fischer Scientific) and processed for immunohistochemistry. Sections were post-fixed for 15 minutes in 4% PFA, followed by blocking in blocking solution (5% bovine serum albumin (BSA), 0.3% Triton-X100 (Sigma), in PBS) for 1 hour at room temperature. Primary antibodies were diluted in blocking solution and incubated overnight at 4ºC. The following primary antibodies were used: goat CTβ (List Biological Laboratories), mouse βIII tubulin (Covance), mouse V5 (Sigma), mouse PLP, rabbit CRMP4 and rabbit L-CRMP4 as previously described (Alabed, Pool et al. 2007). Secondary antibodies were diluted in blocking solution and incubated 1 hour at room temperature. Secondary antibodies used were: rabbit anti-goat biotin; anti-mouse-FITC, Alexa-568; anti-rabbit-FITC, Alexa-568 (Invitrogen). Streptavidin-FITC and Alexa-568 (Invitrogen) were also used to amplify the biotin signal.

3.4.5 Analysis of RGC axon regeneration

Axon regeneration was analyzed by counting the number of CTβ-positive axons that crossed a virtual line parallel to the lesion site divided by optic nerve width (Fig. 2E). The lesion site was identified by darkfield microscopy. CTβ-positive axons were counted at distances of 100 um, 250 um, 500 um, 750 um, and 1000 um from the lesion site in at least four sections per animal from at least 3 animals per condtion. Data analysis was performed using Prism by two-way ANOVA followed by Bonferroni post hoc test.

3.4.6 Immunoblot of Retinal lysates

Rats were given an overdose of 70% chloral hydrate in H_2O, their retinas were quickly dissected away and manually homogenized using a pestle in lysis buffer (20 mM Tris, pH=8.0, 135 mM NaCl, 1% NP-40, 0.1% sodium dodecyl sulfate (SDS), 10% glycerol, and 1X protease inhibitors (Roche)) at 4 ºC. Retinal lysates were sonicated for 20 seconds at 20% amplitude followed by a 10 minute centrifugation at 13,200 rpm at 4 ºC. Supernatant lysate was collected and stored at -20 ºC. 100 μg protein samples were separated on 10% sodium dodecyl sulfate (SDS)-polyacrylamide gels (PAGE) and transferred to polyvinylidene fluoride membranes (PVDF). Membranes were blocked for 1 hour with 5% milk in tris-buffered saline 0.1% Tween-20 (TBST). Primary antibodies were diluted in 5% milk TBST and incubated overnight at 4 ºC. Primary antibodies used were: rabbit CRMP4 and rabbit L-CRMP4. Secondary antibodies were diluted in 5% milk TBST and incubated 1 hour at room temperature. Secondary antibody used was anti-rabbit antibody linked to horse radish peroxidase (HRP). Protein signal was detected used a chemiluminescence reagent (ECL, Amersham Biosciences).

3.5 RESULTS

3.5.1 CRMP4 is expressed in the adult retina

To determine if CRMP4 was expressed in the adult rat retina, retinal lysates were immunoblotted using two different CRMP4 antibodies: a CRMP4 antibody raised against the C-terminal domain common to L-CRMP4 and S-CRMP4, and a L-CRMP4 antibody raised against the unique N-terminus of L-CRMP4. Both L- and S-CRMP4 were expressed in the adult rat retina as detected with both CRMP4 and L-CRMP4 antibodies (Fig. 3A). To localize where CRMP4 was expressed in the retina, adult rat retinas were collected and immunostained with either a CRMP4 or a L-CRMP4 antibody, and a βIII tubulin antibody to visualize the RGCs. Immunostaining with the CRMP4 antibody revealed CRMP4 expression throughout the retina, with strong expression in the RGC and nerve fiber (NF) layers (Fig. 3B, top row). Immunostaining with the L-CRMP4 antibody revealed strong expression in the retinal layers that contained cell bodies: RGC layer, inner nuclear layer (INL), outer nuclear layer (ONL) (Fig. 3C middle row). L-CRMP4 expression was also observed in the outer plexiform layer (OPL) and the outer segment (OS) of the retina. Lower expression level of L-CRMP4 was observed in the IPL and NFL. The differences in expression pattern between CRMP4 and L-CRMP4 raises the possibility that L-CRMP4 and S-CRMP4b are targeted to different compartments with the RGC, where L-CRMP4 preferentially localizes to the cell body and S-CRMP4 preferentially localizes to dendrites and axons. However, L-CRMP4 is localized in RGC axons throughout the optic nerve (Fig. 3B, lower row). Interestingly, strong L-CRMP4 expression was also observed in cell bodies that were in aligned in rows along the long axis of the optic nerve (Fig. 3C). Some of the L-CRMP4 was co-localized with proteolipid protein (PLP) staining, which demonstrates that L-CRMP is also expressed in oligodendocytes. Further, we performed co-localization studies in retinas from eyes that had their RGCs retrogradely labeled with FluoroGold applied to the superior colliculi. L-CRMP4 immunoreactivity was observed in FluoroGold back-labeled RGCs (Fig. 3D, upper row). No immunoreactivity was seen when the L-CRMP4 antibody was pre-incubated with a blocking peptide, which demonstrates the specificity of the antibody (Fig. 3D, lower row).

3.5.2 Adeno-associated virus serotype 2 directs selective C4RIP transgene expression in adult retinal ganglion cells

We used a recombinant AAV serotype 2 to selectively transduce RGCs with C4RIP-V5. AAV-C4RIP-V5 was delivered through a single intraocular injection into the vitreous space of the eye. Retinas and optic nerves were collected 4 weeks following the administration of AAV-C4RIP-V5, which is the time required for transgene expression to reach a plateau in adult rat RGCs (Bennett, Anand et al. 2000; Cheng, Sapieha et al. 2002; Pernet, Hauswirth et al. 2005). Since C4RIP is the unique N-terminal domain of L-CRMP4, we could not use the L-CRMP4 antibody to differentiate between C4RIP-V5 and endogenous L-CRMP4 expression. Therefore, we used an antibody raised against the V5 epitope tag present only in C4RIP-V5 to evaluate AAV-mediated C4RIP-V5 expression in RGCs. Immunohistochemistry was performed on retinas cut in cross section and flatmounted retinas. Strong C4RIP-V5 expression was detected in the RGC cell bodies in retinas from eyes that were injected with AAV C4RIP-V5 but not AAV GFP (Fig. 4A). Additionally, C4RIP-V5 expression was also observed in RGC dendrites extending into the IPL (Fig. 4A), and in RGC axons projecting through the optic nerve head and down the optic nerve (Fig. 4B). We performed immunohistochemistry on flatmount retinas from eyes that were injected with AAV C4RIP-V5 using the V5 antibody to visualize C4RIP-V5 expression and a βIII tubulin antibody to identify RGCs and their processes (Fig. 4C). Qualitative assessment of these retinas revealed that the majority of RGCs were effectively infected with AAV C4RIP-V5. Consistent with our observations from immunohistochemistry performed on cross sections of these retinas, we localized C4RIP-V5 expression in RGC cell bodies, dendrites and axons (Fig. 4C).

3.5.3 AAV C4RIP does not promote neuronal survival or regeneration in adult retinal ganglion cells

Previous studies have demonstrated that RhoA activity plays an important role in the regulation of both neuronal survival and regeneration following CNS nerve injury (Fischer, Petkova et al. 2004; Bertrand, Di Polo et al. 2007). The administration of the RhoA antagonist C3 transferase to RGCs either through AAV-mediated gene transfer or through a cell-permeable protein promotes both neuronal survival and regeneration following optic nerve injury in the adult rat (Fischer, Petkova et al. 2004). Our previous

studies have identified L-CRMP4 as an important RhoA interacting protein that mediates neurite outgrowth inhibition on inhibitory substrates such as myelin and aggrecan (Alabed, Pool et al. 2007; Alabed, Pool et al. 2010). Expression of a RhoA-L-CRMP4 competitive antagonist, C4RIP, is able to significantly attenuate neurite outgrowth inhibition *in vitro* (Alabed, Pool et al. 2007). These findings prompted us to assess the effectiveness of antagonizing RhoA-L-CRMP4 interaction with C4RIP to promote neuronal survival and nerve regeneration *in vivo* following optic nerve injury. Three weeks after a single intraocular injection of either AAV C4RIP-V5 or AAV GFP, RGCs were retrogradely labeled with FluoroGold applied to the superior colliculi, and one week later the optic nerve was axotomized. Retinas were collected two weeks following axotomy and were analyzed for neuronal survival by determining the neuronal densities in the four retinal quadrants (superior, nasal, temporal and inferior). AAV-mediated expression of C4RIP V5 did not promote neuronal survival following axotomy compared to AAV GFP (Fig. 5B).

Four weeks following a single intraocular injection with either AAV C4RIP-V5 or AAV GFP, a forcep crush injury was applied to the optic nerve to transect all RGC axons. Thirteen days following forcep crush injury, an intraocular injection of the anterograde tracer cholera toxin beta-subunit (CTβ) was performed to labeled regenerating axon fibers. Fourteen days following forcep crush injury, the optic nerves were collected and regeneration was assessed through immunohistochemistry with an anti-CTβ antibody. In optic nerves from rats injected with AAV C4RIP-V5, we observed many V5-positive axon fibers proximal to the lesion site indicating that C4RIP-V5 was transported down RGC axons (Fig. 5C). In optic nerves from rats injected with either AAV GFP or AAV C4RIP-V5, we observed many CTβ-positive axons proximal to the lesion site but we did not observed many distal to the lesion site (Fig. 5C). Further, AAV C4RIP-V5 did not promote RGC axon regeneration compared to AAV GFP (Fig. 5D).

3.5.4 AAV C4RIP does not promote axon regeneration in adult retinal ganglion cells in an active growth state

It has been previously shown that in certain cases RGCs must be in an active growth state for regeneration to occur (Fischer, He et al. 2004). One method to activate

the growth state of RGCs is to perform a lens injury, which stimulates RGC survival and axon regeneration in the adult rat optic nerve (Fischer, Pavlidis et al. 2000; Leon, Yin et al. 2000; Fischer, He et al. 2004; Pernet and Di Polo 2006). The introduction of a dominant negative form of Nogo-66 receptor (DN-NgR1) alone does not enhance nerve regeneration following optic nerve injury in adult rats. However, when a lens injury is performed at the time of optic nerve injury, the introduction of DN-NgR1 enhances nerve regeneration compared to lens injury alone (Fischer, He et al. 2004). To assess the effect of AAV-mediated C4RIP expression in RGCs in an active growth state, we performed a lens injury immediately following forcep crush injury. We immediately visualized the lens injury and observed the opacification of the lens (cataract) within a week. We observed many more CTβ-positive axons proximal and distal to the lesion site, thereby validating our ability to promote axon regeneration through lens injury (Fig. 6A). We quantified axon regeneration by counting the number of CTβ-positive axons per optic nerve width at different distances from the lesion site (Fig. 6B). AAV-mediated C4RIP-V5 expression did not promote axon regeneration in RGCs in an active growth state compared to AAV GFP (Fig. 6B).

Together, these findings indicate that AAV-mediated expression of C4RIP-V5 in adult RGCs does not promote neuronal survival or axon regeneration following optic nerve injury. However, during our *in vitro* characterization of C4RIP-V5, we observed that the ability of C4RIP-V5 to function as a competitive antagonist of RhoA-L-CRMP4 interactions was dependent on the molar excess of C4RIP-V5 compared to endogenous L-CRMP4. Therefore, we assessed C4RIP-V5 expression levels by immunoblot with a L-CRMP4 antibody in retinal lysates from eyes that were injected with AAV C4RIP-V5 four weeks prior (Fig. 7). A single intraocular injection of AAV C4RIP-V5 resulted in the expression of C4RIP-V5, which was detected as a 20 kDa band at higher exposure times. On the same immunoblot we were able to visualize a 75 kDa band that corresponded to endogenous L-CRMP4 in the retinal lysates. The expression levels of C4RIP-V5 were robustly lower compared to endogenous L-CRMP4 expression levels. These findings suggest that perhaps the inability of AAV C4RIP-V5 to promote axon regeneration following optic nerve injury in the adult rat is attributed to insufficient C4RIP-V5 protein expression levels. This can be partially explained by the RGC-restricted expression of

AAV C4RIP-V5 but these findings also raise the distinct possibility that AAV C4RIP-V5 fails to promote axon regeneration due to insufficient expression.

3.6 DISCUSSION

In this study, we localize CRMP4 protein expression throughout the adult rat retina and optic nerve. We use a recombinant AAV to investigate the ability of C4RIP, a RhoA-L-CRMP4 competitive antagonist, to promote neuronal survival and axon regeneration in adult rat RGCs following optic nerve injury. Recombinant AAV vectors have a number of important advantages over other gene delivery vectors such as their lack of significant pathogenicity and their ability to induce long-term transgene expression (Di Polo, Aigner et al. 1998; Dudus, Anand et al. 1999; Guy, Qi et al. 1999; Martin, Klein et al. 2002). The efficiency of transduction is dependent on a number of factors including the site of injection, the AAV serotype and titer, the amount of passenger DNA, and the specific gene promoters and enhancing elements used (Martin, Klein et al. 2002). Consistent with previous studies, our recombinant AAV serotype-2 predominately transduces RGCs in the adult rat retina. Four weeks following a single intraocular injection of AAV C4RIP-V5 into the vitreous space, we observe C4RIP-V5 protein expression in the majority of RGC cell bodies, dendrites and axons (Martin, Klein et al. 2002; Fischer, He et al. 2004; Fischer, Petkova et al. 2004; Pernet, Hauswirth et al. 2005; Pernet and Di Polo 2006). However, our studies demonstrate that AAV-mediated expression of C4RIP-V5 does not promote neuronal survival or axon regeneration in RGCs following optic nerve injury, even if the RGCs are stimulated to an active growth state by lens injury.

There are a few possibilities to explain why AAV-mediated C4RIP-V5 expression failed to promote neuronal survival and axon regeneration in adult RGCs following optic nerve injury. Although RhoA antagonist promote neuronal survival and axon regeneration, our previous *in vitro* studies in DRGs only investigated the ability of C4RIP-V5 to attenuate neurite outgrowth inhibition in response to myelin and aggrecan (Alabed, Pool et al. 2007). While this data implicates the RhoA-L-CRMP4 interaction as an important mediator of axon regeneration inhibition, we have no *in vitro* data to suggest that L-CRMP4 regulates neuronal survival.

One unlikely explanation of why C4RIP-V5 did not promote axon regeneration in adult RGCs may be attributed to differences in intracellular signaling mechanisms in

different cell types. Our *in vitro* experiments were performed with embryonic (E13) chick DRGs, while in this *in vivo* study adult RGCs were used. However, there is strong evidence to support a model where RGCs inhibitory signaling following axonal injury is similar to other neurons including DRGs. The administration of RhoA antagonists such as purified cell-permeable C3 or AAV-C3 enhance RGC regeneration following optic nerve injury (Fischer, Petkova et al. 2004; Bertrand, Di Polo et al. 2007). These studies demonstrate that RhoA is an important mediator of axon outgrowth inhibition in RGCs. Furthermore, counteracting Nogo receptor with a dominant negative version enhances RGC axon regeneration if they are in an active growth state (Fischer, He et al. 2004). Importantly, in this study we have determined that adult RGCs express CRMP4. Overall, these findings suggest that adult RGCs are likely to engage the same intracellular signaling cascades that other neurons use to inhibit axonal regeneration.

Therefore, if RhoA-L-CRMP4 interaction mediates RGC axon outgrowth inhibition in response to a CNS injury, then antagonizing this interaction with our competitive protein C4RIP-V5 should promote axon regeneration. Our *in vitro* data suggests that in order for C4RIP-V5 to act as a competitive antagonist, C4RIP-V5 levels must be in molar excess of endogenous L-CRMP4 levels. Our observation that endogenous L-CRMP4 levels in retinal lysates are robustly higher than those seen for C4RIP-V5 suggest that AAV-mediated expression of C4RIP-V5 does not result in adequate C4RIP-V5 levels to act as a competitive antagonist. However, as previously described, our localization of endogenous L-CRMP4 to many different retinal layers, while AAV selective transduces RGCs make these results difficult to interpret. We have attempted to increase AAV-mediated C4RIP-V5 expression by performing multiple injections of AAV C4RIP-V5 but failed to observe a significant increase in C4RIP-V5 expression in retinal lysates.

We have also attempted to perform *in vitro* outgrowth experiments on inhibitory myelin with dissociated postnatal day 8 rat retinas. These experiments would allow us to validate C4RIP in RGCs and to compare the ability of C4RIP to attenuate neurite outgrowth inhibition on inhibitory myelin in DRGs and RGCs. However, while we were

successful at culturing non-infected dissociated mixed retinal neurons and having them respond to myelin, we were unable to do this after viral transduction of the RGCs with C4RIP or mRFP due to virus toxicity. In addition to the poor growth we observe from virus toxicity, our experimental conditions required us to trypsinize the cells off the culture dish following viral infection and reseeding them on a myelin substrate. Despite extensive troubleshooting, we were unsuccessful at achieving culture conditions that yielded consistently good growth.

To address some of the challenges we encountered with AAV-mediated delivery of C4RIP to RGC, in the next chapter, Chapter 4, we develop a cell permeable recombinant TAT C4RIP protein. These have certain advantages and disadvantages when compared to AAVs, which we will discuss in the next chapter.

3.7 ACKNOWLEDGEMENTS

We would like to thank William Hauswirth (University of Florida) for generously providing AAV-C4RIP and AAV-GFP.

3.8 REFERENCES

Alabed, Y. Z., M. Pool, et al. (2010). "GSK3beta regulates myelin-dependent axon outgrowth inhibition through CRMP4." J. Neurosci. **30**(16): 5635-5643.

Alabed, Y. Z., M. Pool, et al. (2007). "Identification of CRMP4 as a convergent regulator of axon outgrowth inhibition." J. Neurosci. **27**(7): 1702-1711.

Atwal, J. K., J. Pinkston-Gosse, et al. (2008). "PirB is a functional receptor for myelin inhibitors of axonal regeneration." Science **322**(5903): 967-970.

Bennett, J., V. Anand, et al. (2000). "Cross-species comparison of in vivo reporter gene expression after recombinant adeno-associated virus-mediated retinal transduction." Meth. Enzymol. **316**: 777-789.

Bertrand, J., A. Di Polo, et al. (2007). "Enhanced survival and regeneration of axotomized retinal neurons by repeated delivery of cell-permeable C3-like Rho antagonists." Neurobiol Dis **25**(1): 65-72.

Bertrand, J., M. J. Winton, et al. (2005). "Application of Rho antagonist to neuronal cell bodies promotes neurite growth in compartmented cultures and regeneration of retinal ganglion cell axons in the optic nerve of adult rats." J. Neurosci. **25**(5): 1113-1121.

Borisoff, J. F., C. C. M. Chan, et al. (2003). "Suppression of Rho-kinase activity promotes axonal growth on inhibitory CNS substrates." Mol Cell Neurosci **22**(3): 405-416.

Byk, T., T. Dobransky, et al. (1996). "Identification and molecular characterization of Unc-33-like phosphoprotein (Ulip), a putative mammalian homolog of the axonal guidance-associated unc-33 gene product." J Neurosci **16**(2): 688-701.

Byk, T., S. Ozon, et al. (1998). "The Ulip family phosphoproteins--common and specific properties." Eur J Biochem **254**(1): 14-24.

Chen, M. S., A. B. Huber, et al. (2000). "Nogo-A is a myelin-associated neurite outgrowth inhibitor and an antigen for monoclonal antibody IN-1." Nature **403**(6768): 434-439.

Cheng, L., P. Sapieha, et al. (2002). "TrkB gene transfer protects retinal ganglion cells from axotomy-induced death in vivo." J. Neurosci. **22**(10): 3977-3986.

Cole, A. R., F. Causeret, et al. (2006). "Distinct priming kinases contribute to differential regulation of collapsin response mediator proteins by glycogen synthase kinase-3 in vivo." J. Biol. Chem. **281**(24): 16591-16598.

Dergham, P., B. Ellezam, et al. (2002). "Rho signaling pathway targeted to promote spinal cord repair." J. Neurosci. **22**(15): 6570-6577.

Di Polo, A., L. J. Aigner, et al. (1998). "Prolonged delivery of brain-derived neurotrophic factor by adenovirus-infected Müller cells temporarily rescues injured retinal ganglion cells." Proceedings of the National Academy of Sciences of the United States of America **95**(7): 3978-3983.

Dubreuil, C., M. Winton, et al. (2003). "Rho activation patterns after spinal cord injury and the role of activated Rho in apoptosis in the …." J. Cell Biol.

Dudus, L., V. Anand, et al. (1999). "Persistent transgene product in retina, optic nerve and brain after intraocular injection of rAAV." Vision Res **39**(15): 2545-2553.

Ferrari, F. K., T. Samulski, et al. (1996). "Second-strand synthesis is a rate-limiting step for efficient transduction by recombinant adeno-associated virus vectors." J Virol **70**(5): 3227-3234.
Fischer, D., Z. He, et al. (2004). "Counteracting the Nogo receptor enhances optic nerve regeneration if retinal ganglion cells are in an active growth state." J. Neurosci. **24**(7): 1646-1651.
Fischer, D., M. Pavlidis, et al. (2000). "Cataractogenic lens injury prevents traumatic ganglion cell death and promotes axonal regeneration both in vivo and in culture." Invest Ophthalmol Vis Sci **41**(12): 3943-3954.
Fischer, D., V. Petkova, et al. (2004). "Switching mature retinal ganglion cells to a robust growth state in vivo: gene expression and synergy with RhoA inactivation." J. Neurosci. **24**(40): 8726-8740.
Fournier, A. E., T. GrandPre, et al. (2001). "Identification of a receptor mediating Nogo-66 inhibition of axonal regeneration." Nature **409**(6818): 341-346.
Fournier, A. E., B. T. Takizawa, et al. (2003). "Rho kinase inhibition enhances axonal regeneration in the injured CNS." J. Neurosci. **23**(4): 1416-1423.
Fukata, Y., T. J. Itoh, et al. (2002). "CRMP-2 binds to tubulin heterodimers to promote microtubule assembly." Nat Cell Biol **4**(8): 583-591.
Gaetano, C., T. Matsuo, et al. (1997). "Identification and characterization of a retinoic acid-regulated human homologue of the unc-33-like phosphoprotein gene (hUlip) from neuroblastoma cells." J Biol Chem **272**(18): 12195-12201.
Goshima, Y., F. Nakamura, et al. (1995). "Collapsin-induced growth cone collapse mediated by an intracellular protein related to UNC-33." Nature **376**(6540): 509-514.
GrandPré, T., F. Nakamura, et al. (2000). "Identification of the Nogo inhibitor of axon regeneration as a Reticulon protein." Nature **403**(6768): 439-444.
Guy, J., X. Qi, et al. (1999). "Reporter expression persists 1 year after adeno-associated virus-mediated gene transfer to the optic nerve." Arch Ophthalmol **117**(7): 929-937.
Hauswirth, W. W., A. S. Lewin, et al. (2000). "Production and purification of recombinant adeno-associated virus." Meth Enzymol **316**: 743-761.
Hedgecock, E. M., J. G. Culotti, et al. (1985). "Axonal guidance mutants of Caenorhabditis elegans identified by filling sensory neurons with fluorescein dyes." Developmental Biology **111**(1): 158-170.
Inatome, R., T. Tsujimura, et al. (2000). "Identification of CRAM, a novel unc-33 gene family protein that associates with CRMP3 and protein-tyrosine kinase(s) in the developing rat brain." J Biol Chem **275**(35): 27291-27302.
Jang, S. Y., Y. K. Shin, et al. (2010). "Injury-induced CRMP4 expression in adult sensory neurons; a possible target gene for ciliary neurotrophic factor." Neuroscience letters **485**(1): 37-42.
Jin, Z. and S. M. Strittmatter (1997). "Rac1 mediates collapsin-1-induced growth cone collapse." J Neurosci **17**(16): 6256-6263.
Kim, J.-E., B. P. Liu, et al. (2004). "Nogo-66 receptor prevents raphespinal and rubrospinal axon regeneration and limits functional recovery from spinal cord injury." Neuron **44**(3): 439-451.

Kottis, V., P. Thibault, et al. (2002). "Oligodendrocyte-myelin glycoprotein (OMgp) is an inhibitor of neurite outgrowth." J Neurochem **82**(6): 1566-1569.
Lehmann, M., A. Fournier, et al. (1999). "Inactivation of Rho signaling pathway promotes CNS axon regeneration." J Neurosci **19**(17): 7537-7547.
Leon, S., Y. Yin, et al. (2000). "Lens injury stimulates axon regeneration in the mature rat optic nerve." J. Neurosci. **20**(12): 4615-4626.
Lord-Fontaine, S., F. Yang, et al. (2008). "Local inhibition of Rho signaling by cell-permeable recombinant protein BA-210 prevents secondary damage and promotes functional recovery following acute spinal cord injury." J Neurotrauma **25**(11): 1309-1322.
Martin, K. R. G., R. L. Klein, et al. (2002). "Gene delivery to the eye using adeno-associated viral vectors." Methods **28**(2): 267-275.
McKerracher, L., S. David, et al. (1994). "Identification of myelin-associated glycoprotein as a major myelin-derived inhibitor of neurite growth." Neuron **13**(4): 805-811.
Mi, S., X. Lee, et al. (2004). "LINGO-1 is a component of the Nogo-66 receptor/p75 signaling complex." Nat. Neurosci. **7**(3): 221-228.
Minturn, J. E., H. J. Fryer, et al. (1995). "TOAD-64, a gene expressed early in neuronal differentiation in the rat, is related to unc-33, a C. elegans gene involved in axon outgrowth." J Neurosci **15**(10): 6757-6766.
Monnier, P. P., A. Sierra, et al. (2003). "The Rho/ROCK pathway mediates neurite growth-inhibitory activity associated with the chondroitin sulfate proteoglycans of the CNS glial scar." Mol Cell Neurosci **22**(3): 319-330.
Mukhopadhyay, G., P. Doherty, et al. (1994). "A novel role for myelin-associated glycoprotein as an inhibitor of axonal regeneration." Neuron **13**(3): 757-767.
Pan, S., Y. Chao, et al. (2009). "Long form collapsin response mediator protein-1 (LCRMP-1) expression is associated with clinical outcome and lymph node metastasis in non-small cell lung cancer patients." Lung Cancer.
Park, J. B., G. Yiu, et al. (2005). "A TNF receptor family member, TROY, is a coreceptor with Nogo receptor in mediating the inhibitory activity of myelin inhibitors." Neuron **45**(3): 345-351.
Pernet, V. and A. Di Polo (2006). "Synergistic action of brain-derived neurotrophic factor and lens injury promotes retinal ganglion cell survival, but leads to optic nerve dystrophy in vivo." Brain **129**(Pt 4): 1014-1026.
Pernet, V., W. W. Hauswirth, et al. (2005). "Extracellular signal-regulated kinase 1/2 mediates survival, but not axon regeneration, of adult injured central nervous system neurons in vivo." J Neurochem **93**(1): 72-83.
Prinjha, R., S. E. Moore, et al. (2000). "Inhibitor of neurite outgrowth in humans." Nature **403**(6768): 383-384.
Quach, T. T., A.-M. Duchemin, et al. (2004). "Involvement of collapsin response mediator proteins in the neurite extension induced by neurotrophins in dorsal root ganglion neurons." Mol Cell Neurosci **25**(3): 433-443.
Quinn, C. C., E. Chen, et al. (2003). "TUC-4b, a novel TUC family variant, regulates neurite outgrowth and associates with vesicles in the growth cone." J. Neurosci. **23**(7): 2815-2823.

Quinn, C. C., G. E. Gray, et al. (1999). "A family of proteins implicated in axon guidance and outgrowth." J Neurobiol **41**(1): 158-164.
Rembutsu, M., M. P. M. Soutar, et al. (2008). "Novel procedure to investigate the effect of phosphorylation on protein complex formation in vitro and in cells." Biochemistry **47**(7): 2153-2161.
Riento, K. and A. J. Ridley (2003). "Rocks: multifunctional kinases in cell behaviour." Nat Rev Mol Cell Biol **4**(6): 446-456.
Rosslenbroich, V., L. Dai, et al. (2005). "Collapsin response mediator protein-4 regulates F-actin bundling." Exp. Cell Res. **310**(2): 434-444.
Shao, Z., J. L. Browning, et al. (2005). "TAJ/TROY, an orphan TNF receptor family member, binds Nogo-66 receptor 1 and regulates axonal regeneration." Neuron **45**(3): 353-359.
Siddiqui, S. S. and J. G. Culotti (1991). "Examination of neurons in wild type and mutants of Caenorhabditis elegans using antibodies to horseradish peroxidase." Journal of Neurogenetics **7**(4): 193-211.
Suzuki, Y., S. Nakagomi, et al. (2003). "Collapsin response mediator protein-2 accelerates axon regeneration of nerve-injured motor neurons of rat." Journal of neurochemistry **86**(4): 1042-1050.
Wang, K. C., J. A. Kim, et al. (2002). "P75 interacts with the Nogo receptor as a co-receptor for Nogo, MAG and OMgp." Nature **420**(6911): 74-78.
Wang, K. C., V. Koprivica, et al. (2002). "Oligodendrocyte-myelin glycoprotein is a Nogo receptor ligand that inhibits neurite outgrowth." Nature **417**(6892): 941-944.
Wang, L. H. and S. M. Strittmatter (1996). "A family of rat CRMP genes is differentially expressed in the nervous system." J Neurosci **16**(19): 6197-6207.
Wang, L. H. and S. M. Strittmatter (1997). "Brain CRMP forms heterotetramers similar to liver dihydropyrimidinase." J Neurochem **69**(6): 2261-2269.
Winton, M. J., C. I. Dubreuil, et al. (2002). "Characterization of new cell permeable C3-like proteins that inactivate Rho and stimulate neurite outgrowth on inhibitory substrates." J Biol Chem **277**(36): 32820-32829.
Wong, S. T., J. R. Henley, et al. (2002). "A p75(NTR) and Nogo receptor complex mediates repulsive signaling by myelin-associated glycoprotein." Nat. Neurosci. **5**(12): 1302-1308.
Yamashita, T., H. Higuchi, et al. (2002). "The p75 receptor transduces the signal from myelin-associated glycoprotein to Rho." J. Cell Biol. **157**(4): 565-570.
Yiu, G. and Z. He (2006). "Glial inhibition of CNS axon regeneration." Nat Rev Neurosci **7**(8): 617-627.
Yuasa-Kawada, J., R. Suzuki, et al. (2003). "Axonal morphogenesis controlled by antagonistic roles of two CRMP subtypes in microtubule organization." Eur J Neurosci **17**(11): 2329-2343.
Zheng, B., J. Atwal, et al. (2005). "Genetic deletion of the Nogo receptor does not reduce neurite inhibition in vitro or promote corticospinal tract regeneration in vivo." Proc Natl Acad Sci USA **102**(4): 1205-1210.
Zolotukhin, S., M. Potter, et al. (1996). "A "humanized" green fluorescent protein cDNA adapted for high-level expression in mammalian cells." J Virol **70**(7): 4646-4654.

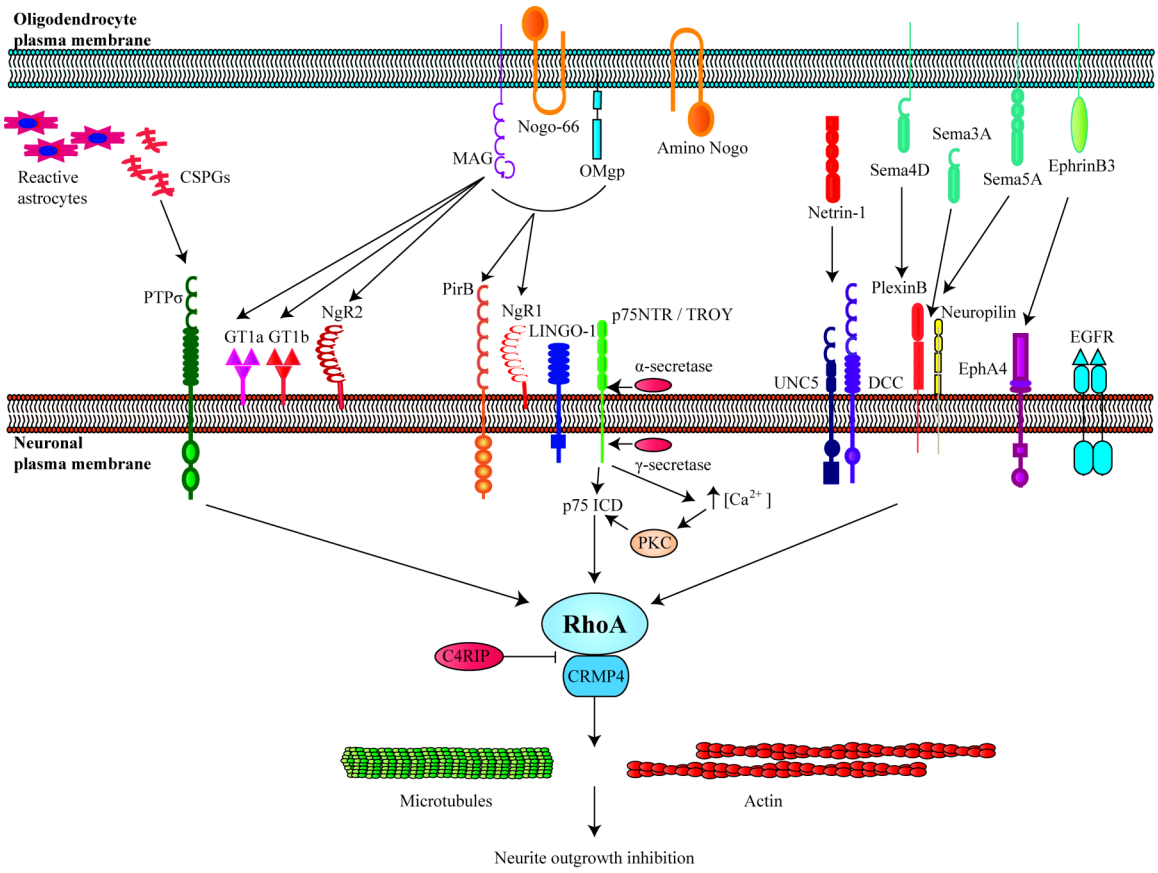

Chapter 3 - Figure 1. Schematic representation of C4RIP blockade of the RhoA-L-CRMP4 interaction.

MAIs, CSPGs and other inhibitory molecules signal through neuronal receptors to activate RhoA. RhoA signals through L-CRMP4 to mediate neurite outgrowth inhibition. The overexpression of the competitive peptide C4RIP disrupts the RhoA-L-CRMP4 interaction and promotes neurite outgrowth on inhibitory substrates. Adapted from *Essentials of Spinal Cord Injury: Targeting Rho inactivation to promote regeneration and treat spinal cord injury: Bench to bedside translational medicine* (In press) by L. McKerracher, M. Fehlings, A.E. Fournier and S. Ong Tone, 2010, NY: Thieme Medical Publishers.

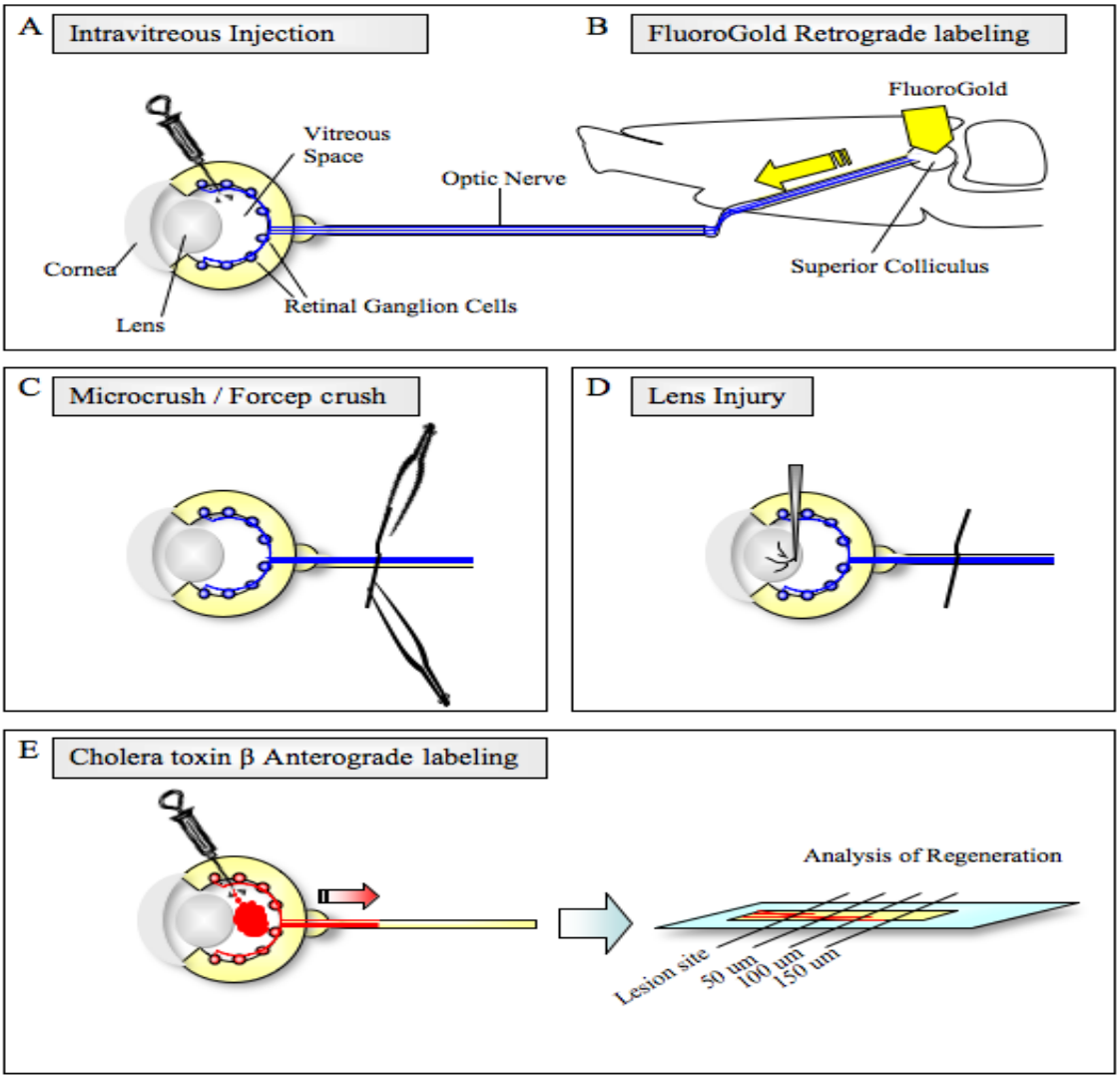

Chapter 3 - Figure 2. Schematic representation of surgical procedures.

(A) AAV C4RIP-V5 and AAV GFP were administered through an intraocular injection into the vitreous space. (B) Retinal ganglion cells were backlabelled through the application of FluoroGold to the superior colliculi. (C) Optic nerve injury was achieved through a microcrush lesion with a 10-0 pt suture or through a forcep crush directly to the nerve. (D) Retinal ganglion cells were induced to an active growth state through a lens injury with a 30 ½ gauge needle. (E) Retinal ganglion cell regeneration was assessed through an intraocular injection of cholera toxin β and subsequent immunohistochemical analysis.

Chapter 3 - Figure 3. CRMP4 expression in the adult retina and optic nerve.

(A) Immunoblot on retinal lysates from 3 separate rats probed with a CRMP4 antibody, which recognizes both L- and S- CRMP4, and a L-CRMP4 specific antibody. (B) Fluorescent micrographs on retinal sections stained for βIII tubulin, DNA and either CRMP4 (top panel) or L-CRMP4 (middle and lower panel). The bottom panel shows L-CRMP4 expression at the optic nerve head and optic nerve. NF= nerve fiber layer, RGC= retinal ganglion cell layer, IPL= inner plexiform layer, INL= inner nuclear layer, OPL= outer plexiform layer, ONL= outer nuclear layer, OS= outer segment, ONH= optic nerve head, ON= optic nerve. Bar, 100 um. (C) Fluorescent micrograph of an optic nerve section stained for proteolioprotein (PLP), DNA and L-CRMP4. Strong L-CRMP4 expression is observed in oligodendrocytes of the optic nerve (arrows). Bar, 100 μm. (D) Fluorescent micrograph of a FluoroGold backlabeled retinal section stained for L-CRMP4. L-CRMP4 is strongly expressed in FluoroGold positive retinal ganglion cells (Top panel). The immunosignal is abolished with the pre-incubation of the L-CRMP4 antibody with its blocking peptide (lower panel). Bar, 20 μm.

FIGURE 3

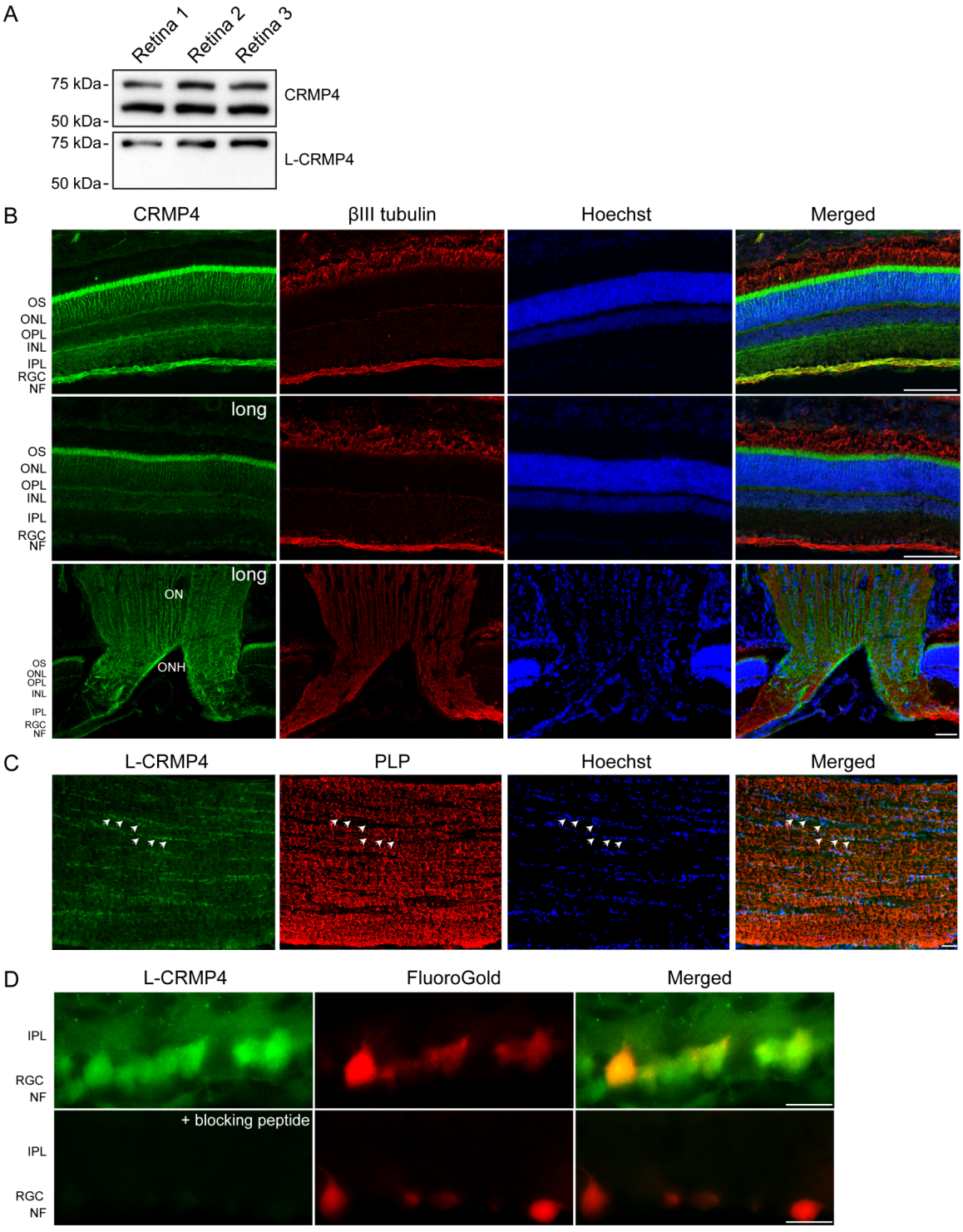
A
Retina 1
Retina 2
Retina 3
75 kDa-
50 kDa-
CRMP4
75 kDa-
50 kDa-
L-CRMP4
B
CRMP4
βIII tubulin
Hoechst
Merged
OS
ONL
OPL
INL
IPL
RGC
NF
long
ON
ONH
C
L-CRMP4
PLP
Hoechst
Merged
D
L-CRMP4
FluoroGold
Merged
IPL
RGC
NF
+ blocking peptide

Chapter 3 - Figure 4. Adeno-associated virus (AAV)-mediated transgene expression of C4RIP-V5 in retinal ganglion cells.

(A) Fluorescent micrographs on retinal sections that were stained with a V5 antibody four weeks following a single intraocular injection of AAV-C4RIP-V5 (top) or AAV-GFP (bottom). Bar, 100 μm. (B) C4RIP-V5 is expressed in retinal ganglion cell bodies, dendrites and axons projecting down through the optic nerve head and optic nerve. ONH=optic nerve head, ON=optic nerve. Bar, 100 μm. (C) Flatmount of an AAV-C4RIP infected retina stained for V5 and βIII tubulin. C4RIP-V5 expression is observed in the majority of retinal ganglion cells. Bar, 100 μm.

FIGURE 4

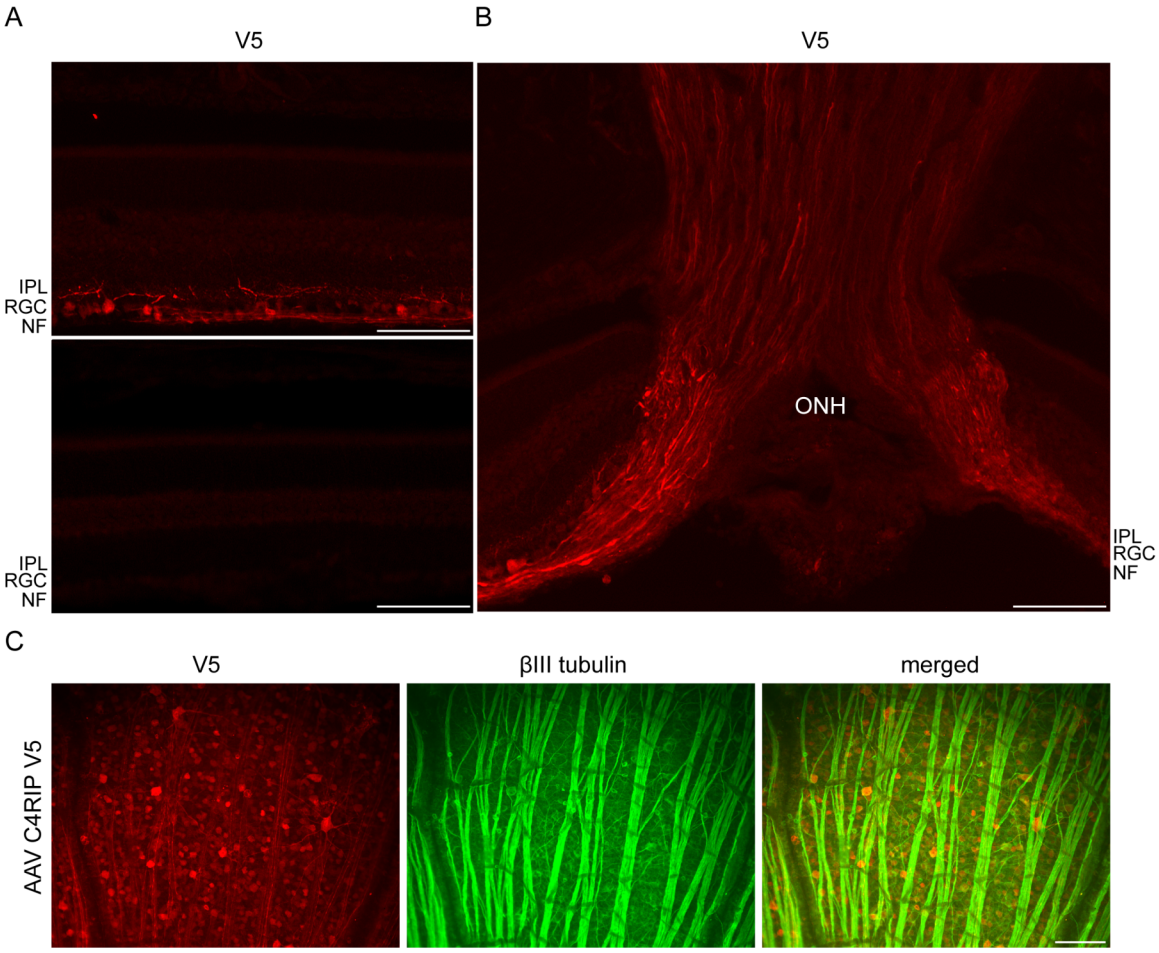
A
V5
IPL
RGC
NF
IPL
RGC
NF
B
V5
ONH
IPL
RGC
NF
C
V5
βIII tubulin
merged
AAV C4RIP V5

Chapter 3 - Figure 5. AAV-mediated transgene expression of C4RIP-V5 in retinal ganglion cells does not promote neuronal survival or axon regeneration.

(A) AAV C4RIP-V5 does not increase the density of FluoroGold backlabeled RGCs two weeks following axotomy. Bar, 100 μm. (B) Quantitative analysis of RGCs survival following injection of AAV-GFP (black bar) or AAV-C4RIP (grey bar). RGC density is calculated by counting the number of RGCs per mm^2 in 12 standard areas of the retina. RGC survival is represented as a percentage of RGC density from intact retinas (white bar). AAV-C4RIP V5 does not promote RGC survival compared to AAV GFP (n=6, Student's *t* test, non-significant = $p>0.05$). (C) AAV C4RIP-V5 does not promote axon regeneration following optic nerve injury. Fluorescent micrographs on optic nerve sections stained for cholera toxin beta-subunit (CTβ) and V5 six week following a single intraocular injection of AAV C4RIP-V5 and two weeks following optic nerve injury. Regenerating fibers were anterogradely labeled with a single injection of CTβ one day before collection of the optic nerve. RGC axons positive for both CTβ and V5 are seen proximal (p) to the lesion site (*), but no regenerating fibers are observed distal to the lesion site (d). Bar, 100 μm. (D) Quantitative analysis of axon regeneration following intraocular injections of either AAV GFP (black bars) or AAV C4RIP-V5 (grey bars). CTβ-positive axons were counted at 100 μm and 500 μm from the lesion site. At least four optic nerve sections were counted per animal. AAV C4RIP-V5 did not promote axon regeneration in RGCs following optic nerve injury compared to AAV GFP (n=3, two-way ANOVA, Bonferroni post hoc test, non-significant= $p>0.05$).

FIGURE 5

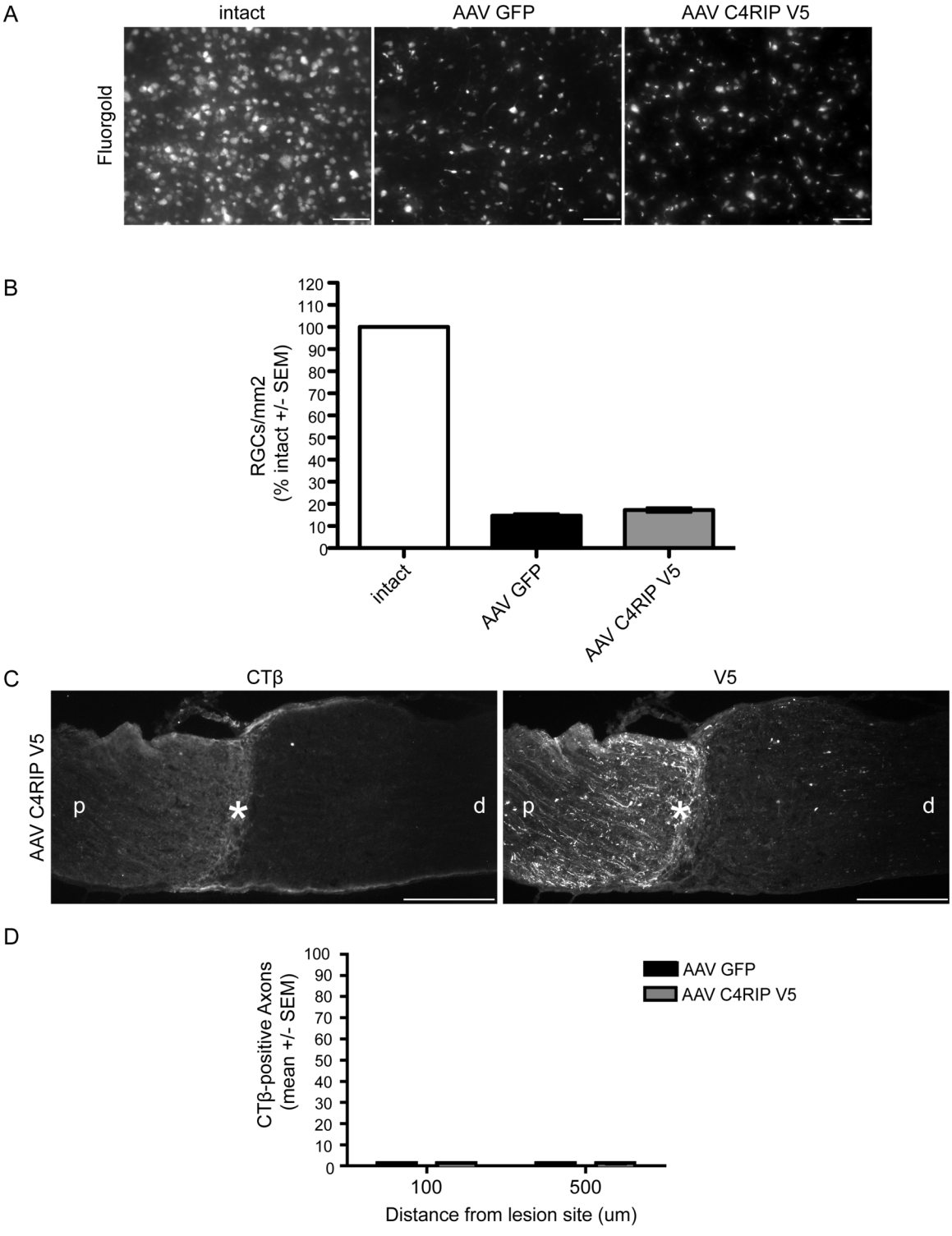
A
intact
AAV GFP
AAV C4RIP V5
Fluorgold
B
RGCs/mm2
(% intact +/- SEM)
120
110
100
90
80
70
60
50
40
30
20
10
0
intact
AAV GFP
AAV C4RIP V5
C
CTβ
V5
AAV C4RIP V5
p
d
*
D
CTβ-positive Axons
(mean +/- SEM)
AAV GFP
AAV C4RIP V5
100
500
Distance from lesion site (um)

Chapter 3 - Figure 6. AAV-mediated transgene expression of C4RIP-V5 in retinal ganglion cells stimulated to an active growth state does not promote axon regeneration.

(A) AAV C4RIP-V5 does not promote axon regeneration in RGCs stimulated to an active growth state following optic nerve injury. Fluorescent micrographs on optic nerve sections stained for CTβ six week following a single intraocular injection of AAV C4RIP-V5 and two weeks following optic nerve injury. RGCs were stimulated to an active growth state through a lens injury performed immediately after the optic nerve injury. Regenerating fibers were anterogradely labeled with a single injection of CTβ one day before collection of the optic nerve. CTβ-positive RGC axons are seen proximal (p) and distal (d) to the lesion site (white line) in both AAV GFP and AAV C4RIP-V5 groups. Bar, 100 μm. (B) Quantitative analysis of axon regeneration following lens injury and injection of AAV GFP (black bar) or AAV C4RIP-V5 (grey bar). CTβ-positive axons were counted at 100 μm, 250 μm, 500 μm, 750 μm and 1000 μm from the lesion site and were divided by the optic nerve width. At least four optic nerve sections were counted per animal. AAV C4RIP-V5 did not promote axon regeneration in RGCs stimulated to an active growth state compared to AAV GFP (n=4, two-way ANOVA, Bonferroni post hoc test, non-significant= $p>0.05$).

FIGURE 6

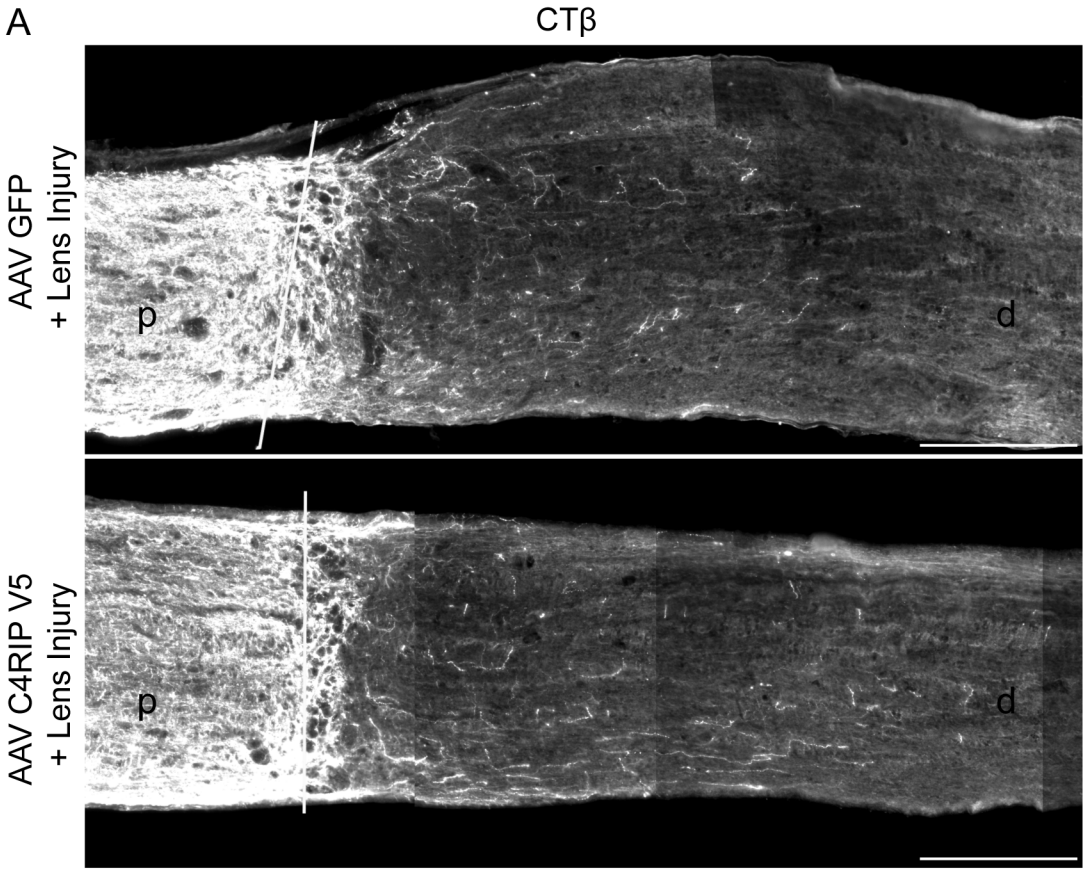
A
CTβ
AAV GFP
+ Lens Injury
p
d
AAV C4RIP V5
+ Lens Injury
p
d

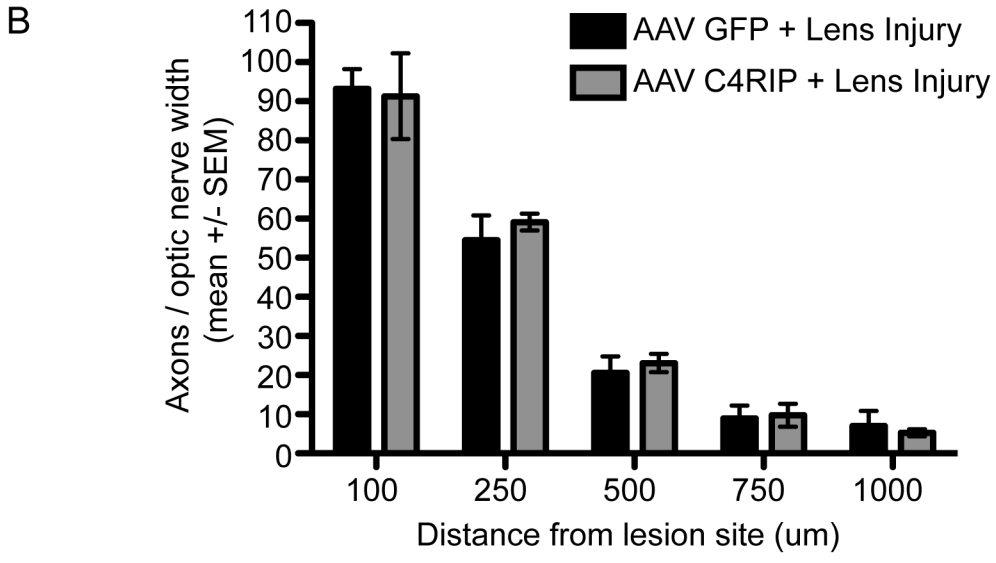
B
AAV GFP + Lens Injury
AAV C4RIP + Lens Injury
Axons / optic nerve width
(mean +/- SEM)
110
100
90
80
70
60
50
40
30
20
10
0
100
250
500
750
1000
Distance from lesion site (um)

Chapter 3 - Figure 7. AAV-mediated transgene expression of C4RIP-V5 in retinal ganglion cells may not be expressed to sufficient levels to antagonize RhoA-L-CRMP4 interactions.

Immunoblot on retinal lysates from 3 separate rats four weeks following a single intraocular injection of AAV C4RIP-V5. C4RIP-V5 is detected only in immunoblots that undergo high exposures, while endogenous L-CRMP4 is detected under low exposures.

FIGURE 7

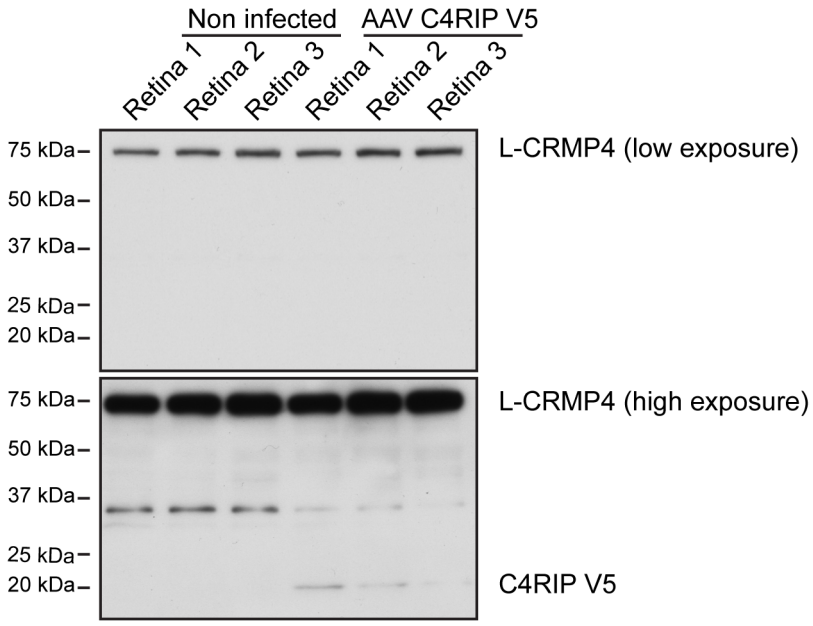
Non infected
AAV C4RIP V5
Retina 1
Retina 2
Retina 3
Retina 1
Retina 2
Retina 3
75 kDa
50 kDa
37 kDa
25 kDa
20 kDa
L-CRMP4 (low exposure)
75 kDa
50 kDa
37 kDa
25 kDa
20 kDa
L-CRMP4 (high exposure)
C4RIP V5

CHAPTER 4

4 THE DEVELOPMENT OF TAT-C4RIP, A CELL PERMEABLE RhoA-L-CRMP4 COMPETITIVE ANTAGONIST

4.1 PREFACE

In Chapter 3, we demonstrate that AAV-mediated expression of C4RIP does not promote retinal RGC neuronal survival or axon regeneration following optic nerve injury in the adult rat. However, C4RIP expression levels may not have been sufficient to antagonize the RhoA-L-CRMP4 interaction, thereby having no effect on axon regeneration. The aim of this study was to develop a recombinant cell permeable TAT C4RIP protein and to evaluate its ability to promote RGC axon regeneration following optic nerve injury in the adult rat.

4.2 ABSTRACT

The ability of the trans-acting activator of transcription (TAT) protein transduction domain (PTD) to transport macromolecules across biological membranes raises the possibility of developing it as a therapeutic delivery tool. Most studies have produced TAT PTD fusion protein in bacteria, which can result in problems such as protein solubility, the formation of inclusion bodies and the lack of eukaryotic post-translational modifications. While some groups have investigated the production of TAT PTD fusion protein in mammalian cells, these strategies are focused on generating TAT PTD fusions that are targeted to the secretory pathway, where furin protease can cleave the TAT PTD. As an alternative to mutating the furin cleavage site in the TAT PTD, which can alter its transduction property, we have developed a novel method to generate cytosolic TAT PTD fusion proteins and purify them from cell lysates. Here, we use this method to generate TAT C4RIP, a cell permeable RhoA- L-CRMP4 competitive antagonist and validate its ability to transduce cells *in vitro* and *in vivo*. We demonstrate that this method generates TAT C4RIP that retains its functional ability to antagonizes RhoA-L-CRMP4 interactions and attenuate myelin inhibition in DRGs *in vitro*. However, the application of TAT C4RIP *in vivo* did not promote retinal ganglion cell axon regeneration following optic nerve injury possibly due to poor distribution of TAT C4RIP. In this study we have developed a novel purification strategy to generate and purify functional TAT PTD fusion proteins from mammalian cell lysates. Future studies should focus on optimizing the delivery and distribution of TAT PTD fusion proteins for therapeutic applications.

4.3 INTRODUCTION

The use of viruses as delivery vehicles for gene transfer has been shown to be a very efficient strategy to correct inherited diseases but its therapeutic use has been quite limited due to the risks of insertional mutagenesis and uncontrolled cellular proliferation (Hacein-Bey-Abina, von Kalle et al. 2003; Hacein-Bey-Abina, Von Kalle et al. 2003). The discovery that the trans-acting activator of transcription (TAT) protein of HIV-1 was able to cross cellular membranes and that chemically coupling TAT to proteins conferred transduction properties raised the possibility of utilizing TAT as a therapeutic delivery tool for macromolecules (Frankel and Pabo 1988; Green and Loewenstein 1988; Fawell, Seery et al. 1994). Furthermore, TAT is able to cross the blood-brain barrier *in vivo*, which would allow therapeutic proteins coupled or fused to TAT to target the brain (Schwarze, Ho et al. 1999).

The TAT protein transduction domain (PTD) allows proteins and peptides to cross biological membranes and enter the cytosolic compartment of a cell. The mechanism by which TAT fusion proteins cross cellular membranes was originally believed to occur in a receptor-, transporter- and endocytic-independent manner. This was largely due to the observation that TAT fusion proteins could still cross cellular membranes in a concentration-dependent manner at low temperatures, where all known mechanisms of entry are inhibited (Vivès, Brodin et al. 1997). However, these reports have been largely dismissed as artifactual and it is currently believed that transduction of TAT fusion proteins through cellular membranes occurs through macropinocytosis, a specialized form of endocytosis (Gump and Dowdy 2007).

The efficacy of various proteins fused to or linked to the TAT PTD produced in bacteria has been demonstrated in various cell types *in vitro* and *in vivo* (Nagahara, Vocero-Akbani et al. 1998; Schwarze, Ho et al. 1999). However, bacterial production of TAT fusion proteins results in several problems that may limit its translation into therapeutic agents such as protein insolubility, formation of inclusion bodies and the lack of eukaryotic post-translational modifications (Beerens, Al Hadithy et al. 2003; Flinterman, Farzaneh et al. 2009). Although many studies have investigated the

transduction properties of bacterially produced TAT PTD fusion proteins, only a few studies have investigated the ability to produce TAT fused proteins using mammalian expression vectors (Yang, Ma et al. 2002; Barka, Gresik et al. 2004; Flinterman, Farzaneh et al. 2009). This is largely because TAT PTD contains multiple arginine and lysine residues, which some endoproteases recognize as a target substrate. The TAT PTD contains the sequence R-Q-R-R, which is a furin cleavage site (R-X-R/K-R), and since furin is found largely in the trans-Golgi network, TAT fusion proteins directed to the secretory pathway are most likely cleaved by furin as they transition through the endoplasmic reticulum and Golgi apparatus (Beerens, Al Hadithy et al. 2003). One strategy to circumvent furin-mediated cleavage of TAT PTD has been to mutate the two furin cleavage sites found in the TAT PTD sequence (Flinterman, Farzaneh et al. 2009). This modified TAT sequence, TATκ, is no longer cleaved by furin and is highly secreted into the media (Flinterman, Farzaneh et al. 2009). This strategy is designed for the continuous *in vivo* secretion of TAT fusion proteins, since direct delivery of recombinant TAT fusion proteins may be quickly degraded by proteases and eliminated by renal filtration, thereby requiring multiple applications (Torchilin and Lukyanov 2003; Flinterman, Farzaneh et al. 2009). However, the need to transplant modified TAT fusion protein secreting cells into humans may limit its role as a therapeutic agent.

In this study, we describe a novel strategy to generate and purify TAT fusion proteins from mammalian cells for therapeutic application. To circumvent furin-mediated cleavage of TAT fusion proteins targeted to the secretory pathway, we target TAT fusion proteins to the cytosolic compartment of mammalian cells and purify it directly from cell lysates. As an example of our purification strategy, we focus on the biological property of C4RIP (CRMP4b-RhoA Inhibitory Peptide) to attenuate myelin-dependent neurite outgrowth inhibition in rat DRG neurons. We demonstrate that purified TAT C4RIP can transduce cells *in vitro* and *in vivo*. Importantly, our purified TAT C4RIP retains its ability to attenuate myelin inhibition in DRG neurons *in vitro*. We also evaluate the therapeutic potential of TAT C4RIP to promote CNS nerve regeneration in a preclinical adult rat optic nerve injury model.

4.4 MATERIALS AND METHODS

4.4.1 Plasmids

Monomeric red fluorescent protein (mRFP) was PCR amplified from pHSV mRFP-actin using the primers: 5'GGGGGATCCGATGGCCTCCTCCGAGGA3' and 5'GGGAAGCTTGGCGCCGGTGGAGTG3'. C4RIP was PCR amplified from pcDNA C4RIP-V5 using the primers: 5'GGGGGGATCCGGCTTGAACCATGGCTTCGGGC3' and 5'GGGGAAGCTTCTACTTGTCCTTGGGACC3'. mRFP or C4RIP were inserted into the BamHI and HindIII sites of the vector pET 28b TAT v2 (generously provided by Steve Dowdy, UCSD). TAT C4RIP and TAT mRFP were PCR amplified using the primers 5'GGGGACAAGTTTGTACAAAAAAGCAGGCTGGGGCAGGAAGAAGCG GAGA3' and 5'GGGGACCACTTTGTACAAGAAAGCTGGGTCTCAGTGGTGGTG GTGGTG3' and were cloned into the vector pDONR221 by BP recombination, and then cloned into a modified pYD5 vector + cassette A compatible for Gateway cloning by LR recombination (Invitrogen). To generate cytosolic TAT fusion proteins, TAT mRFP and TAT C4RIP were PCR amplified from the modified pYD5 vector and inserted into the vector pTT5.

4.4.2 Purification of cytosolic TAT proteins

pTT5-TAT mRFP or pTT5-TAT C4RIP were transfected with polyethylenimine in serum-free medium into suspension growing chinese hamster ovary (CHO) cells. Transfected CHO cells were lysed in lysis buffer (50mM HEPES pH-7.4, 150 mM NaCl). Lysates were sonicated and centrifuged for 20 minutes at 10, 000 rpm. Supernatants were collected at filtered with through a 0.45 μm filter unit. TAT fusion proteins were purified on a Fractogel cobalt column (EMD Bioscience). The Fractogel cobalt column was charged with 5 column volumes of 0.5 M NaCl, followed by 4 column volumes of 200 mM cobalt chloride and 2 column volumes of 0.5 NaCl pH=5±0.2. The Fractogel cobalt column was equilibrated with 10 column volumes of phosphate-buffered saline (PBS). The TAT fusion protein supernatant was applied to the equilibrated column and allowed to flow through by gravity. The flow through was kept for future analysis of the purification efficiency. The Fractogel cobalt column was washed with 10 column volumes of wash buffer #1 (50 mM sodium phosphate pH=7, 300 mM NaCl), followed

by 10 column volumes of wash buffer #2 (50 mM sodium phosphate pH=7, 300 mM NaCl, 25 mM imidazole). TAT fusion protein was eluted in elution buffer (50 mM sodium phosphate pH=7, 300 mM NaCl, 300 mM imidazole). 1 ml elution fractions were collected and Bradford protein assay was performed of the fractions. Fractions that contained the TAT fusion protein were pooled and desalted using a desalting column (Bio-Rad). The desalting columns were first equilibrated in PBS-300 mM NaCl, after which the 3 ml pooled fraction containing the TAT fusion protein was applied to the column. The flow through was collected and an additional 4 mls of PBS-300 mM NaCl was applied to the desalting column and pooled with the flow through. Final protein concentrations were measured at 280 nm using Nanodrop (Thermo Scientific). TAT fusion proteins were aliquoted and kept at -80 °C.

4.4.3 Immunoblot

Cell lysates were separated on an sodium dodecyl sulfate (SDS) – poly acrylamide gel (PAGE) gel and transferred to a polyvinylidene fluoride membrane and blocked in 5% milk in tris-buffered saline and 0.1% Tween-20 (TBST). Primary and secondary antibodies were diluted in 5% milk TBST. Secondary antibody used was anti-rabbit antibody linked to horse radish peroxidase (HRP). Protein signal was detected used a chemiluminescence reagent (ECL, Amersham Biosciences).

4.4.4 *In vitro* cell permeability assay

HeLa cells (ATCC; catalogue number CCL-2) were grown in DMEM (Invitrogen, Burlington, Ontario) supplemented with 10% FBS (HyClone, Logan, UT) and were maintained in 5% CO_2 at 37 °C. HeLa cells were grown on 35 mm glass bottom dishes (MatTek Corp, Ashland, MA). TAT mRFP or TAT C4RIP were added to the culture medium to a final concentration of 100 μg/ml and incubated between 1 hour and 24 hours before processing for immunocytochemistry or live imaging. For immunocytochemistry, HeLa cells were washed with phosphate-buffered saline (PBS), followed by an acid wash (0.2 M acetic acid pH=2.8, 0.5 M NaCl) for 2 minutes, washed again with PBS, and fixed with 4% paraformaldehyde (PFA) in PBS, and stained for T7, filamentous (F) -actin and DNA. F-actin was visualized using phalloidin-488 (Invitrogen) while DNA was visualized using Hoechst 33342 (Invitrogen). In some cases, the mRFP signal was not

amplified with an antibody. Cover slips were mounted using Fluoromount-G (Southern Biotech, Birmingham, AL). For live time-lapse microscopy, HeLa cells were washed with OptiMEM (Invitrogen) to remove any TAT mRFP in the media, and then incubated in OptiMEM. Microscopy was performed on Zeiss Axiovert 200 using a 100X objective equipped with an automated stage and an environmental control chamber, which maintained the cells at 37˚C and 5% CO_2.

4.4.5 Rat dorsal root ganglion neurite outgrowth assay

Dissociated postnatal day 5 (P5) rat DRG neurons were cultured in DRG medium (Neurobasal medium (Invitrogen), 2% B27, 1% penicillin/streptomycin, 1% L-glutamine, 50 ng/ml NGF) in the presence of either PBS-300 mM NaCl, TAT mRFP or TAT C4RIP diluted in a 10X supplement stock (20% B27, 10% penicillin/streptomycin, 10% L-glutamine, 500 ng/ml NGF) on 0.01% poly-L-lysine and 1μg/ml laminin-coated substrates. Rat DRG neurons were grown for approximately 16 hours, fixed in 4% PFA / 20% sucrose in PBS, and stained with anti-βIII tubulin antibody (Covance). Neurite outgrowth length and the number of neurons were analyzed with the neurite outgrowth and multi-wavelength scoring modules of MetaXpress, respectively. Neurite outgrowth per neuron was calculated by dividing the total neurite outgrowth per condition by the total number of neurons.

4.4.6 Intraocular Injection

All animal procedures followed guidelines from the Canadian Council of Animal Care. Surgeries were performed on female Sprague-Dawley rats (180g-200g) under general gas anesthesia (2-3% isofluorane mixed in oxygen, 0.8 L/min). The conjunctiva was dissected away until the sclera was reached. A small puncture wound was made in the superior temporal quadrant through the sclera just temporal to the episcleral vein using a 30-gauge needle. In cases where a second intraocular injection was performed, a second small puncture wound was made in the superior nasal quadrant through the sclera just nasal to the episcleral vein using a 30-gauge needle. Intraocular injections of the TAT proteins (5 μl) into the vitreous space of the left eye were performed using a fine glass

tube attached to a 10 μl-Hamilton syringe. The tip of the needle was inserted through the small puncture wound in the sclera at a 45º angle, with the tip of the needle pointed towards the optic nerve head. This route of administration avoided injury to the lens and iris, which have been shown to promote RGC survival and regeneration (Leon, Yin et al. 2000). The injection was performed over 1 minute, after which the needle was held in place for approximately 2 minutes before slowly removing the needle. The puncture wound was sealed with surgical glue (Indermill, Tyco Health Care, Montreal, Quebec). All subsequent intraocular injections were performed through these two initial injection sites.

4.4.7 Forcep Crush Injury and Immnohistochemistry

The lacrymal glands and extra-ocular muscles were resected to expose the optic nerve. The epineurium was cut along the long axis of the optic nerve, and the optic nerve was crushed approximately 2 mm from the back of the eye with an angled jeweler's forcep (Dumont #5) for 10 seconds. Optic nerve injury was visualized by the clearance of the crush site and the retinal vascular integrity was evaluated by fundoscopic examination. Rats with impaired vascular integrity were excluded from the study. In cases where a Gelfoam sponge (Pfizer) was used to deliver the TAT proteins, a small piece of Gelfoam measuring approximately 1mm X 1mm X 4mm was cut and soaked in 15 μg of TAT protein. Immediately after the optic nerve injury, the soaked Gelfoam sponge was applied directly to the lesion site, where it was wrapped entirely around the optic nerve and kept in place for the remaining two weeks. Thirteen days later, an intraocular injection of 5 μl of 1% cholera toxin beta-subunit (CTβ) (Sigma, Oakville, ON) in PBS through the same puncture wound was performed to anterogradely label regenerating axons. 24 hours later, rats were intracardially perfused with 4% PFA 0.1 M PB and their left eye and optic nerve was removed. The anterior part of the eye and the lens were dissected away, and the eye cup and optic nerve were fixed for an additional 2 hours at 4 ºC. The eye cup and optic nerve were cyroprotected in 30 % sucrose in PBS overnight at 4 ºC, and embedded in OCT (optimal cutting temperature) compound (Tissue-Tek, Miles Laboratories,

Elkhart, IN) and frozen in 2-methylbutane on dry ice. Cryosections (14 μm for optic nerves and 16 μm for retinas) were collected on Superfrost slides (Fischer Scientific) and processed for immunohistochemistry. Sections were post-fixed for 15 minutes in 4% PFA, followed by blocking in blocking solution (5% bovine serum albumin (BSA), 0.3% Triton-X100 (Sigma), in PBS) for 1 hour at room temperature. Primary antibodies were diluted in blocking solution and incubated overnight at 4ºC. The following primary antibodies were used: goat CTβ (List Biological Laboratories), mouse βIII tubulin (Covance), mouse T7 tag (Novagen). Secondary antibodies were diluted in blocking solution and incubated 1 hour at room temperature. Secondary antibodies used were: rabbit anti-goat biotin; anti-mouse-FITC, Alexa-568; anti-rabbit-FITC, Alexa-568 (Invitrogen). Streptavidin-FITC and Alexa-568 (Invitrogen) were also used to amplify the biotin signal.

4.4.8 Analysis of RGC axon regeneration

Axon regeneration was analyzed by counting the number of CTβ-positive axons that crossed a virtual line parallel to the lesion site. The lesion site was identified by differential interference contrast microscopy. CTβ-positive axons were counted at distances of 100 μm and 500 μm from the lesion site in at least four sections per animal from 3 animals per condition. Data analysis was performed using Prism by two-way ANOVA followed by Bonferroni post hoc test.

4.5 RESULTS

4.5.1 Purification of cytosolic TAT fusion proteins from mammalian cell lysates

We initially generated bacterial pET 28b TAT v2 vectors expressing C4RIP or a control mRFP. These vectors contain an N-terminal TAT sequence (RKKRRQRRR) followed by a T7 epitope tag, our in-frame fusion protein (C4RIP or mRFP) and C-terminal 6-histidine sequence. We collected and purified the secreted TAT fusion proteins from conditioned media and observed that this purification resulted in furin-mediated cleavage within the TAT sequence. To circumvent furin-mediated cleavage of the TAT sequence, we generated a mammalian expression vector pTT5 that contained the cDNA for either TAT mRFP or TAT C4RIP. Importantly, this vector did not contain a signal sequence; thereby TAT fusion proteins were targeted to the cytosol and not to the secretory pathway. We transfected pTT5 TAT C4RIP or pTT5 mRFP into chinese hamster ovary (CHO) cells and collected the lysates two days post transfection. We purified TAT C4RIP and TAT mRFP over a Fractogel cobalt column and collected the purified protein. We analyzed fractions collected through out the purification by Coomassie stain and immunoblot with an anti-histidine (His) antibody (Fig. 1A,B). Purification of TAT C4RIP and TAT mRFP using this method resulted in an enrichment of full length TAT fusion proteins from CHO cell lysates.

4.5.2 TAT mRFP crosses biological cell membrane

We investigated the ability of purified TAT mRFP to cross biological membranes by incubating HeLa cells with 100 μg/ml TAT mRFP for 24 hours. Before we fixed the cells, we performed a stringent acid wash to disrupt any non-specific or ionic interactions with the extracellular membrane. We labeled intracellular filamentous (F) -actin with a fluorescently tagged phalloidin. We observed a strong mRFP signal inside HeLa cells treated with TAT mRFP that gave a vesicular-like pattern, while no signal was seen in control PBS-300 mM NaCl treated HeLa cells (Fig. 2A). We also observed a strong nuclear localization of TAT mRFP that seemed to form large aggregates. This is consistent with previous studies that demonstrate a change in localization of TAT proteins following fixation (Richard, Melikov et al. 2003). This has been attributed to the affinity of the positively charged amino acids of TAT to negatively charged DNA.

Therefore, to investigate the localization pattern and to confirm the internalization of TAT mRFP in HeLa cells, we performed live time-lapse microscopy. TAT mRFP was seen diffusely distributed through out the cytoplasm but was strongly localized to vesicles within HeLa cells (Fig. 2B). In contrast to fixed HeLa cells, we did not observe the strong nuclear localization of TAT mRFP in live HeLa cells. We also observed TAT mRFP transduction into HeLa cells as early as 15 minutes following its application. To investigate the ability of purified TAT C4RIP to cross biological membranes, we incubated HeLa cells with 100 μg/ml TAT C4RIP for 3 hours, acid washed the cells and immunostained with a T7 antibody. Both TAT mRFP and TAT C4RIP contained a T7 epitope. Similar to the pattern we observed with TAT mRFP, TAT C4RIP localized to vesicles and also formed large aggregates (Fig. 2C). Based on the differences in localization pattern of TAT mRFP in fixed and live HeLa cells, we believe this distribution pattern is due to fixation. However, the absence of a fluorescent tag in TAT C4RIP precluded us from confirming this. Together, these observations demonstrate that purified TAT mRFP and TAT C4RIP from HeLa cell lysates contain protein transduction properties *in vitro*.

4.5.3 TAT C4RIP attenuates myelin inhibition

We have previously demonstrated that antagonizing RhoA-L-CRMP4 interactions through herpes simplex virus (HSV)-mediated C4RIP expression in DRGs attenuates myelin inhibition (Alabed, Pool et al. 2007). To determine if our purified TAT C4RIP retained the same functional property of attenuating myelin inhibition in DRG neurons, we performed a neurite outgrowth assay in rat DRG neurons. The application of 50 μg/ml TAT C4RIP, but not TAT mRFP, to DRG neurons resulted in the attenuation of myelin inhibition (Fig. 3A,B). These results confirm that our purified TAT C4RIP promotes neurite outgrowth on myelin *in vitro*.

4.5.4 TAT mRFP and TAT C4RIP transduce retinal ganglion cells *in vivo*

To investigate if TAT mRFP and TAT C4RIP were capable of transducing cells *in vivo*, we performed an single intraocular injection of either protein into the adult rat vitreous space and collected the retinas either 3 hours or 24 hours post-injection. To visualize where the TAT proteins localized within the retina, we immunostained retinal

sections with the T7 antibody and βIII tubulin to label neurons (Fig. 3). Both TAT mRFP and TAT C4RIP strongly localized within RGCs at 3 hours and 24 hours post-injection (Fig. 3). TAT mRFP and TAT C4RIP localization was also observed with the inner plexiform layer and the inner nuclear layer. Together, these observations demonstrate that purified TAT mRFP and TAT C4RIP contain protein transduction properties *in vivo*.

We assessed the distribution of TAT mRFP in the retina 24 hours post-injection through T7 and βIII tubulin immunostained retina flatmounts (Fig. 4A). A single intraocular injection of TAT mRFP performed in the superior temporal quadrant of the retina resulted in a limited distribution of TAT mRFP to that quadrant (Fig. 4A, top panel). Furthermore, two separate intraocular injections of TAT mRFP performed in the superior temporal and superior nasal quadrants resulted in a greater distribution of TAT mRFP but still did not transduce all RGCs in the retina (Fig. 4B, bottom panel).

We attempted to deliver TAT mRFP directly to the injured RGC axons by soaking a Gelfoam sponge with TAT mRFP and applying it at the optic nerve lesion site. Gelfoam delivery of C3-transferase, a potent RhoA inhibitor, at the optic nerve lesion site has been shown to be an effective strategy to deliver and promote RGC axon regeneration following optic nerve injury (Lehmann, Fournier et al. 1999). 24 hours after application, we assessed TAT mRFP penetration through immunohistochemistry on optic nerve sections cut along the long axis. We observed that TAT mRFP localized mainly to the periphery of the optic nerve and penetrated very poorly into the central region (Fig. 4B).

4.5.5 TAT C4RIP does not promote axon regeneration in retinal ganglion cells following optic nerve injury

Based on the distribution patterns previously described, we investigated the ability of intraocular injected TAT C4RIP to promote RGC axon regeneration following optic nerve injury. We performed two separate intraocular injections of TAT C4RIP in the superior temporal and superior nasal quadrants immediately following optic nerve injury and five days post-optic nerve injury. This delivery strategy was based on a previous study that demonstrated enhanced RGC survival and regeneration following the repeated delivery of cell-permeable C3-like Rho antagonists (Bertrand, Di Polo et al. 2007). We assessed RGC axon regeneration through a single intraocular injection of cholera toxin beta-subunit (CTβ), which gets transported anterogradely down RGC

axons, followed by immunohistochemistry analysis of CTβ localization in optic nerve sections. Many CTβ-positive axons were observed proximal to the lesion site in TAT mRFP and TAT C4RIP injected animals (Fig. 6A). While a few CTβ-axons were seen distal to the lesion site, TAT C4RIP did not promote RGC axon regeneration compared to TAT mRFP (Fig. 6A, B).

4.6 DISCUSSION

Here we described a novel method to generate and purify TAT fusion proteins targeted to the cytosolic compartment of mammalian cells. These TAT fusion proteins do not enter the secretory pathway where they are cleaved by furin proteases. Mammalian expression allows for the production of TAT fusion proteins that possess relevant post-translational modifications. We demonstrate that TAT fusion proteins generated using this novel method are capable of transducing cells *in vitro* and *in vivo*. We validate this method of generating cytosolic TAT fusion proteins with TAT C4RIP, a competitive RhoA-L-CRMP4 antagonist, and a control TAT mRFP protein. Our data indicates that TAT C4RIP and TAT mRFP transduce HeLa cells *in vitro* and adult RGCs *in vivo*. Importantly, we demonstrate that TAT C4RIP retains its functional ability to attenuate myelin inhibition in rat DRG neurons *in vitro*. We propose that the large-scale production of TAT fusion proteins using this novel method results in functional proteins that can be potentially used for various therapeutic applications.

4.6.1 TAT C4RIP attenuates myelin inhibition *in vitro* but not *in vivo*

We confirmed that our purified TAT C4RIP retained its biological properties by demonstrating that TAT C4RIP attenuates myelin inhibition in DRGs *in vitro* as previously described with HSV-mediated expression of C4RIP (Alabed, Pool et al. 2007). However, the intraocular injection of TAT C4RIP did not promote RGC axon regeneration following optic nerve injury *in vivo*. The inability of TAT C4RIP to promote regeneration in this injury model can be attributed to various reasons. Our *in vitro* data suggests that in order for TAT C4RIP to act as a competitive antagonist, TAT C4RIP levels must be in molar excess of endogenous L-CRMP4 levels. Although we have attempted to increase TAT C4RIP levels through four separate intraocular injections, we have not confirmed if the TAT C4RIP levels reached in RGCs are sufficient to antagonize the RhoA-L-CRMP4 interaction. Indeed, the restricted distribution of TAT mRFP to areas surrounding the injection sites suggests that TAT mRFP is not well distributed throughout the retina.

We have also attempted *in vitro* outgrowth experiments with dissociated postnatal day 8 retinal culture but have encounter some difficulties achieving reproducible growth

with either TAT mRFP or TAT C4RIP on myelin. We are currently troubleshooting these experiments.

4.6.2 TAT PTD fusion proteins as therapeutic agents

The ability of TAT PTD, and other CPPs, to ferry macromolecules through biological membranes has led to many studies investigating its application to treat various diseases such as cancer, ischemic stroke and neurodegenerative diseases. One strategy has been to use a TAT PTD fused to a single double-stranded RNA binding domain to mask the negative charge of nucleic acids (such as small interfering RNA) and transport them across the cellular membrane (Meade and Dowdy 2007; Meade and Dowdy 2009). Other strategies use TAT PTD fused to full length proteins or TAT PTD conjugated to peptides to treat diseases. For example, the use of TAT-survivin in adjuvant therapy for glioma is currently being investigated in preclinical animal models (Kim, Woo et al. 2007). The TAT PTD conjugated to a selective activator peptide of ε-protein kinase C (PKC) confers sustained cardioprotection against ischemia-reperfusion in mice hearts (Inagaki, Begley et al. 2005), while TAT PTD conjugated to a specific inhibitor of δ-PKC improves microvasculature and cerebral blood flow following acute focal ischemia in rats (Bright, Steinberg et al. 2007). Overall, these studies demonstrate that strategies utilizing TAT PTD as a delivery vehicle for therapeutic agents are effective. However, there are still some issues that need to be addressed before translating these therapies into humans. Most of these preclinical studies have been performed using TAT PTD fusion proteins produced in large quantities in bacteria. While adequate purification techniques can eliminate significant endotoxin levels in the final preparation, proteins produced in bacteria lack the post-translational modifications that they normally undergo in mammalian cells. This may result in different biological properties associated with each form of the protein. For example, in one study, they observed that the application of TAT- green fluorescent protein (GFP) produced in bacteria resulted in a cytosolic distribution when incubated with mammalian cells *in vitro*, whereas mammalian-expressed TAT-GFP localized mainly to the nucleus (Yang, Ma et al. 2002). These differences in localization patterns demonstrate that TAT fusion protein produced in bacteria or in mammalian cells are not equivalent. While some mammalian expression

vectors have been used for the production of TAT PTD fusion proteins, these have all directed the TAT fusion proteins to the secretory pathway where they are likely cleaved by furin proteases (Beerens, Al Hadithy et al. 2003; Flinterman, Farzaneh et al. 2009). Modification of the furin cleavage site located in the TAT PTD circumvents this furin-mediated cleavage event but can alter its transduction property. Here, we propose an alternative approach to circumvent furin-mediated cleavage of TAT PTD fusion proteins in the secretory pathway that does not require the mutation of the TAT PTD but still allows eukaryotic post-translational modifications to occur. Furthermore, this strategy allows for proteins that localize to the cytosol access to other modifying proteins that it would normally interact with in that compartment. In contrast, TAT PTD fusion proteins targeted for the secretory pathway may not have access to these interacting proteins. In this study, we purify TAT C4RIP, a RhoA-L-CRMP4 competitive antagonist using this novel method. Both RhoA and L-CRMP4 are normally found in the cytosol, therefore targeting TAT C4RIP to the cytosolic compartment allows for relevant post-translational modifications to occur.

4.6.3 Potential limitations of TAT PTD fusion proteins

While there is certainly a lot of promise for TAT PTD fusion proteins as therapeutic agents, there are also some potential limitations. The highly charged nature of the TAT PTD and its high affinity for glycosaminoglycans might result in the extracellular matrix, which is rich in glycosaminoglycans, binding and sequestering all of the TAT PTD fusion protein (Beerens, Al Hadithy et al. 2003). Indeed, in our study we observe the limited distribution of TAT mRFP within the retina following either a single or double intraocular injection. Future studies should investigate strategies to circumvent this limitation. Further, TAT PTD fusion may also be rapidly degrade by extracellular proteases depending on the amino acid sequence of the fusion protein. This would result in the need for multiple applications of the TAT PTD fusion protein, although the implantation of irradiated mammalian cells that continuously secrete the TAT PTD fusion protein has been proposed as an alternative (Flinterman, Farzaneh et al. 2009). Finally, the major obstacle to overcome in the development of TAT PTD as therapeutic agents is the same property that makes it so attractive: lack of specificity. The presence of

glycosaminoglycans on all cell surfaces results in the non-specific transduction of all cells with the TAT PTD fusion protein, whether they are diseased or healthy. This may lead to unwanted side effects depending on the biological property of the fusion protein. Overall we believe that there are many advantages to using TAT PTD fusion proteins as therapeutic agents but that certain issues exists that must be addressed before translating them into humans. We believe that purification of cytosolic TAT PTD fusion proteins from mammalian cell lysates addresses one of these issues.

4.7 REFERENCES

Alabed, Y. Z., M. Pool, et al. (2010). "GSK3beta regulates myelin-dependent axon outgrowth inhibition through CRMP4." J. Neurosci. **30**(16): 5635-5643.

Alabed, Y. Z., M. Pool, et al. (2007). "Identification of CRMP4 as a convergent regulator of axon outgrowth inhibition." J. Neurosci. **27**(7): 1702-1711.

Barka, T., E. S. Gresik, et al. (2004). "Production of cell lines secreting TAT fusion proteins." J Histochem Cytochem **52**(4): 469-477.

Beerens, A. M. J., A. F. Y. Al Hadithy, et al. (2003). "Protein transduction domains and their utility in gene therapy." Curr Gene Ther **3**(5): 486-494.

Bertrand, J., A. Di Polo, et al. (2007). "Enhanced survival and regeneration of axotomized retinal neurons by repeated delivery of cell-permeable C3-like Rho antagonists." Neurobiol Dis **25**(1): 65-72.

Bertrand, J., M. J. Winton, et al. (2005). "Application of Rho antagonist to neuronal cell bodies promotes neurite growth in compartmented cultures and regeneration of retinal ganglion cell axons in the optic nerve of adult rats." J. Neurosci. **25**(5): 1113-1121.

Borisoff, J. F., C. C. M. Chan, et al. (2003). "Suppression of Rho-kinase activity promotes axonal growth on inhibitory CNS substrates." Mol Cell Neurosci **22**(3): 405-416.

Bright, R., G. K. Steinberg, et al. (2007). "DeltaPKC mediates microcerebrovascular dysfunction in acute ischemia and in chronic hypertensive stress in vivo." Brain Res. **1144**: 146-155.

Byk, T., T. Dobransky, et al. (1996). "Identification and molecular characterization of Unc-33-like phosphoprotein (Ulip), a putative mammalian homolog of the axonal guidance-associated unc-33 gene product." J Neurosci **16**(2): 688-701.

Byk, T., S. Ozon, et al. (1998). "The Ulip family phosphoproteins--common and specific properties." Eur J Biochem **254**(1): 14-24.

Dergham, P., B. Ellezam, et al. (2002). "Rho signaling pathway targeted to promote spinal cord repair." J. Neurosci. **22**(15): 6570-6577.

Derossi, D., S. Calvet, et al. (1996). "Cell internalization of the third helix of the Antennapedia homeodomain is receptor-independent." J. Biol. Chem. **271**(30): 18188-18193.

Dubreuil, C., M. Winton, et al. (2003). "Rho activation patterns after spinal cord injury and the role of activated Rho in apoptosis in the …." J. Cell Biol.

Fawell, S., J. Seery, et al. (1994). "Tat-mediated delivery of heterologous proteins into cells." Proceedings of the National Academy of Sciences of the United States of America **91**(2): 664-668.

Fischer, D., Z. He, et al. (2004). "Counteracting the Nogo receptor enhances optic nerve regeneration if retinal ganglion cells are in an active growth state." J. Neurosci. **24**(7): 1646-1651.

Fischer, D., V. Petkova, et al. (2004). "Switching mature retinal ganglion cells to a robust growth state in vivo: gene expression and synergy with RhoA inactivation." J. Neurosci. **24**(40): 8726-8740.

Flinterman, M., F. Farzaneh, et al. (2009). "Delivery of therapeutic proteins as secretable TAT fusion products." Mol Ther **17**(2): 334-342.
Fournier, A. E., B. T. Takizawa, et al. (2003). "Rho kinase inhibition enhances axonal regeneration in the injured CNS." J. Neurosci. **23**(4): 1416-1423.
Frankel, A. D. and C. O. Pabo (1988). "Cellular uptake of the tat protein from human immunodeficiency virus." Cell **55**(6): 1189-1193.
Gaetano, C., T. Matsuo, et al. (1997). "Identification and characterization of a retinoic acid-regulated human homologue of the unc-33-like phosphoprotein gene (hUlip) from neuroblastoma cells." J Biol Chem **272**(18): 12195-12201.
Goshima, Y., F. Nakamura, et al. (1995). "Collapsin-induced growth cone collapse mediated by an intracellular protein related to UNC-33." Nature **376**(6540): 509-514.
Green, M. and P. M. Loewenstein (1988). "Autonomous functional domains of chemically synthesized human immunodeficiency virus tat trans-activator protein." Cell **55**(6): 1179-1188.
Gump, J. M. and S. F. Dowdy (2007). "TAT transduction: the molecular mechanism and therapeutic prospects." Trends Mol Med **13**(10): 443-448.
Gump, J. M., R. K. June, et al. (2010). "Revised role of glycosaminoglycans in TAT protein transduction domain-mediated cellular transduction." J. Biol. Chem. **285**(2): 1500-1507.
Hacein-Bey-Abina, S., C. von Kalle, et al. (2003). "A serious adverse event after successful gene therapy for X-linked severe combined immunodeficiency." N Engl J Med **348**(3): 255-256.
Hacein-Bey-Abina, S., C. Von Kalle, et al. (2003). "LMO2-associated clonal T cell proliferation in two patients after gene therapy for SCID-X1." Science **302**(5644): 415-419.
Hedgecock, E. M., J. G. Culotti, et al. (1985). "Axonal guidance mutants of Caenorhabditis elegans identified by filling sensory neurons with fluorescein dyes." Developmental Biology **111**(1): 158-170.
Inagaki, K., R. Begley, et al. (2005). "Cardioprotection by epsilon-protein kinase C activation from ischemia: continuous delivery and antiarrhythmic effect of an epsilon-protein kinase C-activating peptide." Circulation **111**(1): 44-50.
Inatome, R., T. Tsujimura, et al. (2000). "Identification of CRAM, a novel unc-33 gene family protein that associates with CRMP3 and protein-tyrosine kinase(s) in the developing rat brain." J Biol Chem **275**(35): 27291-27302.
Jin, Z. and S. M. Strittmatter (1997). "Rac1 mediates collapsin-1-induced growth cone collapse." J Neurosci **17**(16): 6256-6263.
Kaplan, I. M., J. S. Wadia, et al. (2005). "Cationic TAT peptide transduction domain enters cells by macropinocytosis." J Control Release **102**(1): 247-253.
Kim, C.-H., S.-J. Woo, et al. (2007). "Enhanced antitumour immunity by combined use of temozolomide and TAT-survivin pulsed dendritic cells in a murine glioma." Immunology **122**(4): 615-622.
Kim, J.-E., B. P. Liu, et al. (2004). "Nogo-66 receptor prevents raphespinal and rubrospinal axon regeneration and limits functional recovery from spinal cord injury." Neuron **44**(3): 439-451.

Lehmann, M., A. Fournier, et al. (1999). "Inactivation of Rho signaling pathway promotes CNS axon regeneration." J Neurosci **19**(17): 7537-7547.

Leon, S., Y. Yin, et al. (2000). "Lens injury stimulates axon regeneration in the mature rat optic nerve." J. Neurosci. **20**(12): 4615-4626.

Lord-Fontaine, S., F. Yang, et al. (2008). "Local inhibition of Rho signaling by cell-permeable recombinant protein BA-210 prevents secondary damage and promotes functional recovery following acute spinal cord injury." J Neurotrauma **25**(11): 1309-1322.

Meade, B. R. and S. F. Dowdy (2007). "Exogenous siRNA delivery using peptide transduction domains/cell penetrating peptides." Adv Drug Deliv Rev **59**(2-3): 134-140.

Meade, B. R. and S. F. Dowdy (2009). "The road to therapeutic RNA interference (RNAi): Tackling the 800 pound siRNA delivery gorilla." Discov Med **8**(43): 253-256.

Minturn, J. E., H. J. Fryer, et al. (1995). "TOAD-64, a gene expressed early in neuronal differentiation in the rat, is related to unc-33, a C. elegans gene involved in axon outgrowth." J Neurosci **15**(10): 6757-6766.

Monnier, P. P., A. Sierra, et al. (2003). "The Rho/ROCK pathway mediates neurite growth-inhibitory activity associated with the chondroitin sulfate proteoglycans of the CNS glial scar." Mol Cell Neurosci **22**(3): 319-330.

Nagahara, H., A. M. Vocero-Akbani, et al. (1998). "Transduction of full-length TAT fusion proteins into mammalian cells: TAT-p27Kip1 induces cell migration." Nat Med **4**(12): 1449-1452.

Pan, S., Y. Chao, et al. (2009). "Long form collapsin response mediator protein-1 (LCRMP-1) expression is associated with clinical outcome and lymph node metastasis in non-small cell lung cancer patients." Lung Cancer.

Quach, T. T., A.-M. Duchemin, et al. (2004). "Involvement of collapsin response mediator proteins in the neurite extension induced by neurotrophins in dorsal root ganglion neurons." Mol Cell Neurosci **25**(3): 433-443.

Quinn, C. C., E. Chen, et al. (2003). "TUC-4b, a novel TUC family variant, regulates neurite outgrowth and associates with vesicles in the growth cone." J. Neurosci. **23**(7): 2815-2823.

Quinn, C. C., G. E. Gray, et al. (1999). "A family of proteins implicated in axon guidance and outgrowth." J Neurobiol **41**(1): 158-164.

Richard, J. P., K. Melikov, et al. (2003). "Cell-penetrating peptides. A reevaluation of the mechanism of cellular uptake." J. Biol. Chem. **278**(1): 585-590.

Riento, K. and A. J. Ridley (2003). "Rocks: multifunctional kinases in cell behaviour." Nat Rev Mol Cell Biol **4**(6): 446-456.

Schwarze, S. R., A. Ho, et al. (1999). "In vivo protein transduction: delivery of a biologically active protein into the mouse." Science **285**(5433): 1569-1572.

Siddiqui, S. S. and J. G. Culotti (1991). "Examination of neurons in wild type and mutants of Caenorhabditis elegans using antibodies to horseradish peroxidase." Journal of Neurogenetics **7**(4): 193-211.

Torchilin, V. P. and A. N. Lukyanov (2003). "Peptide and protein drug delivery to and into tumors: challenges and solutions." Drug Discov Today **8**(6): 259-266.

Tyagi, M., M. Rusnati, et al. (2001). "Internalization of HIV-1 tat requires cell surface heparan sulfate proteoglycans." J. Biol. Chem. **276**(5): 3254-3261.

Vives, E. (2003). "Cellular uptake [correction of utake] of the Tat peptide: an endocytosis mechanism following ionic interactions." J Mol Recognit **16**(5): 265-271.

Vivès, E., P. Brodin, et al. (1997). "A truncated HIV-1 Tat protein basic domain rapidly translocates through the plasma membrane and accumulates in the cell nucleus." J Biol Chem **272**(25): 16010-16017.

Wadia, J. S., R. V. Stan, et al. (2004). "Transducible TAT-HA fusogenic peptide enhances escape of TAT-fusion proteins after lipid raft macropinocytosis." Nat Med **10**(3): 310-315.

Wang, L. H. and S. M. Strittmatter (1996). "A family of rat CRMP genes is differentially expressed in the nervous system." J Neurosci **16**(19): 6197-6207.

Wang, L. H. and S. M. Strittmatter (1997). "Brain CRMP forms heterotetramers similar to liver dihydropyrimidinase." J Neurochem **69**(6): 2261-2269.

Wender, P. A., D. J. Mitchell, et al. (2000). "The design, synthesis, and evaluation of molecules that enable or enhance cellular uptake: peptoid molecular transporters." Proc Natl Acad Sci USA **97**(24): 13003-13008.

Winton, M. J., C. I. Dubreuil, et al. (2002). "Characterization of new cell permeable C3-like proteins that inactivate Rho and stimulate neurite outgrowth on inhibitory substrates." J Biol Chem **277**(36): 32820-32829.

Yang, Y., J. Ma, et al. (2002). "HIV-1 TAT-mediated protein transduction and subcellular localization using novel expression vectors." FEBS Lett **532**(1-2): 36-44.

Yiu, G. and Z. He (2006). "Glial inhibition of CNS axon regeneration." Nat Rev Neurosci **7**(8): 617-627.

Yuasa-Kawada, J., R. Suzuki, et al. (2003). "Axonal morphogenesis controlled by antagonistic roles of two CRMP subtypes in microtubule organization." Eur J Neurosci **17**(11): 2329-2343.

Zheng, B., J. Atwal, et al. (2005). "Genetic deletion of the Nogo receptor does not reduce neurite inhibition in vitro or promote corticospinal tract regeneration in vivo." Proc Natl Acad Sci USA **102**(4): 1205-1210.

Chapter 4 - Figure 1. Purification of cytosolic TAT C4RIP and TAT mRFP from CHO cell lysates.

pTT5-TAT C4RIP (A) or pTT5-TAT mRFP (B) were transfected into CHO cells and cell lysates were collected two days post-transfection. TAT fusion proteins were purified on a Fractogel cobalt column and the flow through was kept for analysis. The Fractogel cobalt column was washed with 10 column volumes of wash buffer #1 (50 mM sodium phosphate pH=7, 300 mM NaCl), followed by 10 column volumes of wash buffer #2 (50 mM sodium phosphate pH=7, 300 mM NaCl, 25 mM imidazole). TAT fusion protein was eluted in elution buffer (50 mM sodium phosphate pH=7, 300 mM NaCl, 300 mM imidazole) and fractions that contained the TAT fusion protein were pooled and desalted using a desalting column. Collected fractions were run on a SDS-polyacrylamide gel and Coomassie stained or immunoblotted with an anti-histidine antibody.

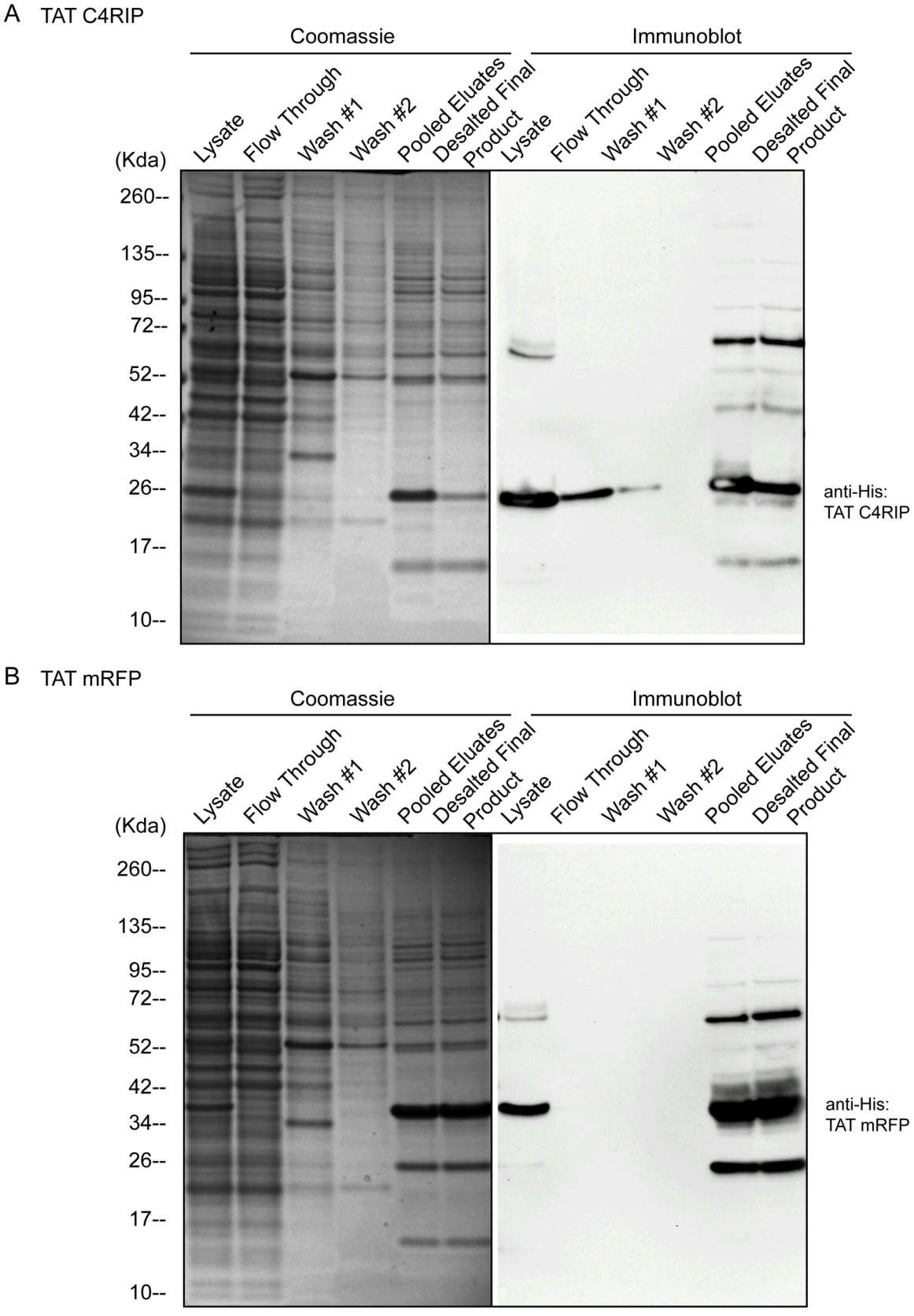
A
TAT C4RIP
Coomassie
Immunoblot
Lysate
Flow Through
Wash #1
Wash #2
Pooled Eluates
Desalted Final
Product
(Kda)
260--
135--
95--
72--
52--
42--
34--
26--
17--
10--
anti-His:
TAT C4RIP
B
TAT mRFP
anti-His:
TAT mRFP

Chapter 4 - Figure 2. Intracellular generated TAT mRFP crosses biological cell membranes.

(A) HeLa cells were incubated with 100 μg/ml TAT mRFP (top panels) or equivalent volume of PBS-300 mM NaCl (bottom panels) for 24 hours before acid wash to remove proteins that were non-specifically bound to the extracellular plasma membrane, and subsequent fixation and staining with phalloidin-Alexa 488. Bar, 10 μm. (B) Fluorescent micrographs from time-lapse microscopy performed on HeLa cells incubated with 100 μg/ml TAT mRFP for 3 hours, washed three times with media, and incubated in OptiMEM. TAT mRFP localizes to small vesicles, which are seen moving through out the cell (arrow). There is also a more diffuse cytosolic distribution of TAT mRFP observed through out the cell. t= time, s=seconds. Bar, 10 μm. (C) Fluorescent micrographs of HeLa cells incubated with either PBS-300 mM NaCl (top panel), 100 μg/ml TAT mRFP (middle panel) or 100 μg/ml TAT C4RIP (bottom panel) for 3 hours, acid washed and stained for T7 and DNA. mRFP signal was visualized without any amplification of the fluorescent signal.

FIGURE 2

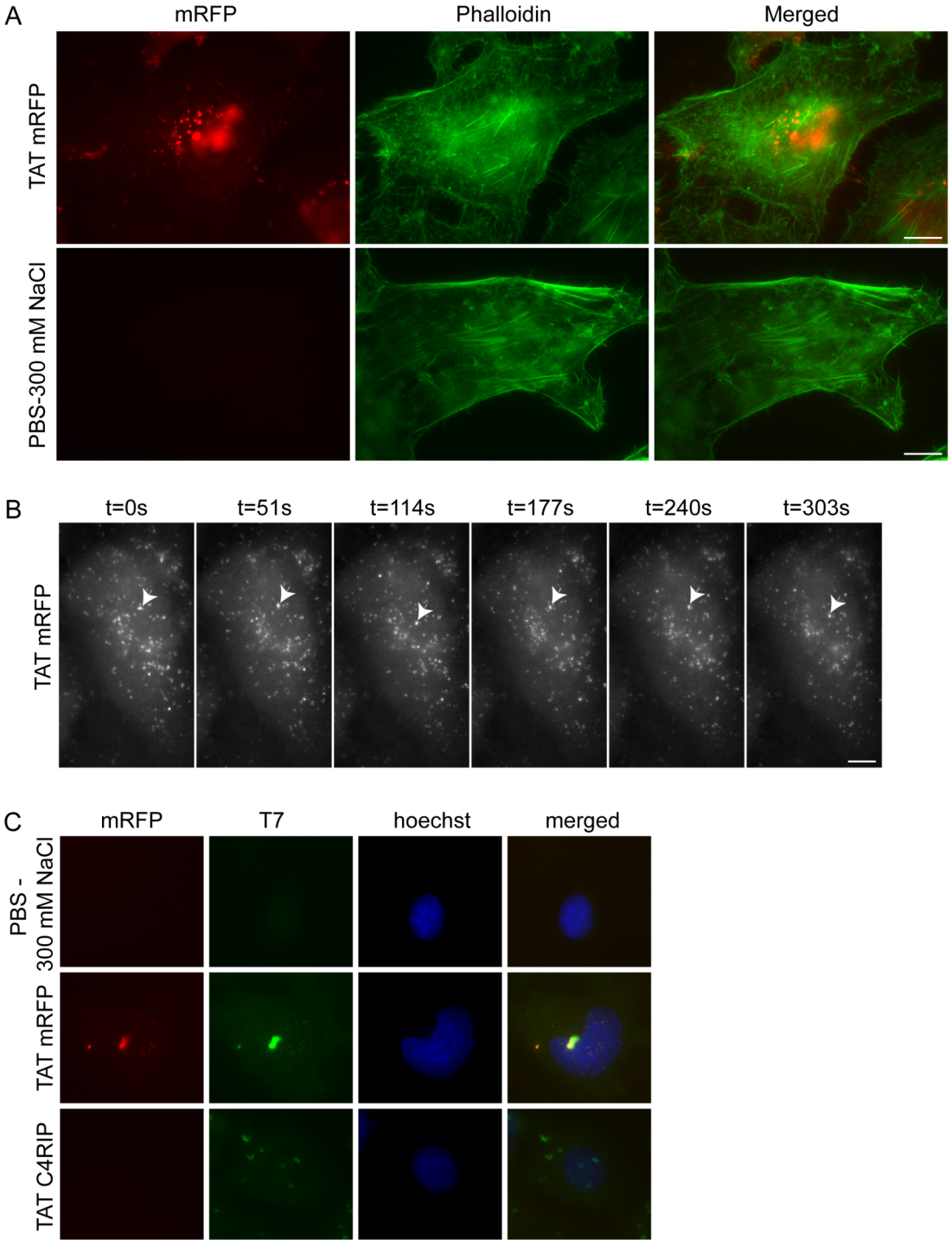
A
mRFP
Phalloidin
Merged
TAT mRFP
PBS-300 mM NaCl
B
t=0s
t=51s
t=114s
t=177s
t=240s
t=303s
TAT mRFP
C
mRFP
T7
hoechst
merged
PBS - 300 mM NaCl
TAT mRFP
TAT C4RIP

Chapter 4 - Figure 3. TAT C4RIP attenuates myelin inhibition.

(A) Representative fluorescent micrographs of βIII tubulin stained dissociated rat dorsal ganglion neurons treated with either PBS-300 mM NaCl, TAT mRFP (50 μg/mL), or TAT C4RIP (50 μg/mL), and plated on a control substrate or myelin. Bar, 100 μm. (B) TAT C4RIP attenuates myelin inhibition. Outgrowth per neuron was determined by measuring the total outgrowth per well divided by the total number of neurons per well. For each experiment, values from duplicate wells were averaged and normalized to outgrowth on 0 μg of myelin (n=3, two-way ANOVA, ***$p<0.001$).

FIGURE 3

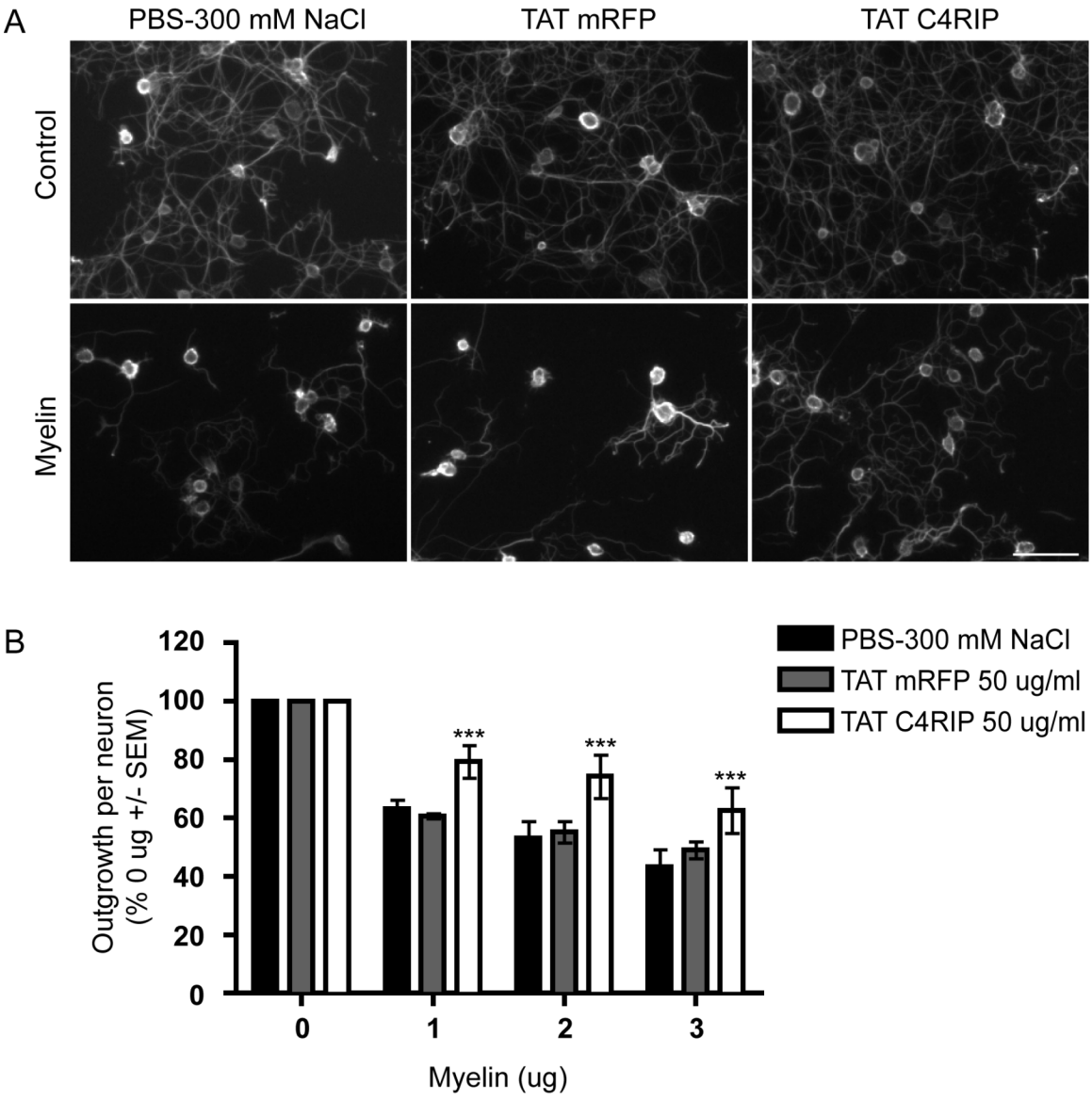
A
PBS-300 mM NaCl
TAT mRFP
TAT C4RIP
Control
Myelin
B
PBS-300 mM NaCl
TAT mRFP 50 ug/ml
TAT C4RIP 50 ug/ml
Outgrowth per neuron
(% 0 ug +/- SEM)
120
100
80
60
40
20
0
***
***
***
0
1
2
3
Myelin (ug)

Chapter 4 - Figure 4. Intracellular generated TAT proteins transduce adult rat retinal ganglion cells in vivo.

Fluorescent micrographs from retinal sections injected with 4 μg of either TAT mRFP or TAT C4RIP. Retinal sections were stained for T7, βIII tubulin and DNA. Both TAT mRFP and TAT C4RIP proteins can transduce into retinal ganglion cells as early as 3 hours post-injection, and is detected 24 hours post-injection. No T7 signal is observed in the non-injected control retina (top panel). NF= nerve fiber layer, RGC= retinal ganglion cell layer, IPL= inner plexiform layer, INL= inner nuclear layer, OPL= outer plexiform layer, ONL= outer nuclear layer, OS= outer segment. Bar, 100 μm.

FIGURE 4

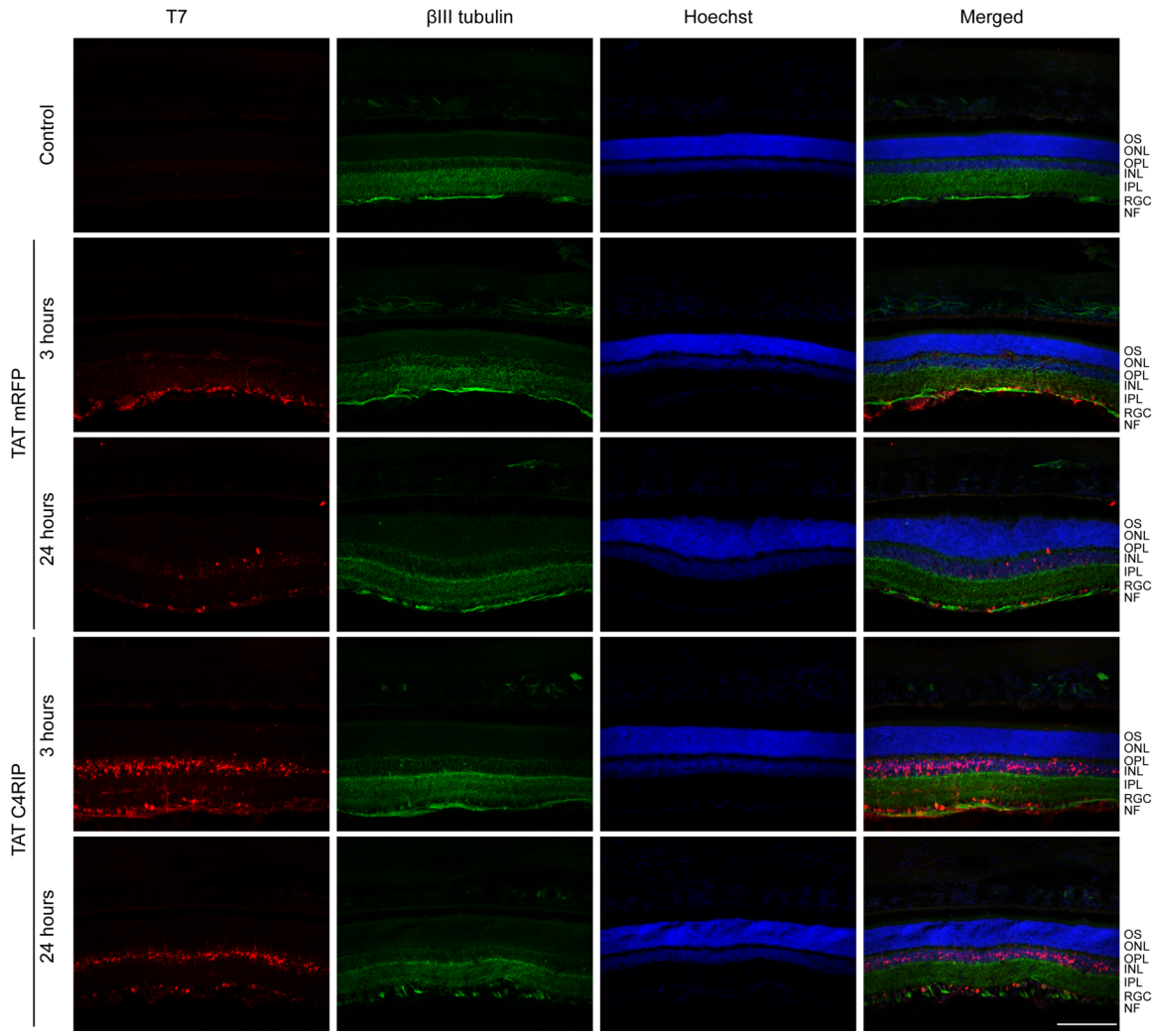
T7
βIII tubulin
Hoechst
Merged
Control
TAT mRFP
3 hours
24 hours
TAT C4RIP
3 hours
24 hours
OS
ONL
OPL
INL
IPL
RGC
NF

Chapter 4 - Figure 5. Optimizing the delivery method of TAT proteins to promote retinal ganglion cell axon regeneration.

(A) Fluorescent micrographs of retinal flatmounts stained for T7 and βIII tubulin 24 hours following either a single temporal injection of 4 μg of TAT mRFP (top panel) or single injections performed at two different locations in the sclera (nasal and temporal) of 4 μg of TAT mRFP (bottom panel). Two injections result in a greater distribution of TAT mRFP within the retina. Bar, 1000 μm. (B) Fluorescent micrographs of optic nerve sections stained for T7 and βIII tubulin 24 hours following the sustained delivery of TAT mRFP directly to the lesion site with Gelfoam. Gelfoam delivery of TAT mRFP results is very poor distribution of TAT mRFP through out the lesion site. The strongest TAT mRFP signal is seen at the periphery of the optic nerve (arrow). Bar, 100 μm.

FIGURE 5

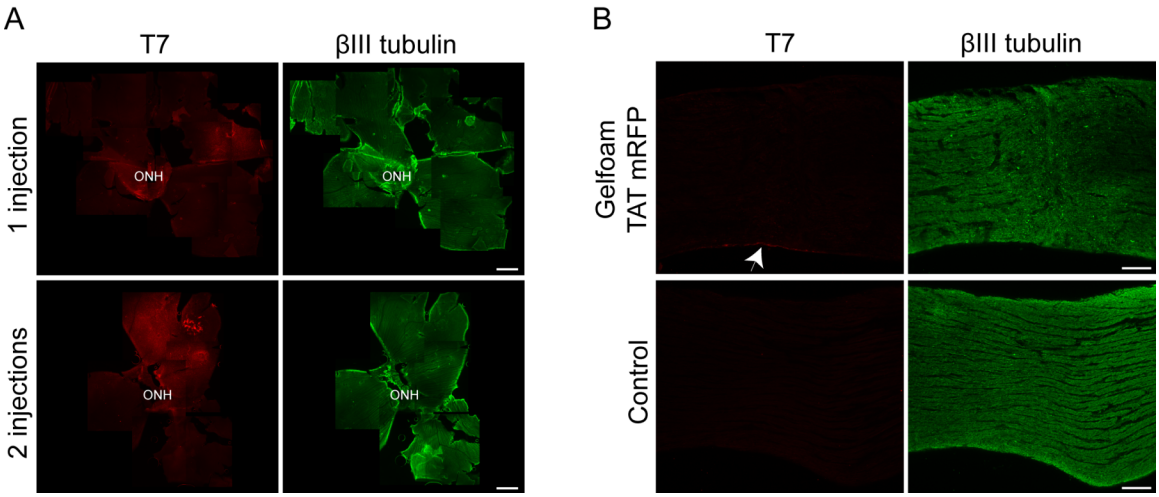
A
T7
βIII tubulin
1 injection
2 injections
ONH
ONH
ONH
ONH
B
T7
βIII tubulin
Gelfoam
TAT mRFP
Control

Chapter 4 - Figure 6. TAT C4RIP does not promote axon regeneration in retinal ganglion cells following optic nerve injury.

(A) Fluorescent micrographs from optic nerve sections stained for CTβ two weeks following optic nerve injury and intraocular injections with 4 μg of either TAT mRFP or TAT C4RIP. Single injections at two different locations in the sclera (nasal and temporal) of 4 μg of TAT mRFP (top panel) or TAT C4RIP (bottom panel) were performed at the time of optic nerve injury and 5 days post-injury. In both groups, CTβ-positive axons are seen in the optic nerve proximal (p) to the lesion site (*), while very few are seen distal (d) to the lesion site. Bar, 100 μm. (B) Quantitative analysis of axon regeneration following intraocular injections of either TAT mRFP (black bars) or TAT C4RIP (grey bars). CTβ-positive axons were counted at 100 μm and 500 μm from the lesion site. At least four optic nerve sections were counted per animal. TAT C4RIP did not promote axon regeneration in RGCs following optic nerve injury (n=3, two-way ANOVA, Bonferroni post hoc test, non-significant= $p>0.05$).

FIGURE 6

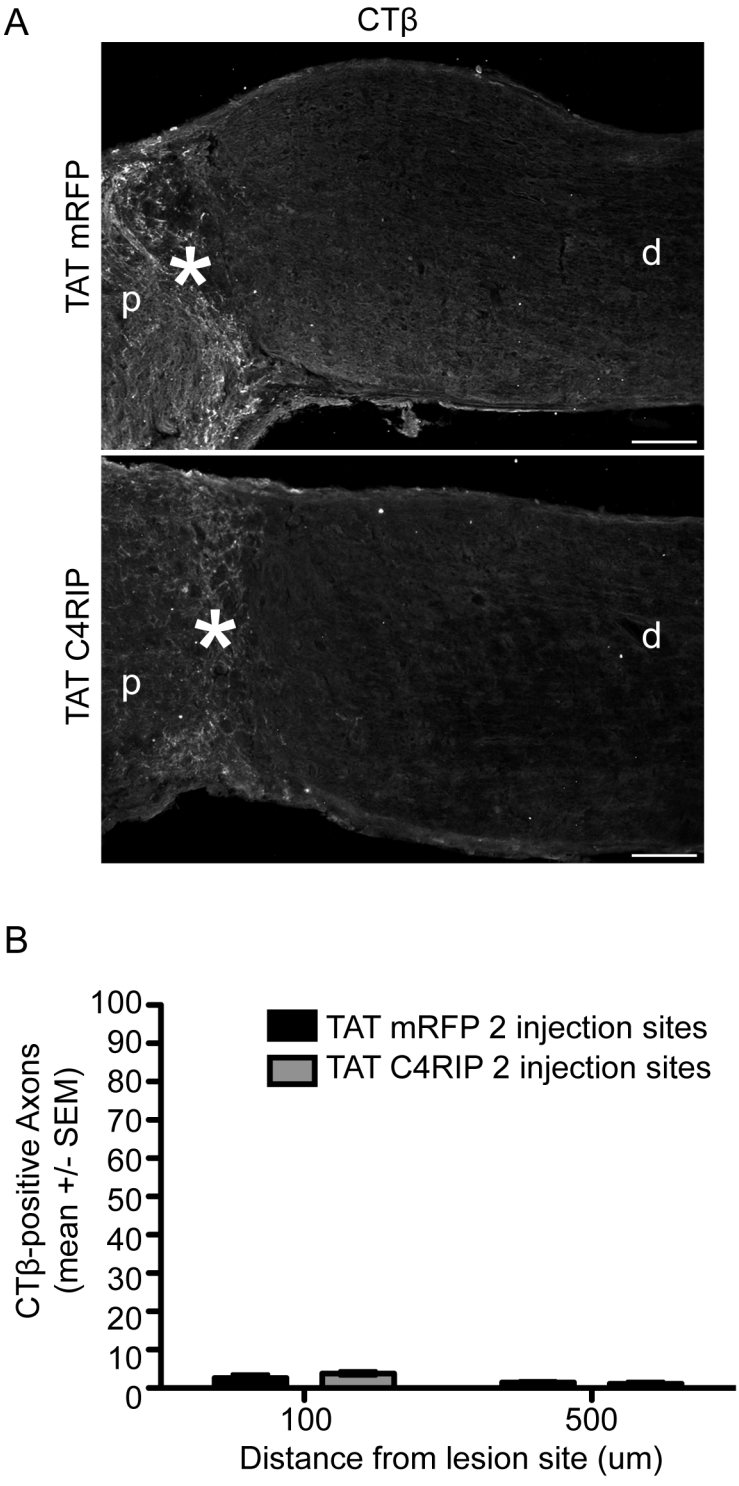
A
CTβ
TAT mRFP
p
d
TAT C4RIP
p
d
B
CTβ-positive Axons
(mean +/- SEM)
100
90
80
70
60
50
40
30
20
10
0
TAT mRFP 2 injection sites
TAT C4RIP 2 injection sites
100
500
Distance from lesion site (um)

CHAPTER 5

5 GENERAL DISCUSSION

5.1 Summary

The major aim of this thesis was to study the role of Collapsin Response Mediator Protein 4 during mitosis and CNS regeneration. The first part of this thesis identifies CRMP4 as a novel regulator of mitosis. The second part of this thesis describes two different *in vivo* strategies we undertook to develop a RhoA-L-CRMP4 antagonist as a therapeutic agent to promote CNS nerve regeneration following trauma.

In Chapter 2, we identify CRMP4 as a novel regulator of mitotic chromosomal alignment in HeLa cells. We observe that CRMP4 depletion results in chromosomal misalignment and delays mitotic progression, possibly through its altered spindle morphology. We also demonstrate that CRMP4 undergoes GSK3-dependent phosphorylation through out mitosis and that CRMP4 phosphorylation at its GSK3 sites is important for its mitotic function.

In Chapters 3 and 4, we investigate the role of CRMP4 in CNS regeneration through the introduction of a RhoA-L-CRMP4 competitive antagonist C4RIP. While we have previously characterized C4RIP and its ability to attenuate myelin inhibition *in vitro*, whether these finding translate into an *in vivo* model of CNS injury was the aim of these chapters. In Chapter 3, we demonstrate that CRMP4 is expressed in the different layers of the adult rat retina including the RGCs and their processes. We show that AAV-mediated transgene expression of C4RIP in RGCs does not promote RGC neuronal survival and axon regeneration following optic nerve injury even if the RGCs are in an active growth state. However, we also identify insufficient AAV-mediated C4RIP protein expression in RGCs as a potential reason why we do not observe any increase in axon regeneration following optic nerve injury. In Chapter 4, as an alternative strategy to deliver C4RIP, we develop a recombinant cell permeable TAT C4RIP protein. We describe a novel method to generate and purify TAT PTD fusion proteins from mammalian cell lysates. Previous strategies used to generate TAT PTD fusion proteins in mammalian cells target them to the secretory pathway, where they are most likely cleaved by furin proteases (Beerens, Al Hadithy et al. 2003; Flinterman, Farzaneh et al. 2009). As an alternative to mutating the furin cleavage site located in the TAT PTD which can change its transduction properties, we target TAT PTD fusion proteins, TAT C4RIP and TAT mRFP, to the cytosol where they are not cleaved by furin proteases and

also undergo normal post-translational modifications. We were able to successfully purify cytosolic TAT C4RIP and TAT mRFP from mammalian cell lysates and demonstrate that these TAT PTD fusion proteins transduce cells *in vitro* and *in vivo*. Importantly, we confirm that purified TAT C4RIP retains its functional ability to attenuate neurite outgrowth inhibition in DRGs *in vitro*. Although, the *in vivo* application of TAT C4RIP did not promote RGC axon regeneration following optic nerve injury, this may be attributed to the poor distribution of TAT C4RIP throughout the retina and optic nerve or to a lack of RGC survival. Overall, we believe that this novel strategy to produce TAT PTD fusion proteins is a significant step forward in the development of TAT PTD fusion proteins as therapeutic delivery vehicles. This method allows for the generation and purification of mammalian expressed TAT PTD fusion proteins without the need to mutate the TAT PTD sequence.

5.2 The importance of CRMP4 during mitosis

The effects we observed following CRMP4 depletion in HeLa cells indicate that CRMP4 plays a role during mitosis. However, if CRMP4 was an essential mitotic protein we would expect it to be expressed in all proliferating cells. Studies characterizing CRMP expression patterns *in vivo* indicate that CRMP4 is not ubiquitously expressed, rather its expression pattern is mostly localized to cells within the nervous system, the developing heart and muscles, and to certain cancers (Wang and Strittmatter 1996; Quinn, Gray et al. 1999; Shih, Yang et al. 2001; Shih, Lee et al. 2003). Therefore, we believe that while CRMP4 depletion results in mitotic defects in HeLa cells, that in other cell types that lack CRMP4 expression, other proteins compensate in its absence. Interestingly, CRMP4 expression in adult nervous tissue is highest in areas where ongoing neurogenesis occurs: the subventricular zone, the dentate granular layer of the hippocampus, the olfactory bulbs and the rostral migratory stream (Nacher, Rosell et al. 2000; Liu, Yang et al. 2003; Liu and Martin 2003). Based on this expression pattern, we can speculate that CRMP4 may be an important mitotic regulator during neurogenesis.

We also demonstrate that phosphorylated CRMP4 at its GSK3 sites is important for chromosomal alignment and spindle morphology. While we have not fully elucidated the mechanisms through which CRMP4 mediates these effects during mitosis, our previous studies in neurons may provide some insight. In neurons, GSK3-dependent

phosphorylation of CRMP4 in response to myelin inhibitors regulates its interaction with RhoA, whereby phosphorylation drives this interaction apart (Alabed, Pool et al. 2010). While the significance of GSK3-dependent phosphorylation of CRMP4 on its interaction with RhoA during mitosis remains to be elucidated, there is some evidence in the literature to support a model in which RhoA mediates its mitotic effects through CRMP4. Neutralization of Lfc, a Rho GEF, with a function-blocking antibody or Lfc depletion with RNA interference results in a decrease in spindle length, increase in chromosome missegregation and an increase in the cells arrested in prophase/prometaphase (Benais-Pont, Punn et al. 2003; Bakal, Finan et al. 2005). This phenotype is similar to the one we observe with CRMP4 depletion, although we do not observe the mitotic arrest. This difference may be attributed to the presence of other physiological substrates that RhoA can signal through, such as mDia. The identification of CRMP4 binding proteins during mitosis should provide more insight into how CRMP4 regulates this process.

5.3 Limitations of C4RIP as a therapeutic agent to promote CNS regeneration

We have previously demonstrated that C4RIP expression in DRGs promotes neurite outgrowth on inhibitory myelin and aggrecan substrates *in vitro* (Alabed, Pool et al. 2007). We have biochemical evidence showing that overexpression of C4RIP selectively disrupts the interaction between RhoA and L-CRMP4 but not between RhoA and S-CRMP4 (Alabed, Pool et al. 2007). Based on these findings, we speculate that C4RIP antagonizes the interaction between RhoA and L-CRMP4 through steric hindrance. One possibility is that C4RIP is competing with endogenous L-CRMP4 for binding sites located with the RhoA protein. However, the inability of C4RIP to bind directly to RhoA suggests that C4RIP may be acting as a dominant negative form of L-CRMP4 that can bind and sequester endogenous L-CRMP4 from its partners (Alabed, Pool et al. 2010). Therefore, the ability of C4RIP to act as a dominant negative form of endogenous L-CRMP4 relies heavily on the ratio of C4RIP to endogenous L-CRMP4, where a molar excess of C4RIP is required. Additionally, C4RIP has to be localized to the same subcellular compartments as endogenous L-CRMP4. In our experiments, we observed AAV-mediated C4RIP expression in RGC cell bodies and their axons but we were unable to confirm if the expression levels we achieved were sufficient to antagonize endogenous L-CRMP4 function. We attempted to increase AAV-mediated C4RIP

expression by performing multiple injections of AAV-C4RIP but were unsuccessful at achieving higher C4RIP protein levels. The difficulties we encountered using AAV as delivery vector highlights the major limitation of developing a competitive antagonist / dominant negative molecule for therapeutic applications: achieving adequate expression levels to competitively antagonize endogenous levels. While C4RIP expression was driven from a chick beta actin promoter, the levels we attained were most likely insufficient to act as a dominant negative to endogenous L-CRMP4.

As an alternative to AAV-mediated expression of C4RIP, we developed a cell permeable form of C4RIP, TAT C4RIP. While the use of a recombinant protein gave us the opportunity to repeatedly deliver large protein quantities to the intraocular space and directly to the lesion site, we lost the advantage of specificity when using AAV serotype 2 vectors since TAT PTD transduces cells non-specifically. Although we were able to confirm TAT C4RIP protein transduction into the RGC cell bodies, we encountered difficulties in transducing all the RGCs within the retina. It is reasonable to speculate that this can be attributed to the high concentration of heparan sulfate preotoglycans within the retina, which bind and sequester the TAT proteins around the injection site.

5.4 The importance of neuroprotection in promoting axon regeneration

In addition to its role as part of the NgR1 signaling complex that mediates outgrowth inhibition in response to myelin associated inhibitors, $p75^{NTR}$ signaling can also induce apoptosis (Barker 2004). Following spinal cord injury (SCI), injured neurons and glial cells upregulate the expression of $p75^{NTR}$ and these apoptotic cells have high levels of active RhoA (Dubreuil, Winton et al. 2003; Madura, Yamashita et al. 2004). Application of the RhoA inhibitor, C3-05, following injury blocks the increase in $p75^{NTR}$ expression and reduces the number of apoptotic cells. These results provide evidence that blocking RhoA protects cells from $p75^{NTR}$–dependent apoptosis. Additional studies using either C3-07 or AAV-C3 transferase demonstrate that RhoA inhibition is also neuroprotective to RGCs following optic nerve injury (Fischer, Petkova et al. 2004; Bertrand, Winton et al. 2005; Bertrand, Di Polo et al. 2007). Therefore, the inactivation of RhoA as a strategy to promote both neuronal survival and axonal regeneration seems very promising.

Importantly, the beneficial effects on survival and regeneration observed with RhoA inhibition translate into improvements in neurological function in different types of SCI models. The most common method of assessing behavioral recovery following SCI is the Basso, Beattie, Bresnahan (BBB) locomotor rating scale, which evaluates open field locomotion (Basso, Beattie et al. 1995). The application C3 in a fibrin gel directly to the lesion site following an over-hemisection lesion results in an improvement in behavioral recovery by 24 hours post-injury (Dergham, Ellezam et al. 2002). These functional improvements are unlikely due to long distance regeneration but are more likely the result of the neuroprotective effects seen with RhoA inhibition. This finding highlights how neuroprotection can translate into significant functional improvements following SCI.

While we have previously demonstrated that the overexpression of C4RIP in rat DRGs attenuates neurite outgrowth inhibition in response to myelin *in vitro*, we were unable to translate these findings to an *in vivo* model of CNS regeneration. Our data demonstrates that AAV-mediated C4RIP expression in adult rat RGCs has no effect on increasing neuronal survival 2 weeks following optic nerve injury compared to AAV-mediated GFP expression. Under these conditions, approximately 15% of RGCs survive two weeks following injury. Therefore, it is possible that the effects of C4RIP on axonal regeneration may only be observed in the context of increased neuronal survival. Our studies combining AAV-mediated C4RIP expression and lens injury did not show an increase in regeneration compared to AAV-mediated GFP expression and lens injury. However, since it has been shown that lens injury alone can stimulate both neuronal survival and nerve regeneration (Pernet and Di Polo 2006), it is possible that these pro-regenerative effects associated with lens injury alone is masking the ability of C4RIP to promote regeneration. Therefore, the combination of C4RIP with a therapeutic compound that exclusively increases neuronal survival, and not regeneration, may yield synergistic results. The exogenous administration of brain-derived neurotrophic factor (BDNF) to injured adult RGC results in an increase in neuronal survival but no effect on axonal regeneration (Pernet and Di Polo 2006). The neuroprotective effect of BDNF is mediated through activation of extracellular signal-regulated kinases 1/2 (Erk1/2) and phosphatidylinositol 3 kinase (PI3K) (Cheng, Sapieha et al. 2002; Pernet, Hauswirth et al.

2005). However, it is important to note that while the combination of BDNF and lens injury act synergistically to enhance RGC neuronal survival, the combination leads to regeneration failure following optic nerve injury (Pernet and Di Polo 2006). It has been proposed that either the downstream signaling pathways of BDNF overcome those activated by lens injury or that BDNF sends a stop signal to the RGC growth cone of the injured axon to inhibit regeneration (Pernet and Di Polo 2006). The combination of BDNF and lens injury leads to the formation of large, hypertrophic axonal swellings in the proximal injured optic nerve suggesting abnormal structural integrity of growth cones (Pernet and Di Polo 2006). Intriguingly, we have demonstrated that GSK3β, a downstream molecule in the PI3K pathway, is inactivated by myelin associated inhibitors, consequently regulating the phosphorylation status of L-CRMP4 and its interaction with RhoA (Alabed, Pool et al. 2010). Thus, in addition to its neuroprotective effects mediated through activated Erk1/2, BDNF-activated PI3K intracellular signaling may also result in the inactivation of GSK3β, an increase the L-CRMP4-RhoA interaction and the inhibition of axonal regeneration. In this context, we hypothesize that the introduction of C4RIP would disrupt the L-CRMP4-RhoA interaction but still allow for other neuroprotective PI3K signaling to occur, resulting in both neuroprotection and nerve regeneration. Future studies combining C4RIP expression, either with AAV-C4RIP or TAT C4RIP, and BDNF may result in an increase in neuronal survival and axon regeneration following optic nerve injury.

5.5 The role of CRMP4 in CNS regeneration: future studies

5.5.1 C4RIP

Through the work we have presented in this thesis, specifically in chapters 3 and 4, we have attempted to elucidate the role of L-CRMP4 in CNS regeneration through the introduction of the competitive antagonist C4RIP. While these *in vivo* studies have yielded largely negative results, its is difficult to conclude that CRMP4 does not participate in CNS regeneration due to the many limitations we have encountered with both AAV-C4RIP and TAT C4RIP. Further, we have also demonstrated that siRNA-mediated CRMP4 depletion in rat DRGs attenuates neurite outgrowth inhibition in response to myelin (Alabed, Pool et al. 2007). Similarly, we have also found that the

introduction of C4RIP, either through Herpes Simplex Virus-mediated expression or through a cell permeable recombinant protein, attenuates myelin inhibition in rat DRGs (Alabed, Pool et al. 2007). While our *in vivo* studies in adult rat retinal ganglion cells have yielded largely negative results, it is possible that the *in vivo* application of C4RIP to adult DRGs following dorsal column injury could promote nerve regeneration.

5.5.2 CRMP4 knockdown

To further elucidate the role of CRMP4 in CNS regeneration ongoing studies not included in this thesis are investigating two different *in vivo* strategies aimed at depleting endogenous CRMP4 protein: (1) the generation of a conventional CRMP4 knockout mouse and (2) the selective depletion of CRMP4 in adult rat RGCs through an AAV vector encoding a CRMP4 shRNA.

We searched the Texas A&M Institute for Genomic Medicine C57BL/6N mouse gene trap library for Dpysl3 gene trapped embryonic stem (ES) cell clones. These ES cell clones have been shown to contribute to the germline and produce knockout mice (Hansen, Markesich et al. 2008). We selected 3 ES cell clones trapped at different locations within the Dpysl3 gene for the generation of chimeras (IST10930D2, 3rd intron; IST12341A8, 3rd intron; and IST14728H3, 1st intron). We anticipate that these ES cell clones will generate mice depleted of both L-CRMP4 and S-CRMP4. We are currently breeding the chimeric mice with wild type C57BL/6N mice to generate heterozygotes. Once we have generated and validated our CRMP4 knockout mice, we will investigate the role of CRMP4 in various CNS and PNS lesion models.

To further investigate the role of CRMP4 *in vivo*, we have generated an AAV-2 expressing green fluorescent protein (GFP) from a chick beta actin promoter and, from a U6 promoter, a CRMP4 shRNA or a control scramble shRNA. AAV-CRMP4shRNA injection into the adult rat vitreous space should result in the selective viral transduction of RGCs, high levels of CRMP4 shRNA expression and depletion of endogenous CRMP4 protein. This strategy for *in vivo* protein knockdown has been effective in demonstrating that Mammalian sterile 20-like kinase-3b (Mst3b) regulates axon regeneration in the mature CNS (Lorber, Howe et al. 2009). We have validated that expression of our CRMP4 shRNAs result in endogenous CRMP4 protein knockdown in rat DRGs and we are currently optimizing the *in vivo* conditions for CRMP4 protein

knockdown in adult rat RGCs. While Lorber and colleagues have used their AAV-Mst3b shRNA to selectively knockdown Mst3b in adult rat RGCs, Liu and colleagues have used a Cre-expressing AAV to delete *Pten*, a negative regulator of mTOR, in the sensorimotor cortex and corticospinal tract of homozygous conditional Pten mutant ($Pten^{loxP/loxP}$) mice (Lorber, Howe et al. 2009; Liu, Lu et al. 2010). Our future studies could take advantage of the ability of AAV to infect cortical neurons in the sensorimotor cortex and we could assess the effect of CRMP4 knockdown on the regenerative ability of adult corticospinal neurons following corticospinal tract injury. These experiments would complement our regenerative studies in the conventional CRMP4 knockout mouse.

5.6 General conclusion

In this thesis we investigate the diverse roles of CRMP4 during mitosis and nerve regeneration. We identify CRMP4 as a novel mitotic regulator and demonstrate that CRMP4 depletion increases chromosome misalignment, delays mitotic progression, yields monopolar syntelic attachments, reduces cold stable microtubules and alters mitotic spindle morphology. Furthermore, we identify CRMP4 as an important physiological substrate of the mitotic kinase GSK3 and show that CRMP4 phosphorylation at its GSK3 sites is critical for its mitotic functions. These findings suggest that despite their low expression levels outside the developing nervous system, CRMPs may play a larger role in other biological processes, particularly in those that rely on cytoskeletal rearrangements.

While our *in vivo* studies using C4RIP as a therapeutic agent to promote CNS regeneration follow injury were unsuccessful, we were able to develop a novel method to generate and purify mammalian expressed recombinant TAT PTD proteins. We hope that this novel purification technique will facilitate the translation of other therapeutic agents, where access to the intracellular compartment of the cell is a priority, into clinically relevant therapies.

5.7 References

Alabed, Y. Z., M. Pool, et al. (2010). "GSK3beta regulates myelin-dependent axon outgrowth inhibition through CRMP4." J. Neurosci. **30**(16): 5635-5643.

Alabed, Y. Z., M. Pool, et al. (2007). "Identification of CRMP4 as a convergent regulator of axon outgrowth inhibition." J. Neurosci. **27**(7): 1702-1711.

Bakal, C. J., D. Finan, et al. (2005). "The Rho GTP exchange factor Lfc promotes spindle assembly in early mitosis." Proc Natl Acad Sci USA **102**(27): 9529-9534.

Barker, P. A. (2004). "p75NTR is positively promiscuous: novel partners and new insights." Neuron **42**(4): 529-533.

Basso, D. M., M. S. Beattie, et al. (1995). "A sensitive and reliable locomotor rating scale for open field testing in rats." J Neurotrauma **12**(1): 1-21.

Beerens, A. M. J., A. F. Y. Al Hadithy, et al. (2003). "Protein transduction domains and their utility in gene therapy." Curr Gene Ther **3**(5): 486-494.

Benais-Pont, G., A. Punn, et al. (2003). "Identification of a tight junction-associated guanine nucleotide exchange factor that activates Rho and regulates paracellular permeability." The Journal of Cell Biology **160**(5): 729-740.

Bertrand, J., A. Di Polo, et al. (2007). "Enhanced survival and regeneration of axotomized retinal neurons by repeated delivery of cell-permeable C3-like Rho antagonists." Neurobiol Dis **25**(1): 65-72.

Bertrand, J., M. J. Winton, et al. (2005). "Application of Rho antagonist to neuronal cell bodies promotes neurite growth in compartmented cultures and regeneration of retinal ganglion cell axons in the optic nerve of adult rats." J. Neurosci. **25**(5): 1113-1121.

Cheng, L., P. Sapieha, et al. (2002). "TrkB gene transfer protects retinal ganglion cells from axotomy-induced death in vivo." J. Neurosci. **22**(10): 3977-3986.

Dergham, P., B. Ellezam, et al. (2002). "Rho signaling pathway targeted to promote spinal cord repair." J. Neurosci. **22**(15): 6570-6577.

Dubreuil, C. I., M. J. Winton, et al. (2003). "Rho activation patterns after spinal cord injury and the role of activated Rho in apoptosis in the central nervous system." J Cell Biol **162**(2): 233-243.

Fischer, D., V. Petkova, et al. (2004). "Switching mature retinal ganglion cells to a robust growth state in vivo: gene expression and synergy with RhoA inactivation." J. Neurosci. **24**(40): 8726-8740.

Flinterman, M., F. Farzaneh, et al. (2009). "Delivery of therapeutic proteins as secretable TAT fusion products." Mol Ther **17**(2): 334-342.

Hansen, G. M., D. C. Markesich, et al. (2008). "Large-scale gene trapping in C57BL/6N mouse embryonic stem cells." Genome Res **18**(10): 1670-1679.

Liu, K., Y. Lu, et al. (2010). "PTEN deletion enhances the regenerative ability of adult corticospinal neurons." Nat Neurosci **13**(9): 1075-1081.

Liu, P.-C., Z.-J. Yang, et al. (2003). "Induction of CRMP-4 in striatum of adult rat after transient brain ischemia." Acta Pharmacol Sin **24**(12): 1205-1211.

Liu, Z. and L. J. Martin (2003). "Olfactory bulb core is a rich source of neural progenitor and stem cells in adult rodent and human." J. Comp. Neurol. **459**(4): 368-391.

Lorber, B., M. L. Howe, et al. (2009). "Mst3b, an Ste20-like kinase, regulates axon regeneration in mature CNS and PNS pathways." Nat Neurosci **12**(11): 1407-1414.
Madura, T., T. Yamashita, et al. (2004). "Activation of Rho in the injured axons following spinal cord injury." EMBO Rep **5**(4): 412-417.
Nacher, J., D. R. Rosell, et al. (2000). "Widespread expression of rat collapsin response-mediated protein 4 in the telencephalon and other areas of the adult rat central nervous system." J. Comp. Neurol. **424**(4): 628-639.
Pernet, V. and A. Di Polo (2006). "Synergistic action of brain-derived neurotrophic factor and lens injury promotes retinal ganglion cell survival, but leads to optic nerve dystrophy in vivo." Brain **129**(Pt 4): 1014-1026.
Pernet, V., W. W. Hauswirth, et al. (2005). "Extracellular signal-regulated kinase 1/2 mediates survival, but not axon regeneration, of adult injured central nervous system neurons in vivo." J Neurochem **93**(1): 72-83.
Quinn, C. C., G. E. Gray, et al. (1999). "A family of proteins implicated in axon guidance and outgrowth." J Neurobiol **41**(1): 158-164.
Shih, J.-Y., Y.-C. G. Lee, et al. (2003). "Collapsin response mediator protein-1: a novel invasion-suppressor gene." Clin Exp Metastasis **20**(1): 69-76.
Shih, J. Y., S. C. Yang, et al. (2001). "Collapsin response mediator protein-1 and the invasion and metastasis of cancer cells." J Natl Cancer Inst **93**(18): 1392-1400.
Wang, L. H. and S. M. Strittmatter (1996). "A family of rat CRMP genes is differentially expressed in the nervous system." J Neurosci **16**(19): 6197-6207.